Design and analysis of a stand-alone renewable hybrid power system for telecom Base Transceiver Station: In East Bale, Ethiopia

Ashebir Demissie Gebre

A Thesis Submitted to the Department of Electrical Power and Control Engineering
School of Electrical Engineering & Computing

Presented in Partial Fulfillment of the Requirements for the Degree of Master's of Science in Electrical Power Engineering

Office of Graduate Studies

Adama Science and Technology University

August, 2021

Adama, Ethiopia

Design and analysis of a stand-alone renewable hybrid power system for telecom Base Transceiver Station: In East Bale, Ethiopia

By: Ashebir Demissie Gebre

Advisor: Dr. Molla Biwota

A Thesis Submitted to the Department of Electrical Power and Control Engineering
School of Electrical Engineering & Computing

Presented in Partial Fulfillment of the Requirements for the Degree of Master's of Science in Electrical Power Engineering

Office of Graduate Studies

Adama Science and Technology University

August, 2021

Adama, Ethiopia

DECLARATION

I hereby declare that this Master Thesis entitled "Design and analysis of a stand-alone renewable hybrid power system for telecom Base Transceiver Station: In East Bale, Ethiopia" is my original work. That is, it has not been submitted for the award of any academic degree, diploma or certificate in any other university. All sources of materials that are used for this thesis have been duly acknowledged through citations.

Name of student: Ashebir Demissie Gebre (PGE/18853/11)

Signature: 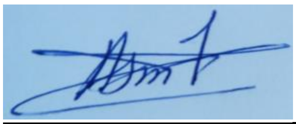 Date 10.09.2021

RECOMMENDATION

I, the advisor of this thesis, hereby certify that I have read the revised version of the thesis entitled “Design and analysis of a stand-alone renewable hybrid power system for telecom Base Transceiver Station: In East Bale, Ethiopia” prepared under my guidance by Ashebir Demissie Gebre submitted in partial fulfillment of the requirements for the degree of Master’s of Science in Electrical Power Engineering. Therefore, I recommend the submission of revised version of the thesis to the department following the applicable procedures.

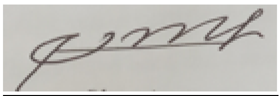

Dr. Molla Biwota		15.09.2021
Major Advisor	Signature	Date

Approval page of M.Sc. Thesis

I, the advisors of the thesis entitled “Design and analysis of a stand-alone renewable hybrid power system for telecom Base Transceiver Station: In East Bale, Ethiopia” and developed by Ashebir Demissie Gebre, hereby certify that the recommendation and suggestions made by the board of examiners are appropriately incorporated into the final version of the thesis.

Dr. Molla Biwota		15.09.2021
Major Advisor	Signature	Date

We, the undersigned, members of the Board of Examiners of the thesis by Ashebir Demissie Gebre have read and evaluated the thesis entitled “Design and analysis of a stand-alone renewable hybrid power system for telecom Base Transceiver Station: In East Bale, Ethiopia” and examined the candidate during open defense. This is therefore, to certify that the thesis is accepted for partial fulfillment of the requirement of the degree of Master of Science in Electrical Power Engineering.

Dr.Prathibha E.		15.09.21
Chairperson	Signature	Date
Dr.Milkias Berhanu		15.09.21
Internal Examiner	Signature	Date
Getachew Biru (Dr.-Ing.)		10.09.21
External Examiner	Signature	Date

Finally, approval and acceptance of the thesis is contingent upon submission of its final copy to the Office of Postgraduate Studies (OPGS) through the Department Graduate Council (DGC) and School Graduate Committee (SGC).

Department Head	Signature	Date
School Dean	Signature	Date
Office of Postgraduate Studies, Dean	Signature	Date

ACKNOWLEGEMENT

I wish to express my profound gratitude and indebtedness to the following for their assistance in making this work a reality. First of all my advisor Dr. Molla Biwota for his very constructive suggestions, encouragement, inspirational guidance and patience until the end of my study.

Next, I would like to thank ASTU (Adama Science and Technology University) for facilitating the thesis work in this coved-19 time. Besides, I want to acknowledge SER Ethio-Telecom for their cooperation to provide the raw data. I owe a lot of appreciation to my family for their goodwill and understanding while this work lasted. Above all, I am most grateful to Almighty God.

Thank You God

TABLE OF CONTENTS

CHAPTER FIVE
RESULTS AND DISCUSSION

LIST OF TABLE

TABLE PAGE

LIST OF FIGURE

FIGURE PAGE

List of Acronyms

AC	Alternating Current
BB	Big Back up battery
BTS	Base Transceiver Station
CO_2	Carbone dioxide
CO	Carbone monoxide
CC	Charging current
CD	Combined dispatch strategy
CHP	Combined Heat and Power
COE	Cost of Energy
DC	Direct Current
DER	Distributed Energy Resource
DG	Diesel Generator
DNO	Distribution Network Operator
DS	Distributed Storage
EMS	Energy Management System
HLR	Home location register
HOMER	Hybrid optimization model for electric renewables
HPS	Hybrid Power System
ICC	Initial capital cost
LF	Load flow
MC	Micro grid Central Controller
MO	Market Operator
NCC	National Telecommunications regulatory authority
NO_2	Nitrogen dioxides
NPC	Net Present Cost
OSS	Operation support system
PCC	Common Coupling Point
PM	Particulate matter
PMS	Power Management System
PV	Photovoltaics
RES	Renewable Energy Sources
Rms	Root Mean Squared Value
SER	South East Region
SOC	State of Charge of the Battery
SO_2	Sulphur dioxides
UHC	Unburned hydrocarbons
WT	Wind Turbine

Abstract

Communication services have faced several challenges to provide consistent mobile network service at remote locations where reliable power supply is not available. This paper presents the solution to utilizing a hybrid of wind and photovoltaic (PV) solar power system with a backup battery to provide feasible and reliable electric power for a specific remote mobile base station located at East Bale Zone, Ethiopia. All the necessary configuration, simulation, and techno economic evaluation carried out using Hybrid Optimization Model for Electric Renewable (HOMER Pro) software. The best optimal system configurations namely PV/Battery and wind/PV/Battery hybrid systems compared with the conventional stand-alone dual diesel generator (DG) system. Findings indicated that PV/Battery hybrid system is the most economically viable option with a total cost of $190,340.00 for the whole system project life time, i.e. 25 years and for the dual diesel generator system the total cost is $3,422,719 for the whole system project life time. And the levelized cost of energy (COE) for both systems is $0.374/kWh and $8.454/kWh respectively. This implies the hybrid system saves $3,232,379.00 in terms of NPC and $8.08/kWh in terms of COE and have 9,636kwh/year electric production benefit to the network operator. Also, simulation results show that the renewable energy source based hybrid energy system can decrease amount of air pollutants as compared to the conventional dual diesel generator only configuration by reduction of 40,102kg/year of CO_2, 99 kg/year of CO, 11 kg/year of UHC, 7.46 kg/year of PM, 80.5kg/year of SO_2, and 883 kg/year of NO_2 observed and saves about 29,200 liters of fuel per site per annual to the network operator. So that, it helps telecom to provide reliable network service and reduce fuel consumption, transportation cost & CO_2 emissions through proper power solution analysis using this Result.

Key words: *Hybrid optimization; Base Transceiver Station (BTSs); Hybrid renewable energy.*

CHAPTER ONE
INTRODUCTION

1.1 Introduction

Telecommunication is one of the sectors where the continuous growth in demand for mobile services and the parallel technological development goes hand in hand with regards to energy consumption; it suffices to think that information and communications technology (ICT) is accountable for consumption of about 3% of the world's total electrical energy. By the end of 2030, it is expected that this figure will grow to 1,700 TWh [1]. Telecommunication networks have changed the way people live, work and think. Since many people around the world are connected by telecommunication networks, the challenges to provide reliable and cost effective power solutions to these expanding networks is indispensable for telecom operators. There are various renewable energy sources such as solar energy, wind energy, fuel cells, biodiesel and so on for telecommunication applications. The implementation of renewable energy technologies, such as a stand-alone wind, PV, or wind-solar hybrid systems, to meet energy demands is on a steady increase since resources are naturally available, free, inexhaustible and pollution free. However, the reliability of these renewable sources of power supply poses a challenge since resources availability is seasonal. Hence, hybrid energy systems, improved stand-alone and grid-connected systems in some cases are being developed; incorporating advanced energy storage in order to increase power generation rates, improve reliability and consistency of power supply and to provide secure power supply to the end user. Therefore, the stand-alone systems are recommended especially for off-grid locations. Wind and solar energy sources are the cheapest available natural resources for renewable energy and they best complement each other seasonal alternations and with incorporated energy storage system (such as a battery storage system) to supply energy in case of shortfall by the wind/solar hybrid system as a result of fluctuating weather conditions.

Ethio telecom is an integrated telecommunication solutions provider operating in Ethiopia. It provides various telecommunication services as Global System for Mobile Communication (GSM), Code Division Multiple Access (CDMA) and Public Switch Telephone Network (PSTN) services. Recently, it deployed Third Generation (3G), Evolution Data Optimized (EVDO), 4G (Long Term Evolution), Next Generation Network (NGN) and Optical Network Unit (ONU) based network services. All these telecommunication stations at different location required efficient design and reliable power network. The electric power infrastructure is playing a negative role in the growth of mobile telecommunications in terms of network coverage and great impact on the operation cost of running the system due to non-availability of grid power supply. Due to this there is very limited or no coverage of mobile network for the rural population. Conventional diesel generators with backup battery are used for powering these mobile tower sites (BTS). These off-grid systems, usually located in areas with difficult accessibilities require regular maintenance and are characterized by their high fuel consumption and high transportation and operational cost [3,4]. Also, due to the increasing demand of clean energy technology to reduce the greenhouse gas emission pressure telecom companies for alternative solutions for powering these sites is needed. Therefore, in order to meet the continuous typical load demand of a mobile base station during varying atmospheric conditions, different energy sources need to be integrated for extended usage of alternative energy. This will create a large demand for off-grid power supply in rural areas which renewable energy is best suited to realize Ethio-telecom tower site with renewable energy technologies. Solar and wind are available freely and thus appears to be a promising technology to provide reliable power supplies in the remote areas and telecom industry of Ethiopia. The thesis aims to analyze design and analysis of a stand-alone hybrid renewable energy system for selected SER telecom Base Transceiver Station (BTS), so that can generate and provide cost effective electric power to meet the BTS electric load requirement.

1.2 Statement of the problem

There is a clear challenge to provide reliable cellular mobile service at remote locations where a reliable power supply is not available. Extending the grid connection to power off-grid BS sites is not economically attractive due to high transmission cost & have geographical limitations. And, the idea of using diesel generators as a primary power supply has become less favorable because of the challenges linked to their high operational and maintenance (O&M) cost, replacement costs, fuel transportation cost and significant environmental impacts.

The study areas have been under south east region Ethio-Telecom among 581 base transceiver stations 312 BTS sites use diesel generator as primary source, means 1.1M liter fuel required per year for power generation.

1.3 Objectives

- General Objectives

The main objective of this thesis is to study the design and analysis of a stand-alone renewable hybrid power system for sixteen selected rural telecom Base Transceiver Station sites in East Bale, Ethiopia using the hybrid optimization model for electric renewables (HOMER Pro) software.

- Specific objective

The specific objectives of this thesis are to: -

- Select study sites and components specifications depending on the energy demand.
- Study the renewable (solar and wind) energy potential of the study area.
- Determine the energy demand of the 16 telecom base station in East Bale zone.
- Develop modeling analysis and simulation using the hybrid optimization model for electric renewables (HOMER Pro) software.
- Compare Optimization result of renewable hybrid system with respect to a conventional dual DG/Battery powered solution.
- Plot conclusion and recommendations from the obtained result.

1.4 Significance of the thesis

SER Telecom base stations require about $1.5million per year for backup diesel generators operation. Renewable energy could contribute significantly to the reduction of this energy cost if properly integrated into the BTS energy sources. Hybrid Power Systems (HPSs) have been described above as among the popular cost-saving renewable energy applications in the telecommunications industry. But till date, these systems (HPSs) which have wind energy have not found in Ethiopia for telecom equipment powering application. This may be attributed to the lack of information on the necessary site and system parameters required to design suitable HPSs to meet given loads of BTS sites. The Model couldn’t be obtained experimentally or practically, because of the cost.

The thesis designed and analyzed to explore the HPS potentials for powering South east region sixteen selected telecom sites in east Bale zone of Ethiopia. Therefore, maintaining a stable power supply is a very significant concern for solving the above mentioned issue and from this both Ethio-telecom and end users are beneficiary.

Some of the benefits from this thesis work to Ethio Telecom are:

• Reduction of frequent power interruption.

• Reduction of cost for power generation

• Provide reliable mobile network service.

• Improve high revenue generation.

• Bring about customer satisfaction.

Benefits to end users are:

- Protected environment from CO_2 emission.
- Sustainable network service.

1.5 Scope of the study

This thesis covers, design and analysis on sixteen selected off-grid remote telecom base station (BTS) sites which required 9.4kw(111kwh/day) at various geographical locations and climatic conditions in east Bale zone of Ethiopia.

These locations include: Ginnir, Raytu , Sawina ,Oda Sofumer and Gasera were selected to reflect the various climatic conditions in East Bale zone Ethiopia. The controller used for the hybrid optimization model for electric renewables (HOMER Pro) software & other components developed to optimized telecom power system on the study.

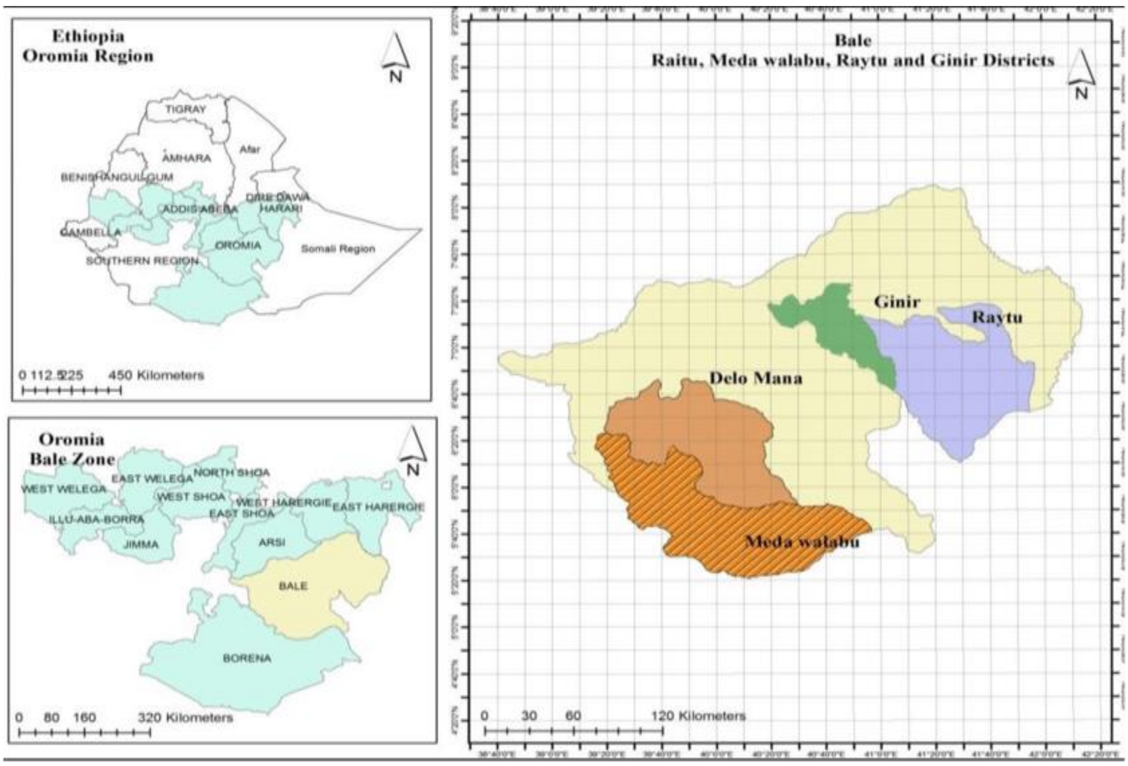

Figure 1.1: Location of the study area[33]

1.6 Organization of the Thesis

This thesis is organized into six chapters:

Chapter one presents the introduction (background), statement of the problem, general and specific objectives, significant of the study, scope of the study has been discussed in the thesis work. In addition, it provides the outline of the thesis.

Chapter two contains exhaustive theoretical background and literature review of the study topics mainly on renewable hybrid energy system in general.

In Chapter three methodology and approaches of the study, data collecting and data analysis methods has been also explained.

Chapter four presents Hybrid system simulation and optimization using HOMER Pro with a detailed description of existing study area.

Chapter five presents result and discussion on the analysis. At last, the sixth chapter brings to an end of this research with results of the thesis, conclusions and recommendations.

CHAPTER TWO

LITERATURE REVIEW

2.1 Background of the study areas

The sun is the largest energy source of life at the same time it is the ultimate source of all energy (except tidal and geothermal power), even the energy in the fossil fuels ultimately comes from the sun. The sun radiates 174 trillion kWh of energy to the earth per hour. In other words, the earth receives 1.74 x 10^{17} watts of power from the sun [14]. The sun is a typical star with mass 2×1030 kg, beam length 700,000 km and it has roughly 5 billion more years of life. Its surface temperature is about 5800 Kelvin while the internal temperature is approximately 15 million Kelvin.

This temperature derives from reactions which were based on the transformation of hydrogen to helium, the process called nuclear fusion, which produces high temperature of the sun and the continuous emission of large amounts of energy. It is calculated that for each gram of hydrogen that is converted to helium sun radiates energy equal to 1.67×10^{5} kWh. The solar energy is emitted to the universe mainly by electromagnetic radiation. Approximately one-third of energy radiated from sun is reflected back. The rest is absorbed and retransmitted to the space while the earth reradiates just as energy as it receives and creates a stable energy balance at a temperature suitable for life.

Photovoltaic (PV) is a method of generating electrical power by converting solar radiation into direct current electricity using semiconductors that exhibit the photovoltaic effect. PV power generation uses solar panels comprising a number of cells containing a semi-conducting material. As long as light is shining on the solar cell, it generates electrical power. When the light stops, the electricity stops. Many PV have been in continuous outdoor operation on Earth or space for over 30 years [15].

2.1.1 General overview of Base Transceiver Station (BTS)

The Base Transceiver station is a term used to denote a base station in GSM terminology. A BTS consists of an antenna and the radio equipment necessary to communicate by radio with a Mobile Stations(MS). Each BTS covers a defined area, known as a cell. A BTS is under control of a Base Station Controller which is in turn under control of a MSC (Mobile switching center).

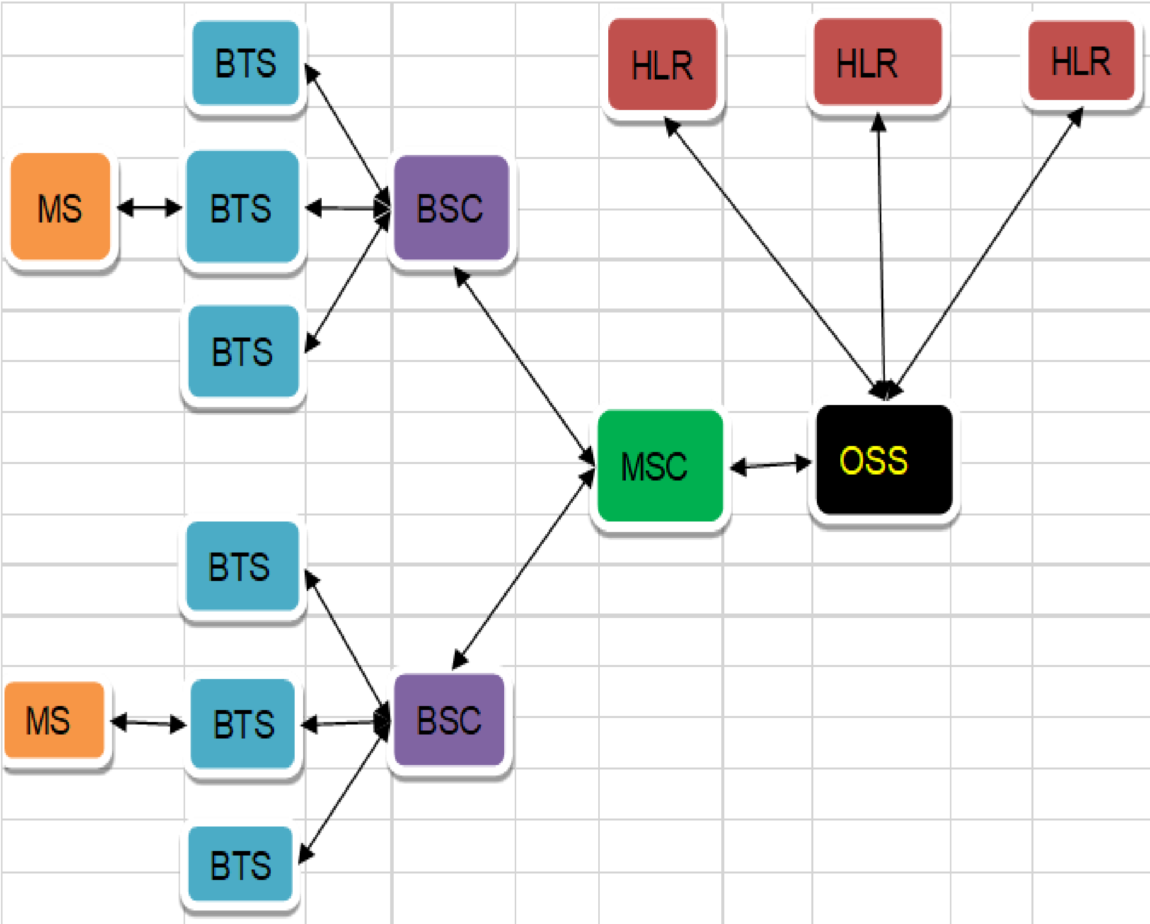

Figure 2.1: GSM Architecture

The Base Station Controller (BSC) is in control of and supervises a number of Base Transceiver Stations (BTS)The BSC is responsible for the allocation of radio resources to a mobile call and for the handovers that are made between base stations under his control. The Mobile Switching Centre (MSC) is a telephone exchange that makes the connection between mobile users within the network, from mobile users to the public switched telephone network and from mobile users to other mobile networks.

The MSC also administers handovers to neighboring base stations, keeps a record of the location of the mobile subscribers, mobile registration, authentication, call routing to roaming subscribers, is responsible for subscriber services and billing.

Figure 2.2: Cellular base station

A cellular base station is a wireless system and makes use of microwave radio communication technology. The base station acts as an interface between either two mobile phones or between a mobile phone and a fixed phone. Generally, these base stations are made up of several antennas mounted on a metallic tower and a house of electronics at the base of the tower. The antennas are connected to the base with cables. The base station antennas are used for transmitting as well as receiving the radio signals to and from mobile phones. Generally, these antennas are mounted on the top of the tower so that obstacles such as trees, high rise buildings, hills, etc. should not obstruct the radio signals.

Usually, three antennas are mounted on the top of the tower to cover the specified region. Among three antennas, two are used for receiving and one is for transmitting. Though these antennas operate at different frequencies they are well separated from each other to avoid interference of emitted power from each other. At the bottom of the tower a small house of electronic circuits comprising of power amplifiers, used to generate strong signals and these power amplifiers are connected to mounted antennas with long cables. The base station also has supporting components such as base station controllers using computers and AC/DC rectifiers to convert AC power to DC power.

Many base stations have a DC power back up system in the form of batteries connected either in series or parallel and these batteries supply power to the base station during mains power outage. The area covered by base station signals is called cell [5]. Based on the amount of area covered the base stations can be classified as a Macro cell base station, Micro cell base station, Pico cell station and Femto cell base station. Femto cells cover the smallest area and they are deployed in a room. Pico cells are deployed in offices or shopping malls and they cover more area than Femto cells. Micro cells can cover blocks of buildings in an urban locality and cover area more than pique cells. Macro cells cover the largest area among all the cells and generally they are deployed in rural areas or on highways.

Regarding the typology, the characteristics of different BSs are indicated below [5]:

- Shelter: cabinets made of aluminum and polyurethane foam containing the transmission equipment (housed in special boxes), air conditioning system and all that is needed for the correct functioning of the BS.
- Room: buildings containing the same equipment as a shelter.
- Outdoor: the transmission equipment neither any kind of shelter nor air conditioning systems are present. But uses heat exchanger.

The cooling of indoor air is required in the room or shelter and outdoor cabinet, because of the high temperatures of the indoor environment; this is due to the large amount of heat dissipated by the transmission systems and solar radiations falling on the cabinet.

The methodologies usually used to decrease the temperature inside the shelter can be identified as:

- Free cooling: cooling system that utilizes an atmospheric air temperature to lower the temperature inside the structure: the air enters the room from the outside through a vent.
- Air conditioner: In the case study, for both types of BS (shelter, room), the free cooling system and the air conditioner are located on the same machine and are ON / OFF type.

When free cooling is turned on, an extractor is activated, which stops the enclosure from over pressuring. The on/off of the air conditioner and free cooling is controlled by a PLC (Programmable Logic Controller), with preset “ON” thresholds and associated hysteresis values. The latter represents the temperature drop needed (after reaching the “ON “threshold) so that the cooling machine turns itself off.

2.1.2 Energy Costs in Telecommunication Industries

Energy costs are one of the largest operating expenses for telecommunication network operators. Energy costs account for more than half of the mobile operators' operating expenses and about 65% of this is for the tower site equipment [7]. As an ever-increasing number of people around the world become connected by fixed and mobile telecommunications networks, the challenges related to providing electricity to these expanding networks are becoming greater as well. Telecommunication networks are still driven largely by fossil fuel energy and the energy costs represent a significant
OPEX item. Engr. Eyo Ita advanced that global system for mobile communication (GSM) operators had spent over N500,000 (five hundred thousand naira) on diesel generators per year in each of their base stations with costs being transferred to subscribers in terms of billing [8].

Mobile network operator SER Ethio-Telecom in Ethiopia were powering over 300 Base Transceiver Stations by diesel generators, which consume about 1.1million liters of diesel fuel yearly. This means that the operators will require a minimum of 20.5million ETB (475,600USD) to power their cell sites across the country with the potential for the figure to increase if they add new base stations.

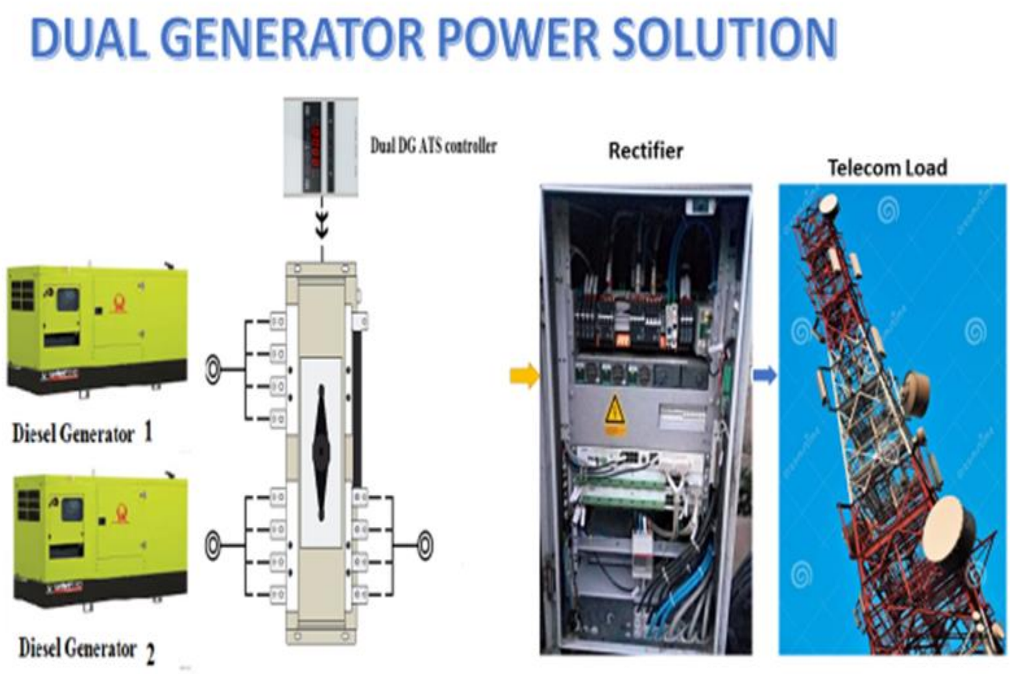

Figure 2.3: Dual Diesel Generator power solution lay out

2.1.3 Environmental Impact and Greenhouse Gas Emissions

The world is experiencing many environmental issues related to usage of fossil fuel. The major environmental impact of diesel generators is constant CO_2 emissions during service life. A diesel generator used to power a BTS consumes about 18,000 liters of fuel per year Carbon Dioxide (CO_2) emission from one liter of diesel fuel is 2.68kg. This emits 46.5 metric tons of CO_2 annually [12].

Hence, contributing to global greenhouse gas (GHG) emissions (CO_2, NO_2, and SO_2). For these reasons, from research and developments, recommended alternative energy sources have been renewable energy [9 - 18]. Utilization of renewable energy is an effective way to solve the energy crisis and environmental pollution problems [9].

To that end, alternative energy sources for wireless base stations consist of eco-efficient solutions that employ cost-effective, reliable and sustainable methods of power generation for both on- and off- the- grid locations. Renewable energy solutions have positive environmental effects.

2.1.4 Energy Consumption & system voltage of telecom BTS Site

The power needed for the radio base station depends on the number of calls at that time. For different region's traffic is different. During night time signal traffic is low when compared to day time. So it is difficult to find an actual power needed for the base station. The power needed for the radio base station varies between 800W to 3200W [6]. The average power for the whole year is 1400W for a Macro base station. The equivalent average power in MWh per year for a macro base station can be computed as 12.3 MWh.

If the site container contains more than one cabinet, then the power needed may be more. As in RBS (radio base station) there are air conditioner and heat exchanger, electronics also present. So the power is used by all the components. The highest amount of power needed for the by macro RBS IS 3200W.Micro base station needs 110W. If mini link is there the power is 150W. RBS and electrical exchanges are connected by mini link [6].

Although other voltages are possible, most radio transceiver loads used in telecom base stations run on a -48V DC bus. This practice originated in the early days of telephony, when 48V DC was found to be suitably high for long telephone lines, but low enough to prevent serious injury from touching the telephone wires. Consequently, most electrical safety regulations consider DC voltage lower than 50V to be a safe low-voltage circuit. It is also practical, because this voltage is easily supplied from the standard valve regulated lead acid (VRLA) batteries by connecting four 12V batteries in series, making it a simple system. The positive grounded or -48V system is another survivor from earlier industry practice. The negative voltage on the line was found to be superior to positive voltage in preventing electrochemical reactions from destroying copper cables if they happen to get wet. Negative voltage also protects against Sulphation on battery terminals. Sulphation, the buildup of crystals of lead sulfate, is the leading cause of early battery failure [7].

The intermittent nature of the solar and wind energy under varying climatic conditions requires a feasibility assessment and optimal sizing of hybrid solar and wind energy system. Without proper technical and financial feasibility study, the hybrid alternative energy systems previously installed in the remote areas showed a poor efficient design.

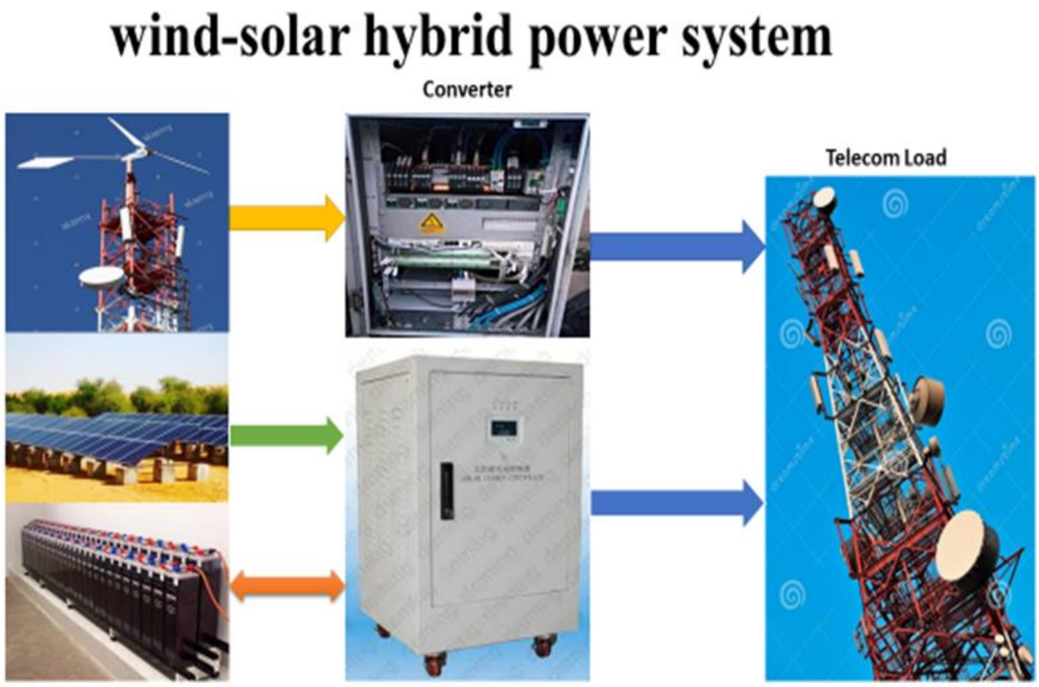

Figure 2.4: Wind-solar hybrid power system layout

The proposed energy system should meet the load demand of the site. The main renewable sources of energy considered in this thesis are solar and wind with Battery. The converter (rectifier or invertor) is added to maintain the flow of energy between the AC and DC components, the controller control DC power from PV array, where as the battery is employed as energy storage systems in order to ensure uninterrupted power and to maintain the desired power quality at the load point because of unpredictable variation in the climatic condition affect nature of the renewable sources. Hybrid model of these two energy sources in parallel with battery storage make the hybrid power system more reliable, efficient and provides a smooth and uninterrupted power supply.

2.1.5 Working Principle of Photovoltaic Cells

PV cells convert sunlight directly into electricity by taking advantage of the photoelectric effect. Cells are constructed from semiconductor materials coated with light-absorbing materials. When photons in sunlight strike the top layer of a PV cell, they provide sufficient energy to knock electrons through the semiconductor to the bottom layer, causing a separation of electric charges on the top and bottom of the solar cell. Connecting the bottom layer to the top with a conductor completes an electrical circuit and allows the electrons to flow back to the top, creating an electric current and enabling the cycle to repeat with more sunlight (Clean Energy Associates). Figure 2.5 illustrates how photovoltaic cells work.

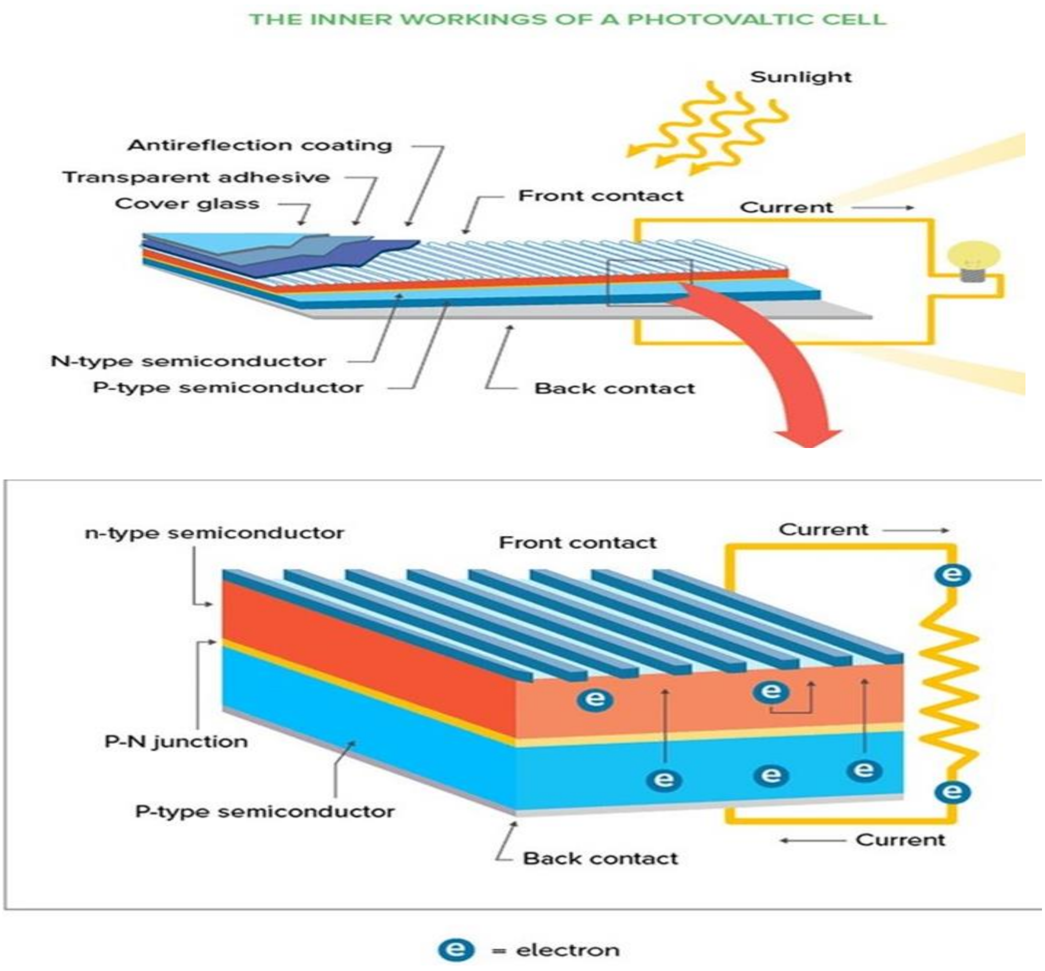

Figure 2.5: Inner workings of photovoltaic cell [19]

The solar cells that are used on calculators and satellites are photovoltaic cells or modules. This PV module consists of many PV cells wired in parallel order to increase current and in series to produce a higher voltage. When we speak of a PV panel it means any number of PV modules and when we speak of array it means any number of PV panels. Individual PV cells are typically only a few inches in diameter, but multiple cells can be connected to one another in modules, modules can be connected in arrays, and arrays can be connected in very large systems.

Therefore, PV panel convert sunlight to DC electricity. The PV generated electricity is „‟silent‟, low in maintenance and does not need in fuel or oil supplies. However, PV energy is available when enough irradiance is accessible.

- Types of PV Cell

The material that is used widely in the industry for the production of photovoltaic cells is silicon. Based on the structure of the basic material from which they are made and the particular way of their preparation the photovoltaic cells of silicon are categorized into three most common types. [9,12]

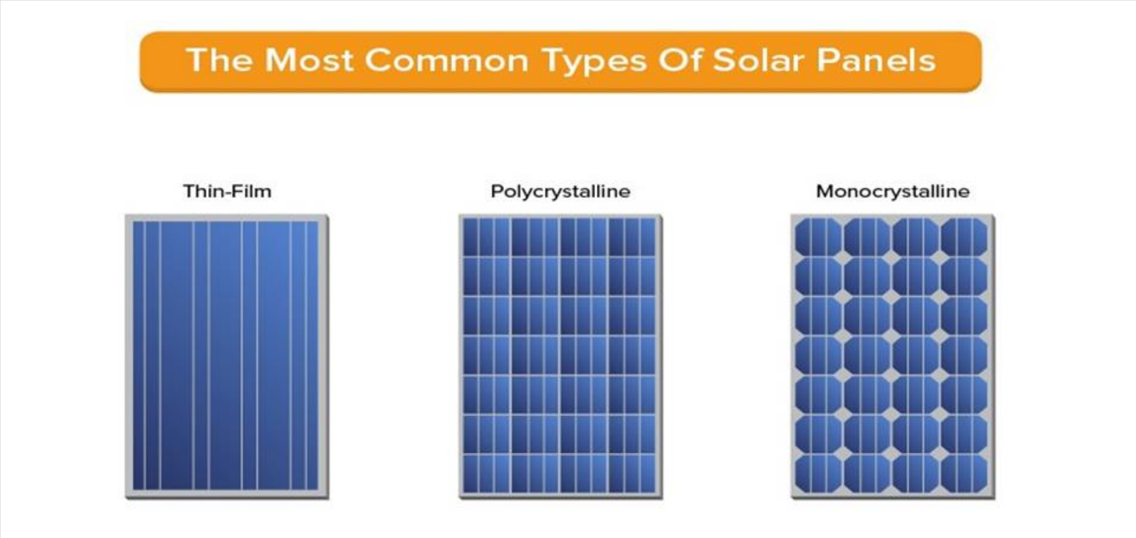

Thin-Film	Polycrystalline panels	Monocrystalline panels
▪ Versatility in usage	▪ Some times referred to us ”Multicrystaline” panels b/c they made up of multifaceted silicon crystals,	▪ One of the oldest & most reliable
▪ Low energy output	▪ Less silicon waste compared to single crystal panels	▪ PV modules are made from single silicon crystals, which are cut into wafers to create
▪ Can be physically flexible	▪ The most popular solar panel around the world	▪ Generally black or dark blue in coloring
▪ Between 8% and 10% energy conservation efficiency	▪ Has an efficiency of less than17%?	▪ Has an efficiency of 15% to 24%
▪ The pros include effectiveness in shaded areas, a uniform appearance and a low cost	▪ The pros of poly include cost effectiveness and a higher temperature co-efficiency.	▪ The pros of monocrystalline panel include longevity, heat resistance and more electricity
▪ The cons include requiring large amounts of space, a faster degradation, and a low energy output.	▪ The cons include less energy conversion and larger panels that tend to take up more space	▪ The cons include high starting costs and the fragility of the panels

Figure 2.6: Common types of solar panel[38]

Cells efficiency decreases with increase in temperature. Crystalline cells are more sensitive to heat than thin films cells. The output of a crystalline cell decreases approximately 0.5% with every increase of one degree Celsius in cell temperature. For this reason, modules should be kept as cool as possible, and in very hot condition amorphous silicon cells may be preferred because their output decreases by approximately 0.2% per degree Celsius increase [9, 12].

2.1.6 Equivalent Electrical Circuit of PV Cell

The complex physics of the PV cell can be represented by the equivalent electrical circuit shown in Figure 2.7 below. The following parameters call for consideration. The current I at the output terminals is equal to the light-generated current I_L, less the diode current I_D and the shunt leakage current I_{sh}. The series resistance R_s represents the internal resistance to the current flow, and depends on the p-n junction depth, impurities, and contact resistance. The shunt resistance R_{sh} is inversely related to the leakage current to the ground. In an ideal PV cell $R_s = 0$ and $R_{sh} = \infty$.

The PV conversion efficiency is sensitive to small variations in Rs, but insensitive to variations in R_{sh}. A small increase in Rs can decrease the PV output significantly.

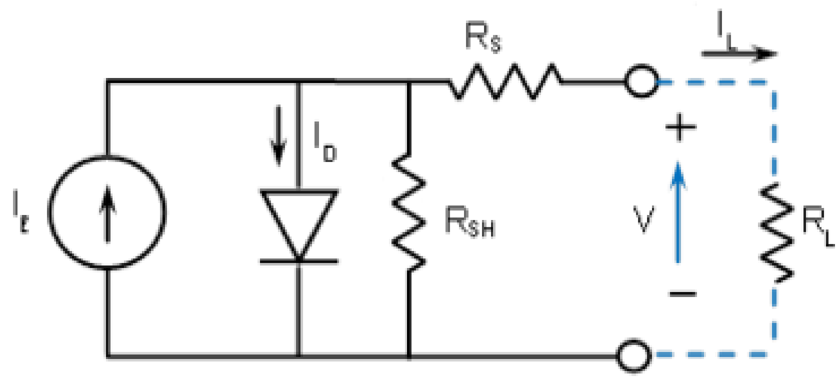

Figure 2.7: A PV cell equivalent electrical circuit [4]

The open-circuit voltage Voc of the cell is obtained when the load current is zero and is given by the following:

$$V_{oc} = (I_L - I_D)R_{sh} \quad (2.1)$$

The diode current is given by the classical diode current expression:

$$I_D = I_o[\exp[\frac{qV_{oc}}{AKT}]-1 \quad (2.2)$$

Where is the saturation current of the diode (A), q is electron charge (1.6×10^{-19} C), A is curve-fitting constant, K is Boltzmann constant (1.38×10^{-23} J/°K), T is temperature on absolute scale ^{o} K.

Thus, the load current is given by the expression:

$I=I_L-I_D-I_{sh}$

$$I = I_D - I_o[\exp\left[\frac{qV_{oc}}{AKT}\right] - \frac{V_{oc}}{R_{sh}}] \ldots\ldots\ldots\ldots\ldots\ldots\ldots\ldots\ldots\ldots \quad (2.3)$$

Where; I_{sh} is the leakage current to the ground. In practical cells, it is negligible compared to I_L and I_o is generally ignored.

The two most important figure of merits widely used for describing PV cell electrical performance are the open-circuit voltage V_{oc} and the short-circuit current I_{sc} under full illumination. The short-circuit current is measured by shorting the output terminals and measuring the terminal current. Ignoring the small diode and ground leakage currents under zero voltage, the short-circuit current under this condition is the photocurrent I_L. The maximum photo voltage is produced under the open-circuit voltage. Again by ignoring the ground leakage current, equation 2.4 with I give the open-circuit voltage as follows:

$$V_{oc} = \frac{AKT}{q}\ln(\frac{I_L}{I_o} + 1) \ldots\ldots\ldots\ldots\ldots\ldots\ldots\ldots\ldots\ldots \quad (2.4)$$

I-V and P-V Curves

The electrical characteristic of the PV cell is generally represented by the current vs voltage (IV) curve. The figure below (Figure 2.8) depicts the I-V curve of typical PV cell. This curve shows the variation of current and voltage when cell resistance varies from zero to infinity. In this curve the point at which the voltage is zero is called the short-circuit current. This is the current we would measure with output terminal shorted. On the other hand, the point at which current is zero is known as open-circuit voltage. This is the voltage we would measure with output terminal open. Somewhere in the middle of the two regions, the curve has a knee point.

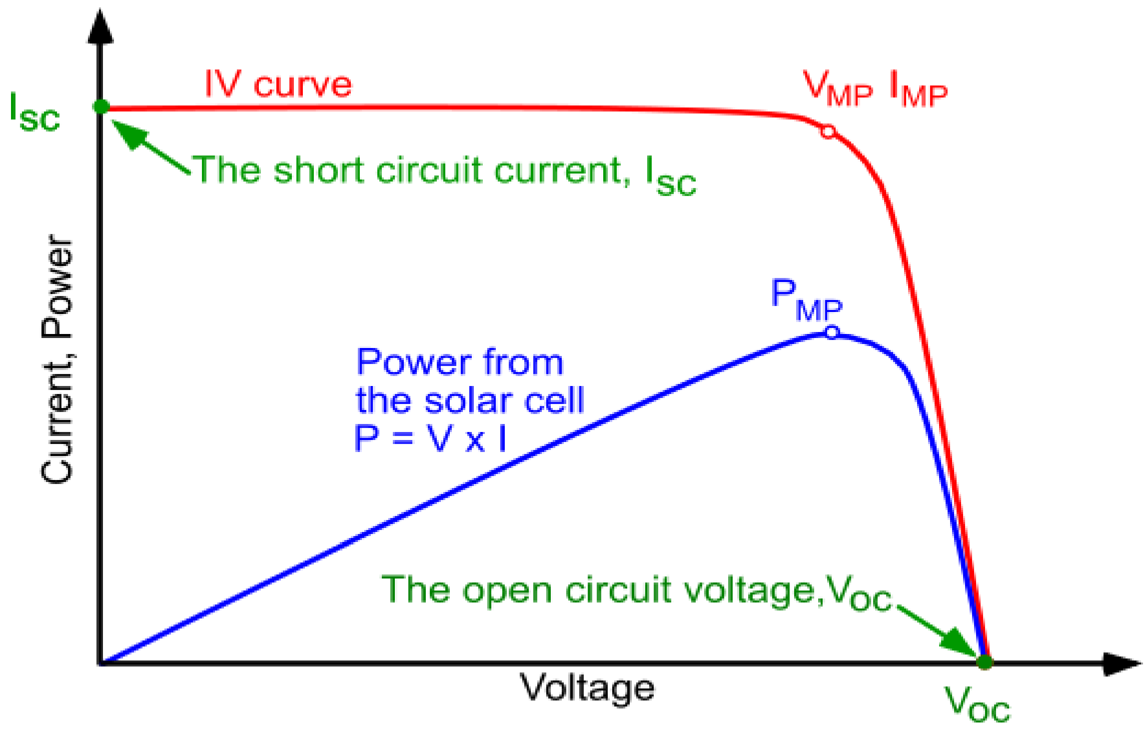

Figure 2.8: IV and PV curve of PV cell [4]

The power output of the panel is the product of the voltage and current outputs. In Figure 2.8, the power is plotted against the voltage which is P-V curve of the PV cell. Note that the cell produces no power at zero voltage or zero current, and produces the maximum power at the voltage corresponding to the knee point of the I-V curve. This is why the PV power circuit is always designed to operate close to the knee point with a slight slant on the left-hand side. The PV circuit is modeled approximately as a constant current source in the electrical analysis of the system.

Finally, in order to measure the photovoltaic cell output power, the following standard test conditions are established internationally. The irradiance level is 1000 W/m², with the reference air mass 1.5 solar spectral irradiance distributions and cell or module junction temperature of 25°C.

2.1.7 Solar Radiation Estimations

For any solar based system design, the most important factors are the position of the sun in the sky, the slope and orientation of a collecting surface, and obstruction and reflection properties of neighboring structures. Figure 2.9 shows the geometry describing orientation of a collector and position of the sun in the sky.

A point on the earth's surface is expressed by its latitude and longitude. The angle between the collector surface and the horizontal is called slope, β (with $0^0 < \beta < 90^0$) for a surface facing towards the equator; $90^0 < \beta < 180^0$ for a surface facing away from the equator). Surface azimuth angle, γ_s is the angle between the normal to the surface and the local longitude meridian, projected on the horizontal plane. In either hemisphere, γ_s equals 0^0 for a surface facing due south, 180^0 due north, 0^0 to 180^0 for a surface facing westward and 0^0 to -80^0eastward. For a horizontal surface, γ_s is always 0^0

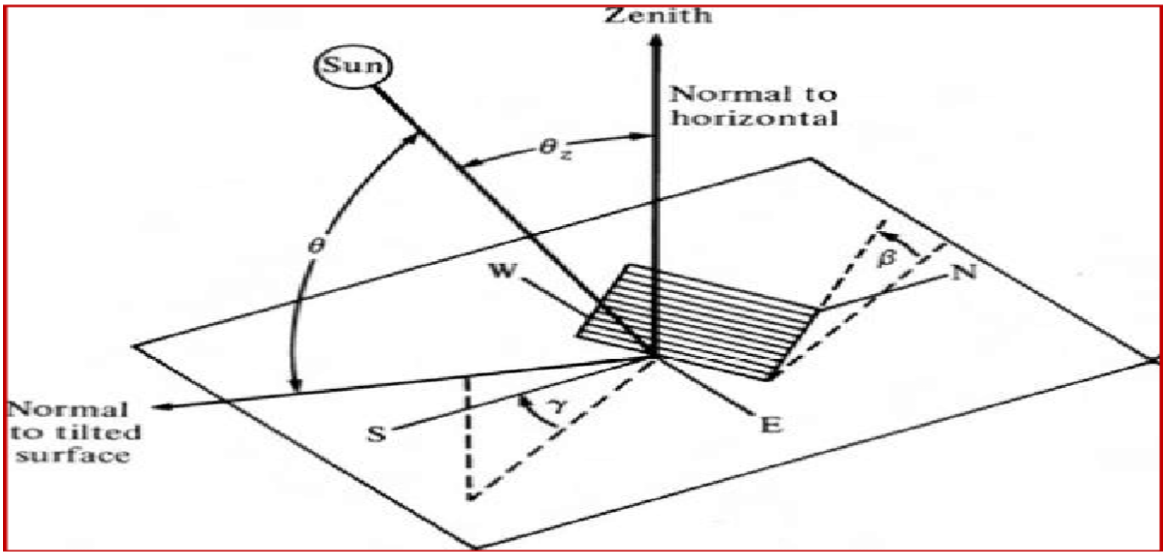

Figure 2.9: Geometry of solar collector and location of sun relative to earth [20]

Location of the sun in the sky, relative to a point on the ground, can be defined in terms of two angles, the solar altitude, (or its complement the solar zenith angle) and the solar azimuth α_s. Solar altitude, angle of solar beam to the horizontal. Solar azimuth α_s is the angle between the solar beam and the longitude meridian projected on the horizontal plane. Sign convention is the same as for surface azimuth angle (γ_s) , solar altitude and solar azimuth are functions of location (latitude, φ), time of the year (declination angle, δ) and time of the day (hour angle, ω). Solar declination angle (δ) is the angle between the earth's equatorial plane and the earth sun line. Solar hour angle ω is the angle Earth has rotated since solar noon. The relation between these angles is given below [20].

$$\delta = 23.45(\sin\frac{360(284+m)}{365}) \quad \ldots\ldots\ldots\ldots\ldots\ldots\ldots\ldots\ldots\ldots\ldots.. (2.5)$$

Where

δ = solar declination angle (^{o})

m = Day number of the year starting at January 1st as 1

$$\omega = (12 - t_L)\, 15^o \ldots\ldots\ldots\ldots\ldots\ldots\ldots\ldots\ldots \text{(2.6)}$$

Where t_L= local solar time in hours

ω= solar hour angle (^{o})

$$\sin\alpha_s = \sin\phi \sin\delta + \cos\phi \cos\delta \cos\omega \ldots\ldots\ldots\ldots\ldots\ldots \text{(2.7)}$$

Where α_s = solar altitude (^{o})

Φ= latitude (^{o})

$$\sin\gamma_s = \frac{\cos\delta \sin\omega}{\cos\alpha_s} \ldots\ldots\ldots\ldots\ldots\ldots\ldots\ldots \text{(2.8)}$$

Where, γ_s= solar azimuth (^{o})

The sunset/sunrise angle is given by:

$$\omega_s = \cos^{-1}(-\tan\emptyset \tan\delta) \ldots\ldots\ldots\ldots\ldots\ldots\ldots\ldots \text{(2.9)}$$

The angle of incident θ_i is the angle between the solar beam and normal to the solar panel which is given by:

$$\sin\theta_i = \sin\delta \sin\emptyset \cos\beta + \sin\delta \cos\emptyset \sin\beta \cos\gamma \cos\delta \cos\emptyset \cos\beta \cos\omega + \cos\delta \sin\emptyset \sin\beta \cos\gamma \cos\omega + \cos\delta \sin\beta \sin\gamma \sin\omega \ldots\ldots \text{(2.10)}$$

The intensity of solar radiation incident per unit area exposed normally to the sun's rays at the average sun-earth distance (about 1.5×10^{11} m), measured outside the earth's atmosphere is called the solar constant, G_{sc} (1367 W/m^2) [12].The intensity of radiation received outside the earth's atmosphere varies as the inverse square of the earth-sun distance and can be expressed in relation to time of the year. The extraterrestrial irradiance on a surface at normal incidence (G_{on}) may be expressed as:

$$G_{on} = G_{sc}[1 + 0.033 \cos\frac{2\pi m}{365}] \ldots\ldots\ldots\ldots\ldots\ldots\ldots\ldots \text{(2.11)}$$

Where m is the number of the day in the year with January 1strep resenting a value of 1 and December 31 a value of 365.

The extra-terrestrial irradiance incident on a horizontal plane at an arbitrary angle of incidence is also of interest and is given by,

$$G_o = G_{on} \cos\theta_z \text{...} (2.12)$$

Where θ_z=zenith angle (angle between the sun and the vertical line from a point on earth) which equals to the incident angle of a horizontal surface at the point of interest.

The whole daily extraterrestrial radiation, Ho from the sunrise to the sunset can be calculated as follows:

$$H_o = \frac{24+3600+G_{sc}}{\pi}(1+.33 * \cos\frac{360m}{365})(\cos\emptyset\cos\delta\sin\omega_s + \frac{\omega_s}{180}\sin\emptyset\sin\delta) \dots\dots\dots\dots\dots\dots\dots\dots\dots\dots\dots\dots\dots\dots\dots\dots\dots\dots\dots\dots (2.13)$$

Where, m = day number starting from January 1^{st} as 1.

Gsc = 1367W/m2

∅= latitude of the location (13^o)

δ= Declination angle (^{o})

ω_s=sunset hour angle

Ideally, the data required to predict the solar potential of any site are several years of measurements of irradiance on the proposed collector plane. These are rarely available, so the required data have to be estimated from meteorological data available either

(i) from the site, or

(ii) from some nearby site having similar irradiance,

(iii) from an official solar atlas or database [14].

Here, the sunshine duration data from the nearby station is used to estimate the monthly average solar radiation using the following angstrom type equation [18, 19,20].

$$\frac{H}{H_o} = a + b\frac{n}{N_s}\text{……………………………………………………} (2.14)$$

Where:

H = monthly average daily radiation on horizontal surface (MJ/m2)

H_o = monthly average daily extraterrestrial radiation on a horizontal surface (MJ/m2)

N_s = the maximum possible daily hours of bright sunshine given by equation

n = monthly average daily number of hours of bright sunshine a and b are regression coefficients having average value of a =0.3and b=0.5 [9].

The day length, Ns, is the maximum possible daily sunshine hour is given by the equation below.

$$N_s = \frac{2}{15}\omega_s\text{………………………………………………………} (2.15)$$

The following relation is used to get the value of Ho and H in kWh (to convert MJ to kWh).

1J = 2.777778*10-7kWh or

1MJ = 277.78Wh …………………………………..……… (2.16)

2.2 Wind Energy System

Winds are produced by uneven solar heating of the earth's land and sea surfaces. Thus, they are a form of "solar" energy. On average, the ratio of total wind power to incident solar power is on the order of two present, reflecting a balance between input and dissipation by turbulence and drag on the surface. Wind is the movement of air caused by the irregular heating of the Earth's surface. It happens at all scales, from local breezes created by heating of land surfaces that lasts some minutes, to global winds caused from solar heating of the Earth. Wind power is the transformation of wind energy into more utile forms, typically electricity using wind turbines [3].

2.2.1 Types of Wind Turbines

A wind turbine is a machine that converts the kinetic energy from the wind into mechanical energy. If the mechanical energy is used directly by machinery, such as a pump or grinding stones, the machine is usually called a windmill. If the mechanical energy is then converted to electricity, the machine is called a wind generator [3]. There are a number of different

wind turbine types available. The horizontal axis turbine, HAWT is by far the most common type of turbine. They come in two different types: the upwind, which face the wind (tower behind rotor) and the downwind arrangement that works away from the wind (tower in front).
Another kind of turbine is the vertical axis, VAWT arrangement that uses drag and lift as the driving forces; the horizontal also uses drag and lift, but in other proportions. The advantages with upwind turbines are that the tower does not act as an obstacle for the wind hitting the rotor. Despite this, the flow behind the passing blade is affected by the tower and causes a slight drop in power. When the blade passes the tower it also decreases the drag on the construction which can cause an on/off bending process causing fatigue stress. This has of course been taking into account when designing the turbine. The upwind design needs a control system that helps the nacelle turn straight to the wind.

In downwind turbines, the tower shades a rotor blade each time it passes by and causes greater power losses compared to the upwind design. An advantage with downwind turbines is that the nacelle is self-adjusting and is not in need of a control system. One drawback with this is the problem with untwisting the cable inside when the nacelle has turned same direction repeatedly.

The VAWT´s are not as commercial and economically competitive as the HAWT´s. Some of the VAWT types suffer from low efficiency due to design difficulties as well as the problem with operation close to the ground. Parts of the vertical turbines will therefore receive low quality winds causing power losses. To keep the construction upright it also needs to be supported with guy cables attached to the ground. The vertical turbine is not in need of yaw control, which of course is an advantage and the wind always hits the turbine tangentially [33]. The modern wind turbine is a sophisticated piece of machinery with aerodynamically designed rotor and efficient power generation, transmission and regulation components. The size of these turbines ranges from a few Watts (Small Wind Turbines) to several Million Watts (Large Wind Turbines). The modern trend in the wind industry is to go for bigger units of several MW capacities in places where the wind is favorable, as the system scaling up can reduce the unit cost of wind-generated electricity. Most of today's commercial machines are horizontal axis wind turbines (HAWT) with three bladed rotors.

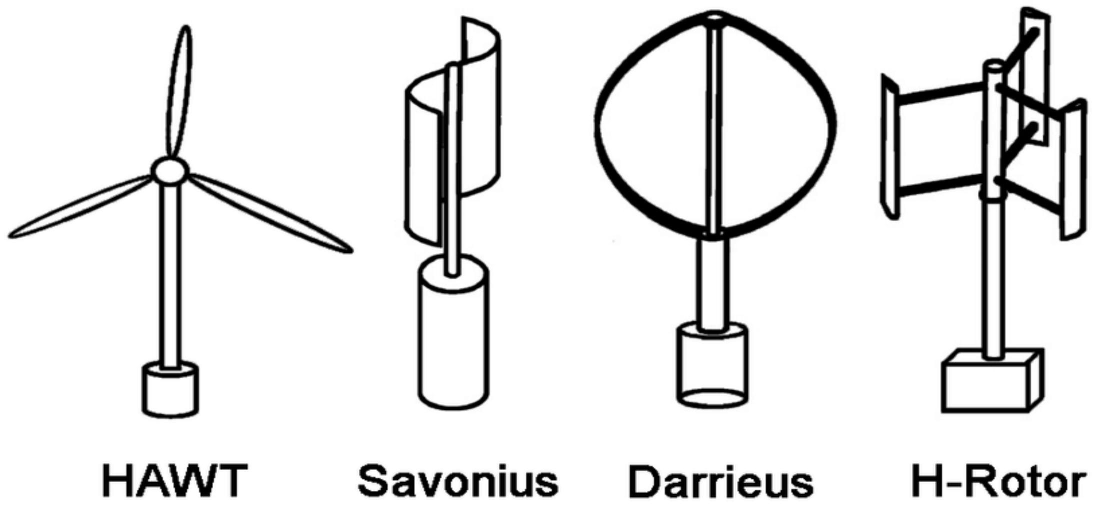

Figure 2.10: Type of wind turbines [14]

Horizontal axis wind turbines (HAWT) are either upwind machine or down wind machines. Vertical axis wind turbines (VAWT=Darrieus) which accept wind from any direction [14].

- **Wind Turbine Components**

The most common turbine type is the horizontal axis wind turbine. A cut-view (Figure 2.11) helps the reader to get familiar with the components of a wind turbine.

- **Anemometer:**

Measures the wind speed and transmits wind speed data to the controller.

- **Hub:**

Hub is the connection point for the rotor blades and the low speed shaft.

- **Gear box:**

Gears connect the low-speed shaft to the high-speed shaft and increase the rotational speeds from about 30 to 60 rotations per minute (rpm) to about 1200 to 1500 rpm, the rotational speed required by most generators to produce electricity. The gear box is a costly (and heavy) part of the wind turbine and engineers are exploring "direct-drive" generators that operate at lower rotational speeds and don't need gear boxes specially for small scale wind turbines.

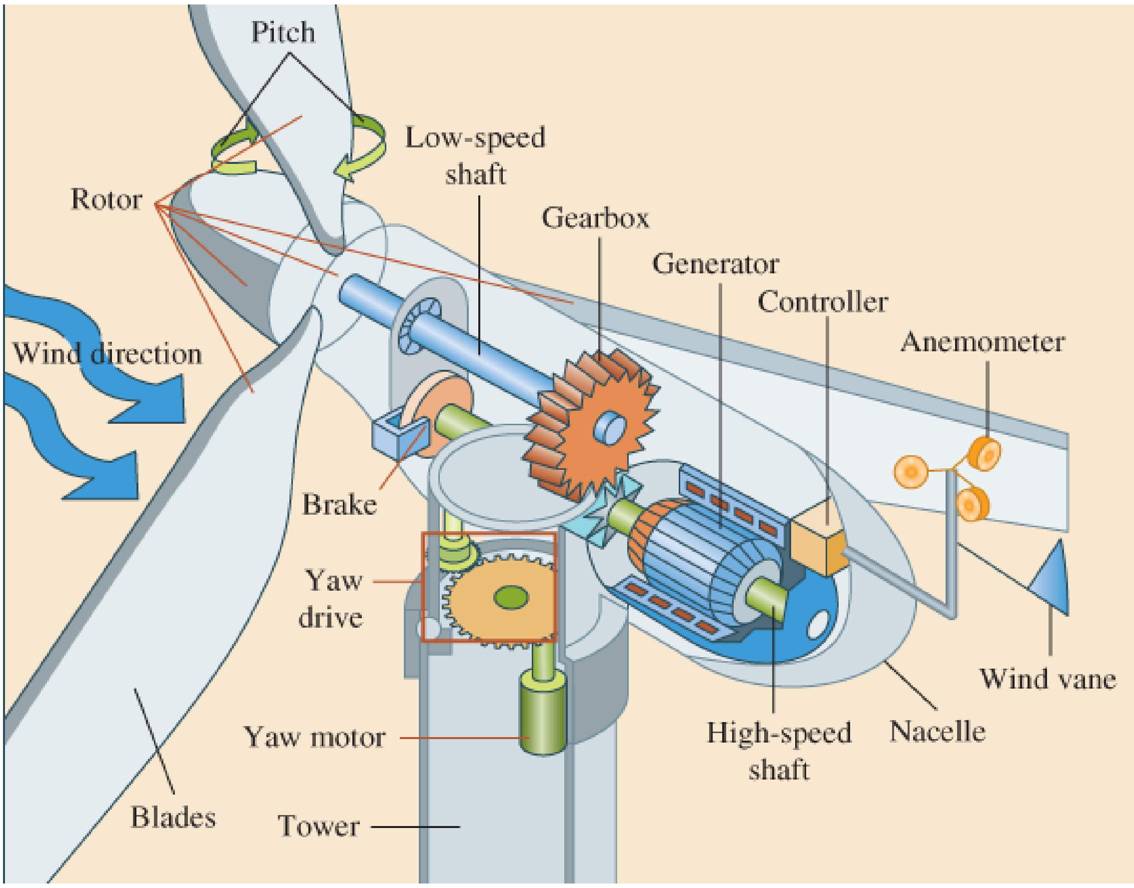

Figure 2.11: Cut-View Wind Turbine [29]

- **Generator:**

The generator is connected to the high-speed shaft and is the component of the system that converts the rotational energy of the shaft into an electrical output.

- **Tower of wind power generation:**

  The tower is used to support the nacelle and rotor blades and typically made of rolled, tubular steel, and built and shipped in sections because of its size and weight. Common tubular towers incorporate a ladder within the hollow structure to provide maintenance access. Small -scale towers range in height from 24-35m and its weight depends on the material from where it is manufactured.

- **Nacelle:** The rotor attaches to the nacelle, which sits at top of the tower and includes the gear box, low and high-speed shafts, generator, controller, and brake. A cover protects the components inside the nacelle. Some nacelles are large enough for a technician to stand inside while working rotor in emergencies.

- **Controller:**

The controller starts up the machine at wind speeds of about 3.5 to 7.2 meters per sec (m/s) and shuts off the machine at about 30 m/s.

- **High-speed shaft:** Drives the generator.
- **Low-speed shaft:**

The rotor turns the low-speed shaft at about 30 to 60 RPM. Pitch: Blades are turned, or pitched, out of the wind to keep the rotor from turning in winds that are too high or too low to produce electricity.

Rotor: The blades and the hub together are called the rotor.

- **Tower:**

Towers are made from tubular steel or steel lattice. Because wind speed increases with height, taller towers enable turbines to capture more energy and generate more electricity.

- **Yaw drive:**

Upwind turbines face into the wind; the yaw drive is used to keep the rotor facing into the wind as the wind direction changes. Downwind turbines don't require a yaw drive; the wind blows the rotor down wind.

- **Yaw motor:** Powers the yaw drive.
- **Electronic equipment:** Such as controls, electrical cables, ground support equipment and interconnection equipment.

2.2.2 Working Principles of Wind Turbines

The blade, using aerodynamic lift, capture energy from wind in order to turn the shaft. In small wind turbines the shaft, usually drives the generator directly. The generator converts the mechanical energy into electricity. The shaft power causes coils to spin past alternate poles of magnets, allowing an electric current to flow. If a permanent magnet device is being used the opposite occur: current flow as magnets spin past coil windings. Most small wind turbines use a permanent magnet alternator. Large wind turbines usually use either induction generator or a Synchronous generator. In addition, in large wind turbines the shaft connected to the generator via a gearbox those steps up the rotational speed or the generator.

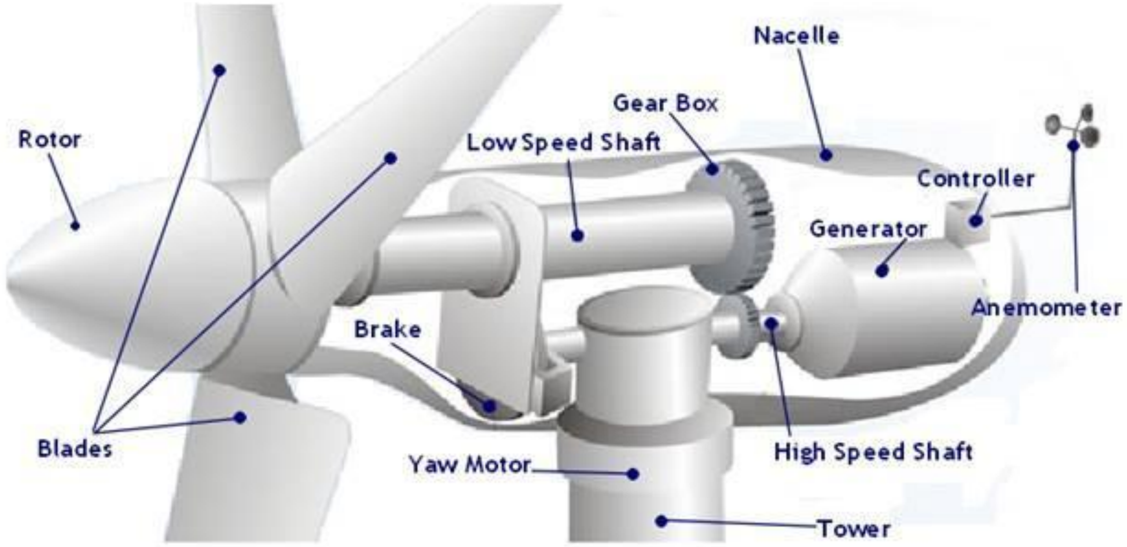

Figure 2.12: wind energy conversion system diagram [33]

2.2.3 Wind Energy Distribution & Extraction by HAWT

- Distribution of wind speed

The distribution of wind is expressed by Weibull distribution over a certain period of time at a particular site. The Weibull probability density function (PDF) is given by equation 2.17 [24].

$$f(u) = \frac{k}{c}\left(\frac{u}{c}\right)^{k-1}\exp\left(-\frac{u^k}{c}\right) \ldots \ldots \quad (2.17)$$

Where, u = the wind speed,

k = a constant known as shape factor, as the value of k increases the curve will have a sharper peak

c = a scale parameter in m/s; the larger the scale parameter, the more spread out the distribution.

The area under the curve is always unity. The power density can in this case be expressed by equation 2.18.

$$\frac{p}{A} = \frac{1}{2}\sum_{j=1}^{n} \rho V_j^3 f_j \ldots \ldots \quad (2.18)$$

Where, V_j is the median velocity in class j and f_j is the frequency of occurrence in the same class.

For k = 2 the Weibull PDF is commonly known as the Rayleigh density function in which case equation 2.17 may be rewritten as in equation 2.19.

$$\boldsymbol{f_u} = \frac{2u}{c^2}\,\mathbf{exp}\left[-\left(\frac{u}{c}\right)^2\right] \ldots\ldots\ldots\ldots\ldots\ldots\ldots\ldots\ldots\ldots\ldots\ldots\ldots\ldots\ldots\ldots\ldots\ldots\ldots\ldots.. (\mathbf{2.19})$$

- Wind Energy Extraction by HAWT

The energy of wind is extracted by using an appropriate wind turbine. The wind energy is tapped by the wind turbine which converts the kinetic energy of the wind into mechanical shaft energy. The rotational energy is converted into electrical energy through the transmission system. The transmission system consists of the rotor shaft with bearings, brake(s), an optional gearbox, as well as a generator and optional clutches.

The energy available in the wind can be expressed using equation 2.20.

$$p_w = \frac{1}{2}\rho A v^3 \ldots\ldots\ldots\ldots\ldots\ldots\ldots\ldots\ldots\ldots\ldots\ldots\ldots\ldots\ldots\ldots.\ldots\ldots (2.20)$$

Where, ρ =Density of air (kg/m3)

A = the swept area (m2)

Pw = power in the wind (W)

v =instantaneous wind velocity (m/s)

Energy conversion from free-flowing fluid streams is limited because full energy extraction implies a decrease of fluid velocity (decrease of kinetic energy of the stream), down to zero which is impossible. Some fluid may not pass through the turbine and may simply flow around it (bypass it). This limitation is expressed in terms of Betz limit defined by the power coefficient Cp as given by equation 2.21.

$$c_{p=}\frac{rotor\ power}{power\ in\ the\ wind} \ldots\ldots\ldots\ldots\ldots\ldots\ldots\ldots\ldots\ldots\ldots..\ldots\ldots\ldots\ldots\ldots (2.21)$$

The power coefficient, CP, is a function of the axial induction factor. The optimum of this function (which is a maximum value for CP) is 0.5926 (=16/27) [20,]. Thus the electrical power output from the wind turbine can be expressed by equation 2.22.

$$p_w out = \acute{\eta}_t C_p \frac{1}{2} \rho A v^3 \quad (2.22)$$

Where, Pw out = output power of wind turbine

$\acute{\eta}_t$ = Overall efficiency of the transmission system/power train

Cp = the power coefficient

The power coefficient and efficiency of wind turbines vary greatly from the manufactures to the manufacturers. As a result, the power output of wind turbines varies from turbine to turbine and is given by power curve, which plots the output power of a turbine against wind speed (see Figure 2.13).

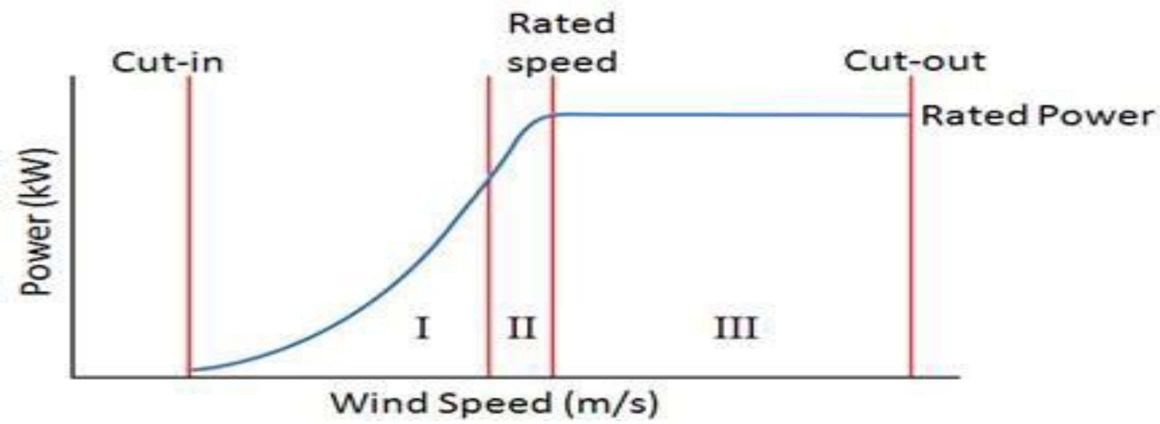

Figure 2.13: General power curve of wind turbine [20]

The wind speed at which a wind turbine starts generating electrical power is called the cut-in speed. The rated wind speed is the wind speed at which the turbine operates at its maximum efficiency of energy conversion. Rated power is the power output of the wind speed which is equal to, or above, the rated speed. The cut-out speed is the wind speed at which the turbine may shut down to protect the rotor and drive train machinery from damage, or high wind stalling characteristics.

2.2.4 Wind Turbines Power Control Mechanism

All wind turbines are designed with some sort of power control. There are different ways to control, aerodynamic forces on the turbine rotor and thus to limit the power in very high wind speeds in order to avoid damage to the turbine. There are three commonly used types of power control in the industry [27].

- Stall Control
- Pitch Control

- Active stall regulation

The simplest, most robust and cheapest control method is the stall control (also called passive control), where the blades are bolted onto the hub at a fixed angle. The fixed-blade pitch is chosen so that the turbine reaches its maximum or rated power at the desired wind speed. The design of the rotor aerodynamic causes the rotor to stall (lose power) when the wind speed exceeds a certain level which limits the aerodynamic power on the blades.

Another type of control is pitch control, where the blades can be turned out or into the wind as the power output becomes too high or too low, respectively. Generally, the advantages of this type of control are good power control, increased energy capture, assisted startup and emergency stop. The pitch change system has to act rapidly. From an electrical point of view, good power control means that at high wind speeds the mean value of the power output is kept close to the rated power of the generator. The extra complexity arising from the pitch mechanism and the higher power fluctuations at high wind speeds can be mentioned as the demerits of this control scheme.

The third possible control strategy is the active stall control, in which the stall of the blade is actively controlled by pitching the blades. At low wind speeds, the blades are pitched similar to a pitch-controlled wind turbine, in order to achieve maximum efficiency. At high wind speeds, the blades go into a deeper stall by being pitched slightly in the direction opposite to that of a pitch-controlled turbine. The active stall wind turbine achieves a smoother limited power, without high power fluctuations as in the case of pitch-controlled wind turbines. This control type has the advantage of being able to compensate variation in air density and inherits the advantages of both pitch and stall control mechanisms.

2.2.5 Wind Speed Measurement

The wind speed is measured with an instrument called an anemometer. These instruments come in several types. The most common type is a cup anemometer which has three or four cups attached to a rotating shaft. When the wind hits the anemometer, the cups and the shaft rotate. The angular speed of the spinning shaft is calibrated in terms of the linear speed of the wind.

Normally, the anemometer is fitted with a wind vane to detect the wind direction. A data logger collects wind speed and wind direction data from the anemometer and wind vane respectively. It is very important that the measuring equipment is set high enough to avoid turbulence created by trees, buildings or other obstructions. The readings would be most useful if they have been taken at hub height where the wind turbine is going to be installed [3].

If the measurement of wind speed was not made at the wind turbine hub height (in this case it is 10 m) it is important to adjust the measured wind speed to the hub height. This can be done using either the logarithmic law, which assumes that the wind speed is proportional to the logarithm of the height above ground, or the power law, which assumes that the wind speed varies exponentially with height. Using the logarithmic law, the wind speed at a certain height above ground level can be given as follows [3]:

$$\mathrm{V}(\mathrm{z}) * \ln\frac{z_r}{z_o} = V(z_r) * \ln\frac{z}{z_o} \qquad (2.23)$$

Where, Z_r = Reference height (m)

Z = Height where wind speed is to be determined (m)

Z_o = Measure of surface roughness (0.1 to 0.25 for crop land)

V (z) = Wind speed at the height of Z m (m/s)

V (Z_r) = Wind speed at the reference height (m/s)

Using power law, the wind speed at a certain height above ground level can be given as follows [24]:

$$V_2 = V_1 (\frac{h_2}{h_1})^a \qquad (2.24)$$

Where: V_1 is wind speed measured at the reference height h_1 (m/s),

V_2 is wind speed estimated at height h_2 (m/s), and

a is the ground surface friction coefficient.

Table 2-1: Friction coefficient a of various terrains[12]

Terrain Type	Friction coefficient α
lake, ocean, and smooth, hard ground	0.1
Foot – high grass on level ground	0.15
Tall crops, hedges, and shrubs	0.2
Wooded country with many trees	0.25
Small town with some trees and shrubs	0.3
City area with tall buildings	0.4

2.2.6 Factor affecting wind electricity production

The wind turbine electricity production can be depending on the following factors, namely wind speed, air density and area swept by the rotor blades. From the figure 2.13 clearly understand, that the above mention factor influencing the electricity production of the wind turbine [22].

➢**Wind speed**

The wind speed is divided into four category based on the operation of wind turbine.

• **Start-up Speed:** - This is the speed at which the rotor and blade assembly begins to rotate.

• **Cut-in Speed:** - Cut-in speed is the minimum wind speed at which the wind turbine will generate usable power. This wind speed is typically between 7mph and 10mphfor most turbines.

• **Rated Speed:** - The rated speed is the minimum wind speed at which the wind turbine will generate its designated rated power. Rated speed for most machines is in the range of 25 to 35 mph. At wind speeds between cut-in and rated, the power output from a wind turbine increases as the wind increases. The output of most machines levels off above the rated speed. Most manufacturers provide graphs, called "power curves," showing how their wind turbine output varies with the wind speed.

• **Cut-out Speed:** -At very high wind speeds, typically between 45 and 80 mph, most wind turbines cease power generation and shut down. The wind speed at which shuts down occurs is called the cut-out speed, or sometimes the furling speed. Having a cut-out speed is a safety feature which protects the wind turbine from damage.

➢Air density

The denser the air, the more energy received by the turbine. Air density varies with elevation and temperature. Air is less dense at higher elevations than at sea level, and warm air is less dense than cold air. All else being equal, turbines will produce more power at lower elevations and in locations with cooler average temperatures. Air density has a significant effect on wind turbine performance. The power available in the wind is directly proportional to air density. As air density increases the available power also increases. Air density is a function of air pressure and temperature. It increases when air pressure increases or the temperature decreases. Both temperature and pressure decrease with increasing elevation. Consequently, changes in elevation produce a profound effect on the generated power as a result changing in the air density.

•The Perfect Gas Law

The air density may be estimated from the perfect gas law.

$$P * V = n * R_{air} * T \text{.. (2.25)}$$

Where

P is the pressure [P_a]

V is the volume considered [m^3]

n is the number of moles

R_{air} is the specific gas constant for dry air (287.05 J/ (kg*K))

T is the temperature [K]

If the density, ρ_{air}, is defined from the number of molecules in a certain volume, n/V=ρ, then the density may now be expressed from the perfect gas law as:

$$\text{Air density } \rho = \frac{\rho}{R_{air}T} \text{...(2.26)}$$

Where

R_{air} = molecular weight of air (J/kg*K) and

is given by: $R_{air} = R/M_{air}$= 287.05J/kg*K

R= universal gas constant (J/kg*K) = 8.31432 J/kg*K

M_{air} = molar mass of air (kg/mol) = 28.9644*10-3kg/mol (assumed constant up to approximately 86km altitude)

P = atmospheric pressure (P_a)

T = temperature (K)

- **Swept area of the turbine**

The larger the swept area (the size of the area through which the rotor spins), the more power the turbine can capture from the wind. Since swept area is $\frac{\pi D^2}{4}$, where D = diameter of the rotor, a small increase in blade length results in a larger increase in the power available to the turbine.

Figure 2.12: Wind turbine model [19]

The below equation is used to calculate the power production from the wind turbine.

$$\text{Power (watts)} = \frac{\rho A v^3}{2} \ldots\ldots\ldots\ldots\ldots\ldots\ldots\ldots\ldots\ldots\ldots\ldots\ldots (2.27)$$

Where ρ=air density (kg/m^3)

A=swept area of the wind turbine rotor (m^2)

V=wind speed (m/s)

We can also calculate power from the wind turbines using:

$$*P_T = c_p * \frac{\rho A v^3}{2} \ldots\ldots\ldots\ldots\ldots\ldots\ldots\ldots\ldots\ldots\ldots\ldots\ldots\ldots (2.28)$$

Where: P_T=Power extracted by wind turbine (watts)

C_p= Coefficient of performance

ρ =Air density (kg/m^3), 1.225 kg/m^3 at sea level, less in higher altitudes

A=swept area of the wind turbine rotor (m^2)

Table 2-2: International standard atmosphere, mean sea level conditions[19]

Pressure	P_o=101325N/m^2=1013.25hP_a
Density	ρ_o=1.225kg/m^3
Temperature	To = 288.15
Speed of sound	α_o = 340.294 m/sec
Acceleration of gravity	G_o = 9.80665 m/sec^2

2.2.7 Temperature modelling

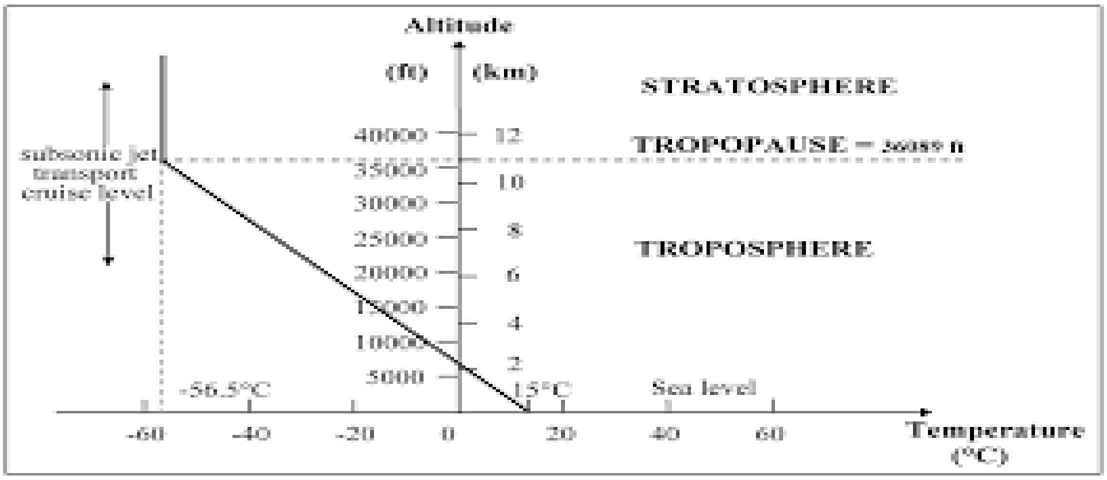

Figure 2.14: International standard atmosphere temperature variation [19]

Temperature decreases with altitude at a constant rate of -6.5oC/1000m(-1.98oC/1000ft) up to the tropopause. The standard tropopause altitude is 11000m (36089ft). Therefore, the air which is considered as a perfect gas in the ISA model presents the following Characteristics within the troposphere.

$$T = T_o - 6.5\frac{h_m}{1000} \qquad (2.29)$$

$$T = T_o - 1.98\frac{h_{ft}}{1000} \qquad (2.30)$$

2.2.8 Pressure modelling

To calculate the standard pressure p at a given altitude, the temperature is assumed standard, and the air is assumed as a perfect gas. The relationship between the pressure at a troposphere altitude and sea level pressure can be obtained by:

$$P = P_o(1 - .0065\frac{h}{T_o})^{5.256} \quad (2.31)$$

where T_o is temperature in Kelvin, and h is height in meters. or

$$P = P_o(1 - 2.5577 * 10^{-5} * h)^{5.256} \quad (2.32)$$

2.3 HOMER Pro

HOMER (Hybrid Optimization of Multiple Electric Renewables), the micro power optimization model, simplifies the task of evaluating designs of both off-grid and grid-connected power systems for a variety of applications. When you design a power system, you must make many decisions about the configuration of the system: what components does it make sense to include in the system design? How many and what size of each component should you use? The large number of technology options and the variation in technology costs and availability of energy resources make these decisions difficult. HOMER's optimization and sensitivity analysis algorithms make it easier to evaluate the many possible system configurations. [32]

- **Simulation**

HOMER simulates the operation of a system by making energy balance calculations in each time step of the year. For each time step, HOMER compares the electric and thermal demand in that time step to the energy that the system can supply in that time step, and calculates the flows of energy to and from each component of the system. For systems that include batteries or fuel-powered generators, HOMER also decides in each time step how to operate the generators and whether to charge or discharge the batteries.

HOMER performs these energy balance calculations for each system configuration that you want to consider. It then determines whether a configuration is feasible, (i.e. whether it can meet the electric demand under the conditions that you specify), and estimates the cost of installing and operating the system over the lifetime of the project. The system cost calculations account for costs such as capital, replacement, operation and maintenance, fuel, and interest.

- **Optimization**

HOMER Pro has two optimization algorithms. The original grid search algorithm simulates all of the feasible system configurations defined by the Search Space. The new HOMER Optimizer? uses a proprietary derivative free algorithm to search for the least cost system.

HOMER then displays a list of configurations, sorted by net present cost (sometimes called lifecycle cost), that you can use to compare system design options.

- **Sensitivity Analysis**

When you define sensitivity variables as inputs, HOMER Pro repeats the optimization process for each sensitivity variable that you specify. For example, if you define wind speed as a sensitivity variable, HOMER will simulate system configurations for the range of wind speeds that you specify.

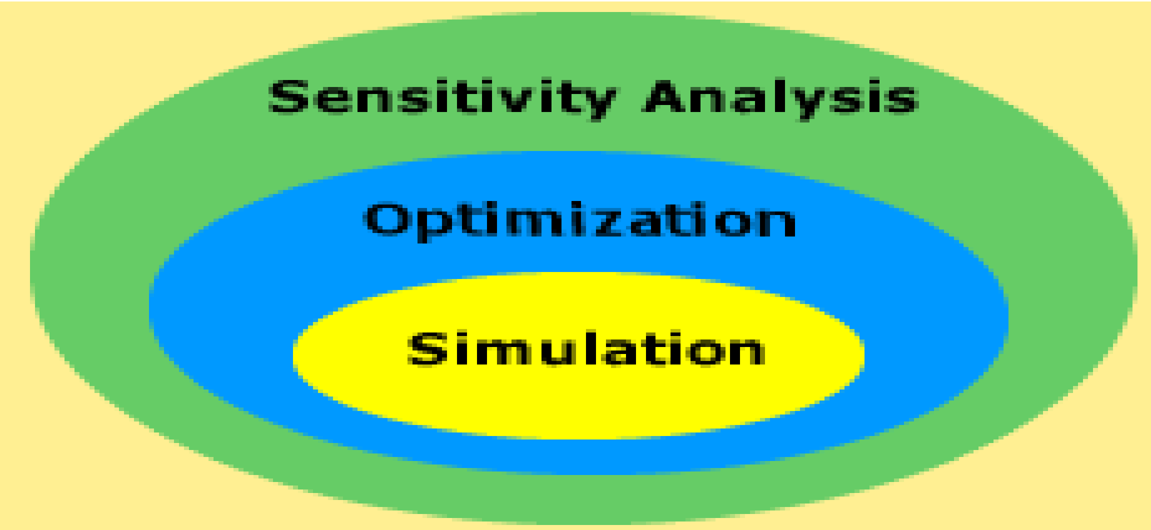

Figure 2.2: HOMER Pro Analysis layer[32]

HOMER Pro simplifies the task of designing distributed generation (DG) systems - both on and off-grid. HOMER's optimization and sensitivity analysis algorithms allow you to evaluate the economic and technical feasibility of a large number of technology options and to account for variations in technology costs and energy resource availability.

Working effectively with HOMER Pro requires understanding of its three core capabilities - simulation, optimization, and sensitivity analysis - and how they interact. [32]

2.4. Literature Review

Different research is carried in the field of renewable energy; applications of stand-alone power system and hybrid renewable energy systems have been conducted for the maximum usage of the resource potential.

A case study [7] in the Somalia region of Ethiopia, the remote rural village called Werder district (6050'N 45030' E) have an average wind speed of 5m/s at 10m elevation and an average daily solar radiation of 7.5kwh/m2/day. Extension of national grid is not economically feasible and the electrical load density in the village is low. The techno economic analysis of this option has been done using HOMER Pro software and hybrid PV/wind/diesel generator system became economically feasible for the proposed site based on some important parameters such as high renewable penetration, less annual diesel consumption, less carbon dioxide emission and less cost of energy.

The study [20] presents the result of techno-economic analysis of hybrid system comprising of solar and wind energy for powering a specific remote mobile base transceiver (BTS) in Kaduna state, Nigeria. But the optimal system configurations obtained through simulation in HOMER. Two best optimal system configurations namely PV-Diesel-Battery and PV-wind-diesel-battery system are compared with the conventional stand-alone diesel generator (DG) system. Finding indicated that PV array (10KW)-DG (5.5KW)-Battery (64 units Trojan L16P) is the most economically viable option with the total net present cost of $69,811 and per unit cost of electricity of $0.409. The simulations indicate that a hybrid system option, compared to a diesel only system, is feasible for each of the three villages.

In the paper [14] they are proposed a hybrid system cost analysis which has wind generation, solar system, and storage battery system and diesel generator using efficient optimization tool HOMER for obtain the optimal cost of the hybrid system. Determine the optimal combination of solar, wind and diesel based hybrid system to fulfill the load requirement and minimize the cost of telecommunication site in BSNL Bhopal, India.

In this paper [11] presents a solution utilizing a hybrid of solar and wind power systems with a table generator to provide reliable power for a mobile base station located behind the Himalayas of south Asia. The design is based on the local mobile subscribers with 350 capacities with 51mE per subscriber traffic and the peak load capacity of 750 W. The meteorological data including solar sunshine hours and hourly wind speed are taken for a site in Mustang district at 3444 m altitude. The power consumption patter of a mobile base station depends up on the traffic pattern of the mobile users. The cost of the hybrid system is also estimated as $81,512.04 Canadian dollars. The proposed system ensures the reliability of power supply to run the 24/7 cellular mobile services at an extremely remote site of Nepal.

Thus, based on the literature reviews, HOMER modeling software is taken for the purposes of this study to carry the feasibility analysis. when compared with other software's HOMER creates a list of feasible system configurations sorted according to cost effectiveness and presents the optimal configuration based on the lowest net percent cost (NPC) the supply in order to design system [20].

This paper also used the HOMER Pro software to design and optimize stand-alone renewable hybrid power system to be provided electricity requirement of the remote telecom sites in Ethiopia.

To improve the communication infrastructure of the rural community the ethio-telecom must use Hybrid RES to provide electrical power depending on the geographical area and the resource availability of the area. Here in these sites, it uses Hybrid Battery and diesel Generator, but power supply is not continuous. However, this thesis differs from the related studies in terms of application, load demand, climatic data, and location of the study areas.

CHAPTER THREE

METHODS and MATERIALS

3.1 Methodology of the Study

This chapter presents all the tools and systems used for the study. These include: the real data collection, the simulation & optimization software, and a supervisory controller for the energy management. The descriptions of all the system components (solar, wind, diesel generator, and hybrid systems), the power converters, the energy storage (battery) and their sizing are also outlined and detailed. From the description of the system components, a mathematical model was formulated. Mathematical modeling of energy systems involves representing the deployment of energy options (either single or hybrid) computationally and simulating its operation over time or under varying conditions or scenarios. In this study, the mathematical models developed by HOMER Pro, based on power generation model and cost model, were presented. A power generation model is a model of the electrical energy generated by the system components. Cost model is the annualized cost of a component which includes annualized capital cost, annualized replacement cost, annual operation and maintenance (O & M) cost, emission cost and annual fuel cost (generator). This model (economic and environmental cost model) was derived through annualized total cost of different configurations of power system. An algorithm was formulated to be used to solve the optimization problem which links the power generation model and the cost model together.

3.2 Methods

Successful evaluation of any renewable energy project requires appropriate criteria to be applied in the selected area to ensure that the operational behavior of different scenarios can be analyzed accurately.

The following analysis frameworks has been adopted in this project:

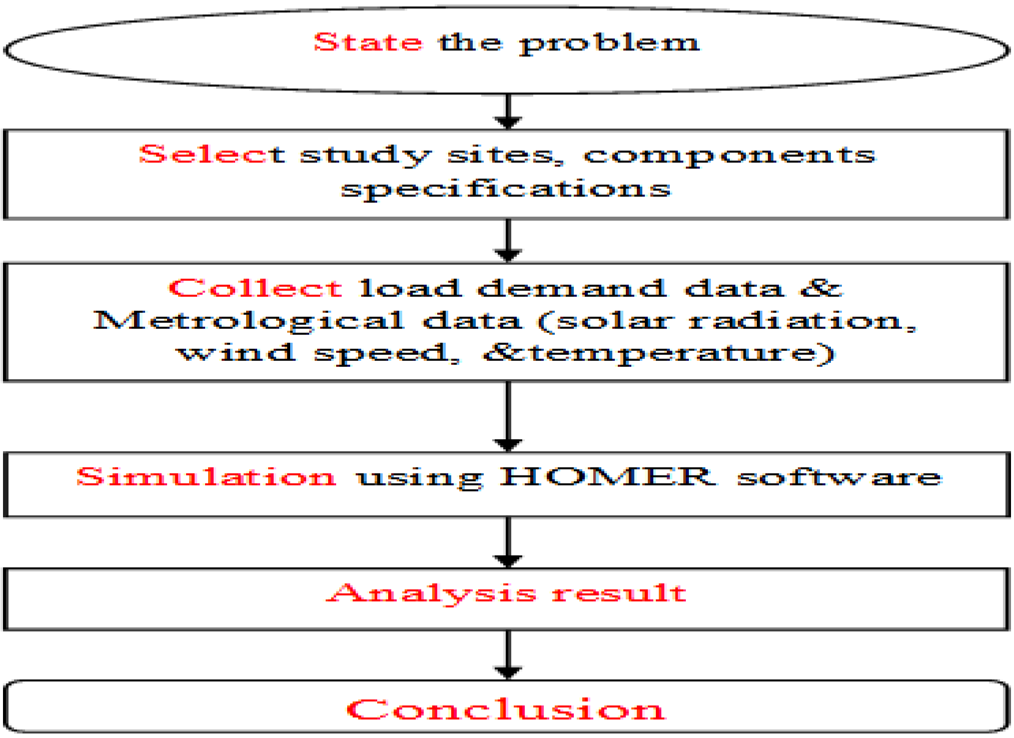

Figure 3.1: Design Analysis framework

Table 3-1: Comparison table of optimization software [20]

Comparison point	**HOMER Pro**	**HYBRID2**	**HOGA**	**TRANSYS**
Free download and use	×	×	×	
PV, Diesel, Batteries	×	×	×	×
Wind	×	×	×	×
Mini-Hydro	×	×	×	×
Fuel cell; electrolyze and hydrogen tank	×	×	×	×
Hydrogen load	×	×	×	×
Thermal load	×			×
Control strategies	×	×	×	
Simulation	×	×	×	×
Economical Optimization	×		×	×
Multi-Objective Optimization, Genetic Algorithms			×	

➢Based on the above comparison table result technical data has been collected using HOMER Pro software uses the monthly average global horizontal radiation, wind speed and ambient temperature as input parameters.

3.3 Data Collection

The main concern is the assessment of resource potential and modeling of the hybrid system by analyzing the data taken from different sources. Sources of data for this study are classified in to two. These are primary data sources and secondary data sources.

➢Primary Data Collection

Primary data are the data collected through field survey by the researcher. Survey has been done to select BTS sites geographical location with climate data & collect sites load consumption data of the study sites and from the region SER ethio-telecom.

- The current study has been conducted for 16 selected specific telecom BTS sites in east Bale zone Ethiopia, under Ginner, Gasser a, Raytu and Sewina woreda of Oromiya Region.
- The sites discussed here in this paper are: The four study locations are models for east bale zone.

Table 3-2: Summarized geographical data of selected 16 SER telecom sites

Study Area	Site ID	Specific Location	Latitude	Longitude	Altitude (ft)	Average telecom load capacity (kw)
Ginnir Area	211356	Ginnir ET office	7.1384	40.7111	9667	5.2
	211358	Kebena	7.1993	40.5823	10217	5.2
	215067	Harewa repeater	7.24409	40.7402	9980	4.5
Gassera-Area	211329	Sahilu	7.2811	40.3063	11150	5.2
	211354	Oda sofumer	6.9908	40.8539	7591	5.2
	215063	Kere Adanu repeater	7.23977	40.3704	10990	5.2
Raytu-Area	211541	Raso Town	6.5485	41.7846	5141	5.2
	211542	Bekol	6.56652	41.6106	5550	5.2
	211544	Beredimtu 1	6.651	41.4445	6601	5.2
	211545	Beredimtu 2	6.7213	41.3568	6628	4.5
	211547	Shekula	6.8165	41.2628	6914	4.5
	211549	Riytu	6.8956	41.1302	7046	4.5
Seweyna-Area	211458	Beltu tele	7.8795	40.9841	8920	4.5
	211578	Hjikogn	7.2345	41.0764	7553	4.5
	211579	Areda gemelo	7.2583	40.8346	9077	4.5
	211581	Hada	7.3264	41.1824	7542	4.5

➢ Secondary Data Collection

Secondary data is a data, which is obtained from other recently done related literatures. Some of the data was solar radiations data of study area taken from online data of NASA meteorological department.

The capital cost of equipment was taken from website and adjusted to local value by including transportation and other costs. The load profile of the sites was determined using the wattage and hour of use of the proposed equipment as explained in subsequent section.

Table 3-3: Secondary data collected from various sources

Data collected& source	**Value/Components type/**
Solar radiation of the study areas (NASA)	22 years solar radiation data
Wind potential of the study areas (NASA)	22 years wind speed data
Average Temperature of the study sites (NASA)	30 year temperature(C) 1984-2013
Hybrid component Size and cost for simulation(HOMER Pro)	Battery storage, PV module, Wind Turbine,, Diesel generator and Converter

Table 3-4: Average monthly inter-annual earth skin temperature(c°) of the study sites data from NASA.

Latitude	**Longitude**	**Parameter**	Jan	Feb	Mar	Apr	May	Jun	Jul	Aug	Sep	Oct	Nov	Dec	Ann
7° 8' 18.24" N	40° 42' 39.96" E	TS	21.2	22.9	23.3	22	22.9	22.2	21.9	20	22.4	20.8	19.8	19.8	21.7
7° 11' 57.48" N	40° 34' 56.28" E	TS	21.2	22.9	23.3	22	21.9	22.2	21.9	22	22.4	20.8	19.8	19.8	21.7
7° 14' 38.76" N	40° 44' 24.72" E	TS	21.2	22.9	23.3	22	21.9	22.2	21.9	22	22.4	20.8	19.8	19.8	21.7
7° 16' 51.96" N	40° 18' 22.68" E	TS	16.6	18.3	19.1	18.5	18.6	18.7	18.2	18.1	18.1	16.7	15.7	15.6	17.7
6° 59' 26.88" N	40° 51' 14.04" E	TS	22.7	24.4	24.4	23.1	22.5	22.7	22.9	23.4	24.1	22.3	21.1	21.4	22.9
7° 14' 23.172" N	40° 22' 13.44" E	TS	16.6	18.3	19.1	18.5	18.6	18.7	18.2	18.1	18.1	16.7	15.7	15.6	17.7
6° 32' 54.6" N	41° 47' 4.56" E	TS	27	28.8	29.6	27.8	26.5	26.8	27.3	28.3	29.1	27.3	26	25.9	27.5
6° 33' 59.472" N	41° 36' 38.16" E	TS	27	28.8	29.6	27.8	26.5	26.8	27.3	28.3	29.1	27.3	26	25.9	27.5
6° 39' 3.6" N	41° 26' 40.2" E	TS	25.2	26.9	27.5	25.6	24.7	25.1	25.6	26.3	27.1	25.1	23.7	23.9	25.5
6° 43' 16.68" N	41° 21' 24.48" E	TS	25.2	26.9	27.5	25.6	24.7	25.1	25.6	26.3	27.1	25.1	23.7	23.9	25.5
6° 48' 59.4" N	41° 15' 46.08" E	TS	25.2	26.9	27.5	25.6	24.7	25.1	25.6	26.3	27.1	25.1	23.7	23.9	25.5
6° 53' 44.16" N	41° 7' 48.72" E	TS	25.2	26.9	27.5	25.6	24.7	25.1	25.6	26.3	27.1	25.1	23.7	23.9	25.5
7° 52' 46.2" N	40° 59' 2.76" E	TS	22.6	24.3	24.7	23.5	23.6	24	23.2	23	23.3	21.9	21.2	21.3	23
7° 14' 4.2" N	41° 4' 35.04" E	TS	24.8	26.4	26.7	25	24.5	24.8	24.9	25.5	26.2	24.4	23.2	23.4	25
7° 15' 29.88" N	40° 50' 4.56" E	TS	21.2	22.9	23.3	22	21.9	22	21.9	22	22.4	20.8	20.8	19.8	21.7
7° 19' 35.04" N	41° 10' 56.64" E	TS	24.8	26.4	26.7	25	24.5	24.8	24.9	25.5	26.2	24.4	23.2	23.4	25

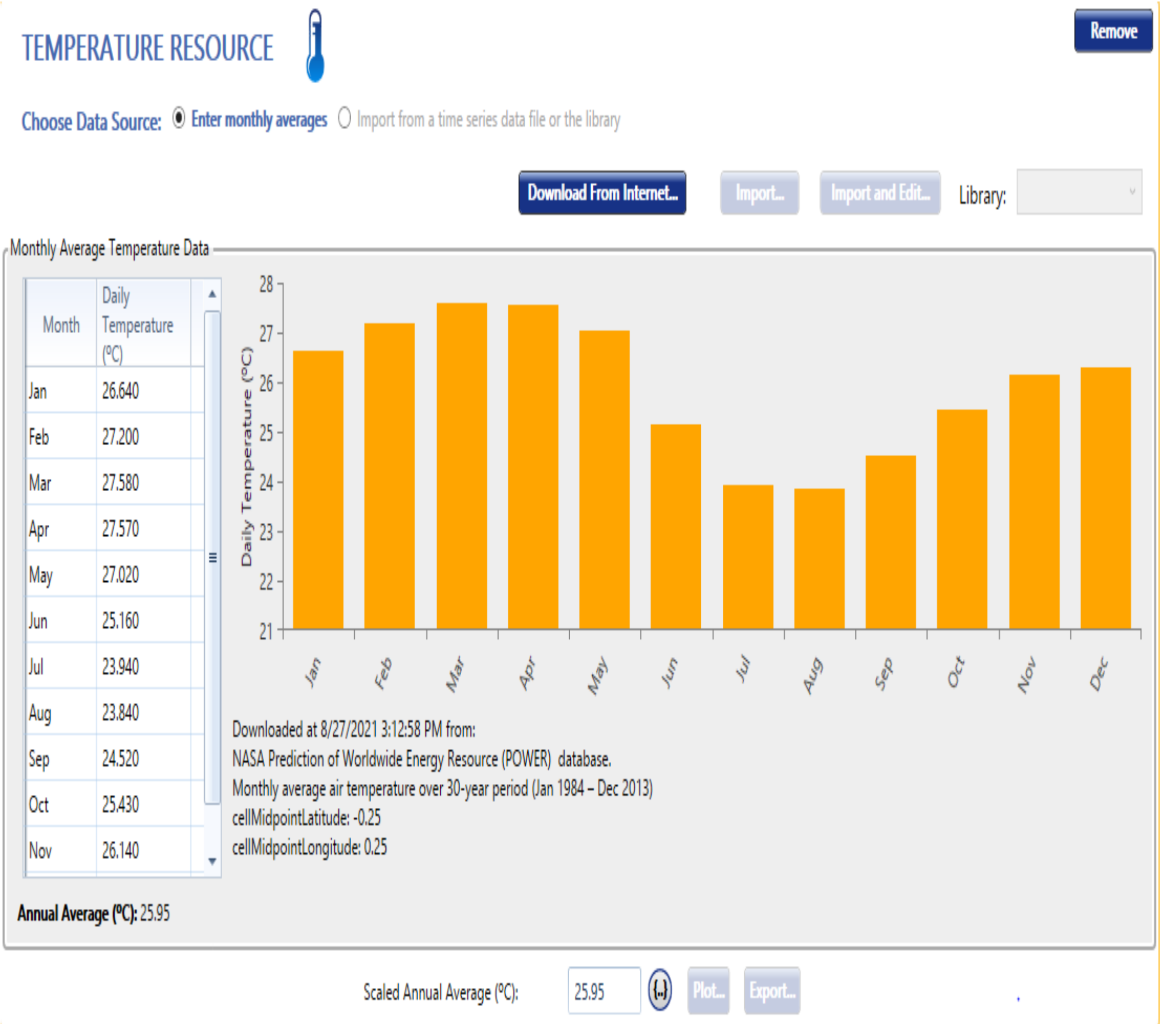

Figure 3.2: HOMER Pro Monthly average temperature data for selected locations

3.4 Solar and Wind Resource assessment in Ethiopia

Ethiopia receives 4.55 to 6.5 kWh/m^2/day annual average of solar radiation throughout the country [2, 4, 8, and 23]. This varies significantly during the year, ranging from a minimum of 4.55 kWh/m^2 in July to a maximum of 6.55 kWh/m^2 in February and March. Other literatures describe the yearly average radiation to be in the range from 4.25 kWh/m^2 in the areas of Itang in the Gambella regional state (western Ethiopia), to 6.25 kWh/m^2 around Adigrat in the Tigray regional state (northern Ethiopia) [19].

Ethiopia has exploitable reserve of 100 GW wind energy with an average speed of 3.5 – 5.5 m/s, flowing for 6 hours/day. There are two basic zones with homogenous periodicity separated by the rift valley. In the first of these, covering most of the highland plateaus, there are two well-defined wind speed maximal occurring, respectively, between March and May and between September and November. In the second zone, covering most of the

Ogaden and the eastern lowlands, average wind velocity reaches maximum values between May and August [7,38].

The government of Ethiopia with the collaboration of Chinese government prepared solar and wind master plan for the whole country, which can be very useful to identify the gross amount and distribution condition of wind and solar energy resources, construction conditions, cost and other limiting factors of wind and solar power generation projects. (Ministry of Water and Energy June 22, 2013).

Based on the analysis of this master plan [31]:

- Ethiopia has 1,350GW Potential installed capacity of wind energy.
- Ethiopia has annual total solar energy reserve of 2.199 million TWh/annum.

Table 3-5: List of wind farm constructed [31]

No.	Farm Name	Installed Capacity(MW)	Average Energy (Gwh/year)
1	Ashegoda	120	450
2	Adama II	153	479
	Total	**273**	**929**

Table 3-6: List of under construction sites of solar PV power development [31]

No.	**Name**	**Capacity (MW)**	**Area (km2)**	**Region**
1	DebreBerhan Pv power station	10	0.39	Amhara
2	Metehara Pv power station	50	1.6	Oromiya
3	Dera Pv power station	60	1.59	Oromiya
	Total	**120**	**3.58**	

Table 3-7: Potential installed capacity in each state & the whole country [31]

Potential Installed Capacity in Each State and the Whole country		
Country /state	**Area(km2)**	**Potential installed capacity(GW)**
Amhara	155	59
Tigray	50.2	78
Afar	94.1	52
SNNP	109.9	26
Gembela	24.6	0
Oromiya	320	75
Benshagul	49.5	0
Somali	300.3	1,060
Total	**1,103.60**	**1,350**

Table 3-8: Wind farm sites selected in Ethiopia [31]

Wind Farm Site Selected in Ethiopia					
No.	Name of site	Capacity	Area	Grading in	Domicile
F1	Nazret wind farm	300	254	100	Oromiya
F2	Mek'ele South wind farm	100	77	85	Tigray
F3	Sheno wind farm	100	56	88	Oromiya
F4	Ch'ach'a wind farm	100	56	86	Amhara
F5	Phase I wind farm in Iteya	100	66	96	Oromiya
F6	Sulalta wind farm	100	60	92	Oromiya
F7	Gondar West wind farm	50	50	82	Amhara
F8	Imdibir wind farm	50	47	90	SNNP
F9	Dire Dawa wind farm	50	40	91	Dire Dawa
F10	Dilla East wind farm	300	268	96	SNNP
F11	Mek'ele North wind farm	200	185	85	Tigray
F12	Debre Markos East wind farm	200	143	87	Amhara
F13	Soddo wind farm	200	160	84	SNNP
F14	Sendafa North wind farm	100	70	88	Oromiya
F15	Sendafa South wind farm	100	70	88	Oromiya
F16	Gondar North wind farm	100	65	80	Amhara
F17	Phase II wind farm inIteya	100	70	95	Oromiya
F18	Bu'i East wind farm	100	80	83	SNNP
F19	Aysha wind farm	100	60	83	Somalia
F20	Phase I wind farm in Bolo	100	60	90	Oromiya
F21	Diche Oto wind farm	50	100	78	Afar
F22	Bahir Dar wind farm	50	80	82	Amhara
F23	Assela wind farm	50	71	93	Oromiya
F24	Jacho wind farm	600	330	73	SNNP
F25	Phase II wind farm in Bolo	500	300	90	Oromiya
F26	Hula wind farm	300	220	64	Oromiya
F27	Dilla West wind farm	300	230	96	SNNP
F28	Dangla wind farm	200	170	67	Amhara
F29	Debre Markos West wind farm	200	150	87	Oromiya
F30	Ambo wind farm	200	130	72	Oromiya
F31	Babile wind farm	200	130	56	Oromiya
F32	Dabat wind farm	100	61	56	Amhara
F33	Phase I wind farm in Weldiya	100	43	70	Amhara

3.4.1 Solar Energy Assessment of the study area

The assessment of the potential for solar radiation of the selected area is done by taking data from NASA. These data is analyzed using mathematical approach based on the sunshine duration collected on the past twenty two consecutive years starting from July 1983 - June

2005. Therefore, for calculating the radiation in kWh/m^2/d from the sunshine duration, the values for the regression coefficients α and b are taken to be 0.3 and 0.5 respectively [39]. Finally, it is found that the analysis of annual average solar radiation data taken from NASA is given in tables 3.9 and table 3.10 respectively. For this study, the calculated monthly average daily radiation summarized in the bellow charts used for modeling the hybrid system. The monthly average solar radiation of selected BTS sites for the data taken from NASA is shown on the bellow tables.

22 years average Solar radiation of the study area in kWh/m^2 /day & Clearness index data from NASA: -

Table 3-9: Average monthly global solar radiation & Clearness index of 9 study areas in kwh/m^2/day data from NASA [39]

LAT	LON	Parameter	JAN	FEB	MAR	APR	MAY	JUN	JUL	AUG	SEP	OCT	NOV	DEC	ANN
7.138	40.711	DNR	7.73	7.7	6.3	5.22	6.22	5.95	5.1	5.08	5.3	5.15	6.65	7.52	6.15
7.138	40.711	K T	0.66	0.66	0.61	0.55	0.6	0.59	0.54	0.55	0.56	0.54	0.61	0.65	0.59
7.199	40.582	DNR	7.73	7.7	6.3	5.22	6.22	5.95	5.1	5.08	5.3	5.15	6.65	7.52	6.15
7.199	40.582	K T	0.66	0.66	0.61	0.55	0.6	0.59	0.54	0.55	0.56	0.54	0.61	0.65	0.59
7.244	40.74	DNR	7.73	7.7	6.3	5.22	6.22	5.95	5.1	5.08	5.3	5.15	6.65	7.52	6.15
7.244	40.74	K T	0.66	0.66	0.61	0.55	0.6	0.59	0.54	0.55	0.56	0.54	0.61	0.65	0.59
7.88	40.984	DNR	7.73	7.7	6.3	5.22	6.22	5.95	5.1	5.08	5.3	5.15	6.65	7.52	6.15
7.88	40.984	K T	0.66	0.66	0.61	0.55	0.6	0.59	0.54	0.55	0.56	0.54	0.61	0.65	0.59
7.235	41.076	DNR	8.06	8.1	6.61	5.17	5.99	5.85	5.01	5.06	5.65	5.34	6.85	7.78	6.28
7.235	41.076	K T	0.68	0.68	0.62	0.55	0.59	0.58	0.54	0.55	0.58	0.56	0.62	0.67	0.6
7.258	40.835	DNR	7.73	7.7	6.3	5.22	6.22	5.95	5.1	5.08	5.3	5.15	6.65	7.52	6.15
7.258	40.835	K T	0.66	0.66	0.61	0.55	0.6	0.59	0.54	0.55	0.56	0.54	0.61	0.65	0.59
7.326	41.182	DNR	8.06	8.1	[illegible]	5.17	5.99	5.85	5.01	5.06	5.65	5.34	6.85	7.78	6.28
7.326	41.182	K T	0.68	0.68	0.62	0.55	0.59	0.58	0.54	0.55	0.58	0.56	0.62	0.67	0.6
7.281	40.306	DNR	7.73	7.7	6.3	5.22	6.22	5.95	5.1	5.08	5.3	5.15	6.65	7.52	6.15
7.281	40.306	K T	0.66	0.66	0.61	0.55	0.6	0.59	0.54	0.55	0.56	0.54	0.61	0.65	0.59
7.24	40.37	DNR	7.73	7.7	6.3	5.22	6.22	5.95	5.1	5.08	5.3	5.15	6.65	7.52	6.15
7.24	40.37	K T	0.66	0.66	0.61	0.55	0.6	0.59	0.54	0.55	0.56	0.54	0.61	0.65	0.59

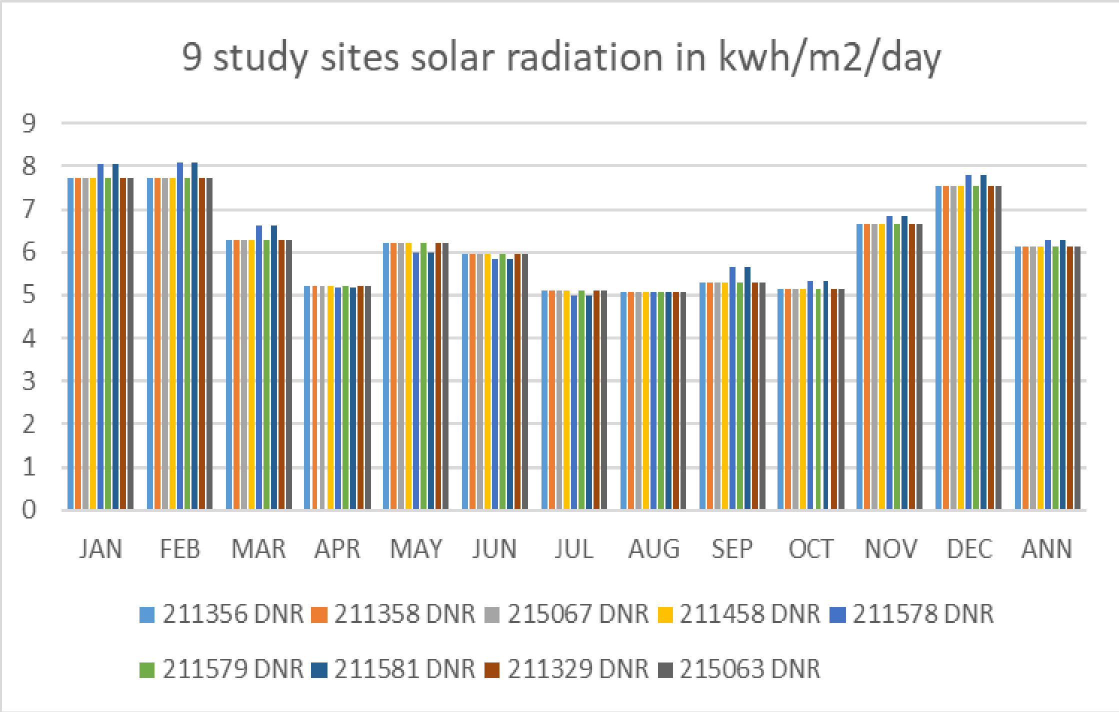

Figure 3.3: Plot of average monthly solar radiation of 9 selected locations [39]

Table 3-10: Average monthly global solar radiation & Clearness index of 7 study area in kwh/m^2/day data from NASA [39]

LAT	LON	Parameter	JAN	FEB	MAR	APR	MAY	JUN	JUL	AUG	SEP	OCT	NOV	DEC	ANN
6.549	41.785	DNR	8.09	8.2	6.64	4.93	5.45	4.94	4.39	4.82	5.7	4.74	6.37	7.74	5.99
6.549	41.785	KT	0.68	0.68	0.62	0.54	0.57	0.54	0.51	0.54	0.58	0.53	0.6	0.66	0.59
6.567	41.611	DNR	8.09	8.2	6.64	4.93	5.45	4.94	4.39	4.82	5.7	4.74	6.37	7.74	5.99
6.567	41.611	KT	0.68	0.68	0.62	0.54	0.57	0.54	0.51	0.54	0.58	0.53	0.6	0.66	0.59
6.651	41.445	DNR	8.09	8.2	6.64	4.93	5.45	4.94	4.39	4.82	5.7	4.74	6.37	7.74	5.99
6.651	41.445	KT	0.68	0.68	0.62	0.54	0.57	0.54	0.51	0.54	0.58	0.53	0.6	0.66	0.59
6.721	41.357	DNR	8.09	8.2	6.64	4.93	5.45	4.94	4.39	4.82	5.7	4.74	6.37	7.74	5.99
6.721	41.357	KT	0.68	0.68	0.62	0.54	0.57	0.54	0.51	0.54	0.58	0.53	0.6	0.66	0.59
6.817	41.263	DNR	8.09	8.2	6.64	4.93	5.45	4.94	4.39	4.82	5.7	4.74	6.37	7.74	5.99
6.817	41.263	KT	0.68	0.68	0.62	0.54	0.57	0.54	0.51	0.54	0.58	0.53	0.6	0.66	0.59
6.896	41.13	DNR	8.09	8.2	6.64	4.93	5.45	4.94	4.39	4.82	5.7	4.74	6.37	7.74	5.99
6.896	41.13	KT	0.68	0.68	0.62	0.54	0.57	0.54	0.51	0.54	0.58	0.53	0.6	0.66	0.59
6.991	40.854	DNR	7.58	7.56	5.95	4.59	4.87	4.03	3.29	3.43	4.36	4.19	5.78	7.18	5.22
6.991	40.854	KT	0.66	0.65	0.59	0.52	0.53	0.49	0.43	0.46	0.51	0.49	0.57	0.64	0.55

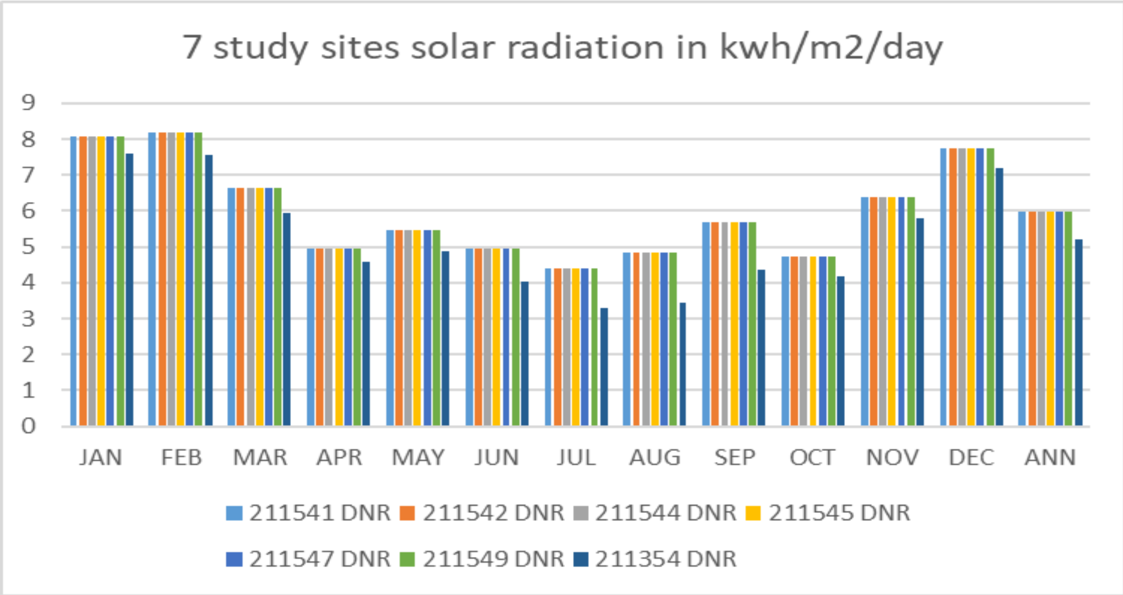

Figure 3.4: Plot of Average monthly solar radiation on 7 selected locations [39]

3.4.2 Wind Potential Assessment in the Study Area

The resource assessment for the wind potential is done by taking the data's only from NASA. This is because of the absence of full data regarding wind speed in the National Metrological Service Agency of Ethiopia. Therefore, the annual average wind speed for The study located area which have different climatic condition at a height of 10m & 50m. This value is used as an input to the wind resource in modeling the hybrid system.

Monthly mean wind speed resources of the site are obtained from NASA surface meteorology and solar energy database. NASA has estimated the rotor speed at rated power is 15.83rpm, the annual average wind speed of the locations is 5.52 m/s at an anemometer height of 10 m & 50m,in the average temperature 25.95^{o}C as shown in Table 3.11,3.12, and 3.13.

Generally, it shows the wind speed data of the site is not that much satisfactory for power generation since it has a very small cut-in wind speeds. So, wind speed extracted from NASA is simply taken to assess wind energy potential of the selected site (resource assessment). This data can be extrapolated to the designated wind turbine height of 50 m.

The lowest wind speed profile is indicated in the months of October, November and December whereas, June, July, August and September are the windiest months.

As wind turbine height increase length from ground the wind speed also increase and hence, power production also rises. The wind speed at any height above ground level can be interpolated either in exponential function or logarithmic function forms [24]. In this paper the logarithmic function used that the logarithmic profile (or log law) assumes that the wind speed is proportional to the logarithm of the height above ground. The following equation therefore gives the ratio of the wind speed at hub height to the wind speed at anemometer height:

$$\frac{V_2}{V_1} = \frac{ln\left(\frac{h_2}{Z_0}\right)}{ln\left(\frac{h_1}{Z_0}\right)} \quad \ldots\ldots\ldots\ldots\ldots\ldots\ldots\ldots\ldots\ldots\ldots\ldots\ldots\ldots\ldots\ldots\ldots\ldots\ldots\ldots\ldots\ldots\ldots\ldots (3.1)$$

Where: Zo: Surface roughness length factor [m]; Surface roughness length describes the roughness of the surroundings terrain in this case few trees, having a value of 0.01. h1: Reference height above ground level [m], h2: Hub height [m].

Table 3-11: Monthly average wind speed(m/s) of 9 study area data from NASA [39]

Site ID	Parameter	JAN	FEB	MAR	APR	MAY	JUN	JUL	AUG	SEP	OCT	NOV	DEC	ANN
211354	WS50M	4.38	4.54	4.5	4.04	5.26	7.68	8.76	8.74	6.98	4.07	3.81	4.15	5.58
	WS10M	3.03	3.19	3.17	2.79	3.57	5.49	6.6	6.65	5.04	2.79	2.6	2.82	3.98
211541	WS50M	4.38	4.54	4.5	4.04	5.26	7.68	8.76	8.74	6.98	4.07	3.81	4.15	5.58
	WS10M	3.03	3.19	3.17	2.79	3.57	5.49	6.6	6.65	5.04	2.79	2.6	2.83	3.98
211542	WS50M	4.38	4.54	4.5	4.04	5.26	7.68	8.76	8.74	6.98	4.07	3.81	4.15	5.58
	WS10M	3.03	3.19	3.17	2.79	3.57	5.49	6.6	6.65	5.04	2.79	2.6	2.83	3.98
211544	WS50M	4.46	4.52	4.55	4.26	5.27	7.54	8.63	8.57	6.18	4.27	4.03	4.35	5.55
	WS10M	3.24	3.35	3.31	2.96	3.52	5.32	6.4	6.37	4.79	2.94	2.84	3.08	4.01
211545	WS50M	4.46	4.52	4.55	4.26	5.27	7.54	8.63	8.57	6.81	4.27	4.03	4.35	5.61
	WS10M	3.24	3.35	3.31	2.96	3.52	5.32	6.4	6.37	4.79	2.94	2.84	3.07	4.01
211547	WS50M	4.46	4.52	4.55	4.26	5.27	7.54	8.63	8.57	6.18	4.27	4.03	4.35	5.55
	WS10M	3.24	3.35	3.31	2.96	3.52	5.32	6.4	6.37	4.79	2.94	2.84	3.08	4.01
211549	WS50M	4.46	4.52	4.55	4.26	5.27	7.54	8.63	8.57	6.18	4.27	4.03	4.35	5.55
	WS10M	3.24	3.35	3.31	2.96	3.52	5.32	6.4	6.37	4.79	2.94	2.84	3.08	4.01
211458	WS50M	4.09	4.3	4.61	4.47	5.16	7.06	8.06	8.1	6.54	4.16	3.87	4	5.38
	WS10M	2.98	3.19	3.35	3.1	3.48	5.05	5.98	6	4.6	2.88	2.72	2.83	3.85
211578	WS50M	4.09	4.3	4.61	4.47	5.16	7.06	8.06	8.1	6.54	4.16	3.87	4	5.38
	WS10M	2.98	3.19	3.35	3.1	3.48	5.05	5.98	6	4.6	2.88	2.72	2.83	3.85

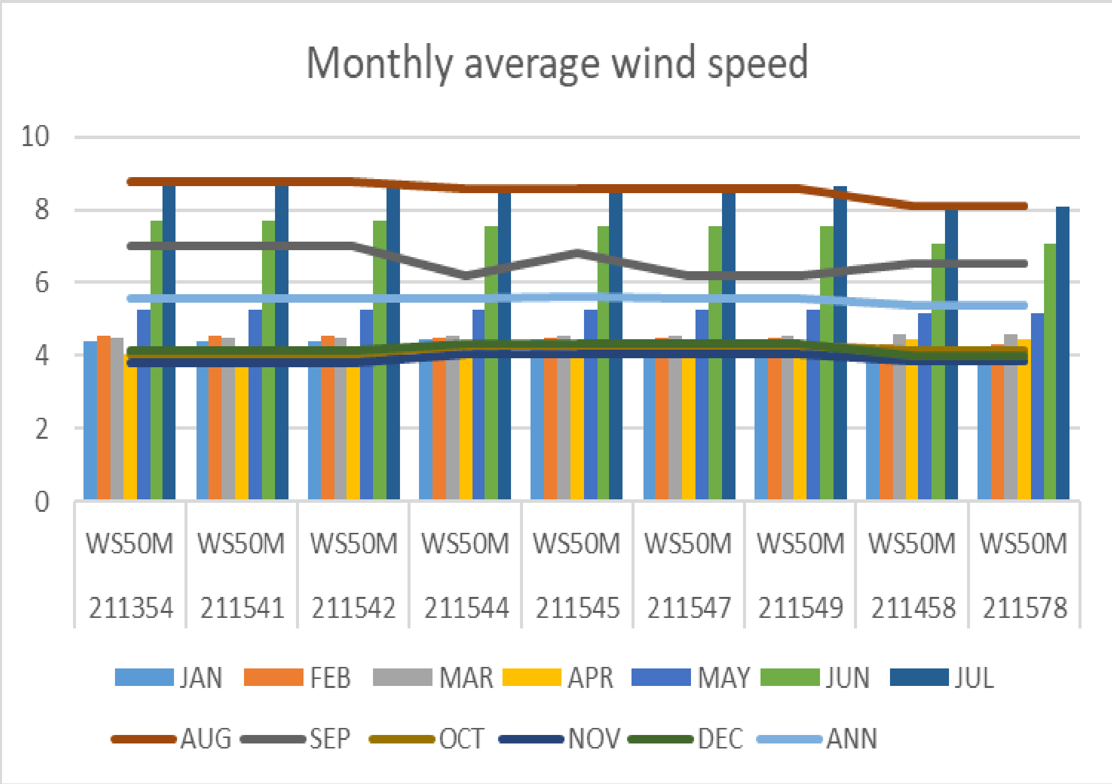

Figure 3.5: Plot of Monthly average wind resource on 9 telecom sites

Table 3-12: Monthly Average wind speed(m/s) of 4 study area data from NASA [39]

Site ID	Parameter	JAN	FEB	MAR	APR	MAY	JUN	JUL	AUG	SEP	OCT	NOV	DEC	ANN
211356	WS50M	3.74	4.02	4.43	4.22	4.36	5.66	6.38	6.48	5.37	3.75	3.53	3.62	4.63
	WS10M	2.75	3	3.27	2.99	2.97	3.99	4.63	4.64	3.65	2.61	2.53	2.6	3.31
211358	WS50M	3.74	4.02	4.43	4.22	4.36	5.66	6.38	6.48	5.37	3.75	3.53	3.62	4.63
	WS10M	2.75	3	3.27	2.99	2.97	3.99	4.63	4.64	3.65	2.61	2.53	2.53	3.29
215067	WS50M	3.74	4.02	4.43	4.22	4.36	5.66	6.38	6.48	5.37	3.75	3.53	3.62	4.63
	WS10M	2.75	3	3.27	2.99	2.97	3.99	4.63	4.64	3.65	2.61	2.53	2.6	3.31
211579	WS50M	3.74	4.02	4.43	4.22	4.36	5.66	6.38	6.48	5.37	3.75	3.53	4.13	4.63
	WS10M	2.75	3.01	3.27	2.99	2.97	3.99	4.63	4.64	3.65	2.61	2.53	2.6	3.31

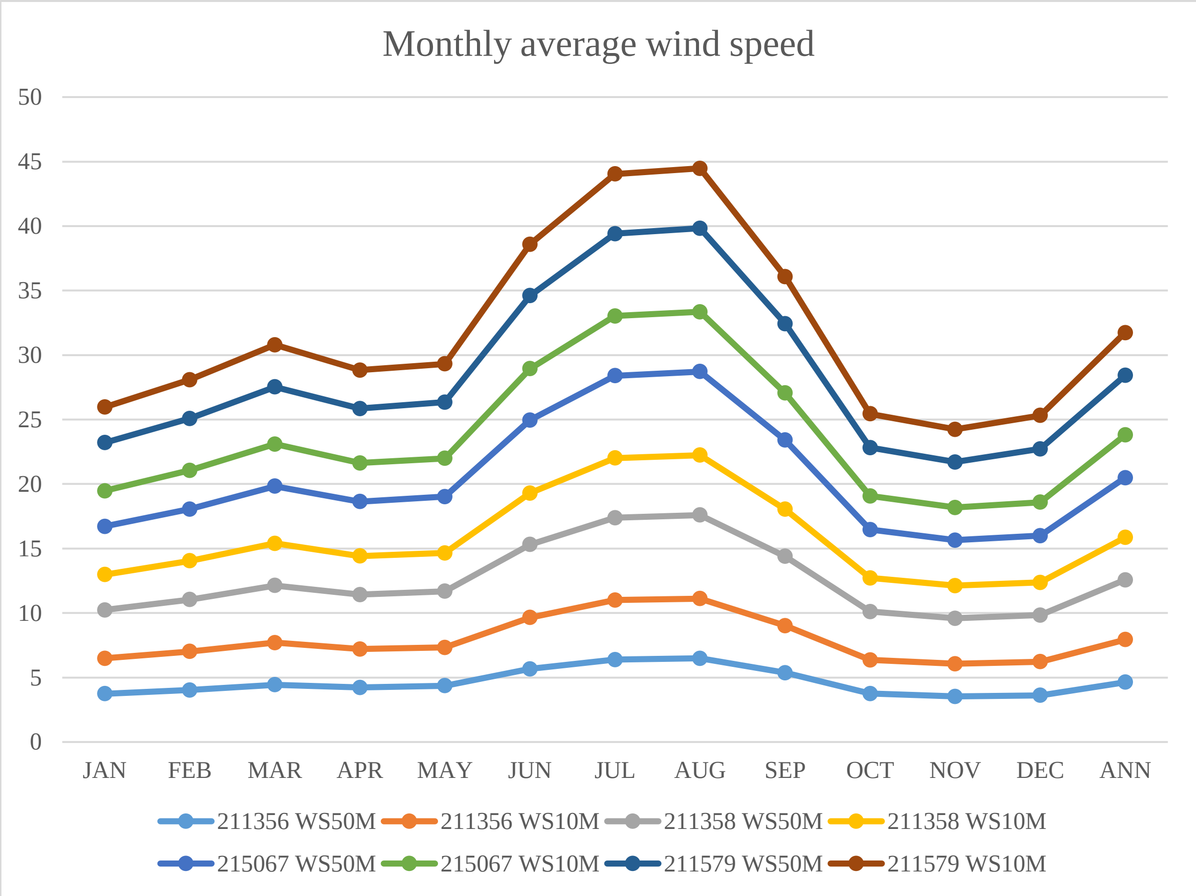

Figure 3.6: Plot of Monthly average wind resource of 4 telecom sites

Table 3-13: Monthly Average wind speed(m/s) of 3 study area data from NASA [39]

Site ID	Parameter	JAN	FEB	MAR	APR	MAY	JUN	JUL	AUG	SEP	OCT	NOV	DEC	ANN
211329	WS50M	3.26	3.53	3.95	3.72	3.48	3.95	4.31	4.42	3.83	3.3	3.24	3.24	3.69
	WS10M	2.49	2.73	3.02	2.77	2.5	2.81	3.12	3.17	2.66	2.42	2.42	2.42	2.71
215063	WS50M	3.26	3.53	3.95	3.72	3.48	3.95	4.31	4.42	3.83	3.3	3.24	3.24	3.69
	WS10M	2.49	2.73	3.02	2.77	2.5	2.81	3.12	3.17	2.66	2.42	2.42	2.42	2.71
211458	WS50M	3.47	3.9	4.49	4.19	3.94	4.37	4.42	4.58	4.33	3.37	3.17	3.23	3.96
	WS10M	2.53	2.87	3.26	2.96	2.71	3.04	3.06	3.12	2.87	2.35	2.26	2.31	2.78

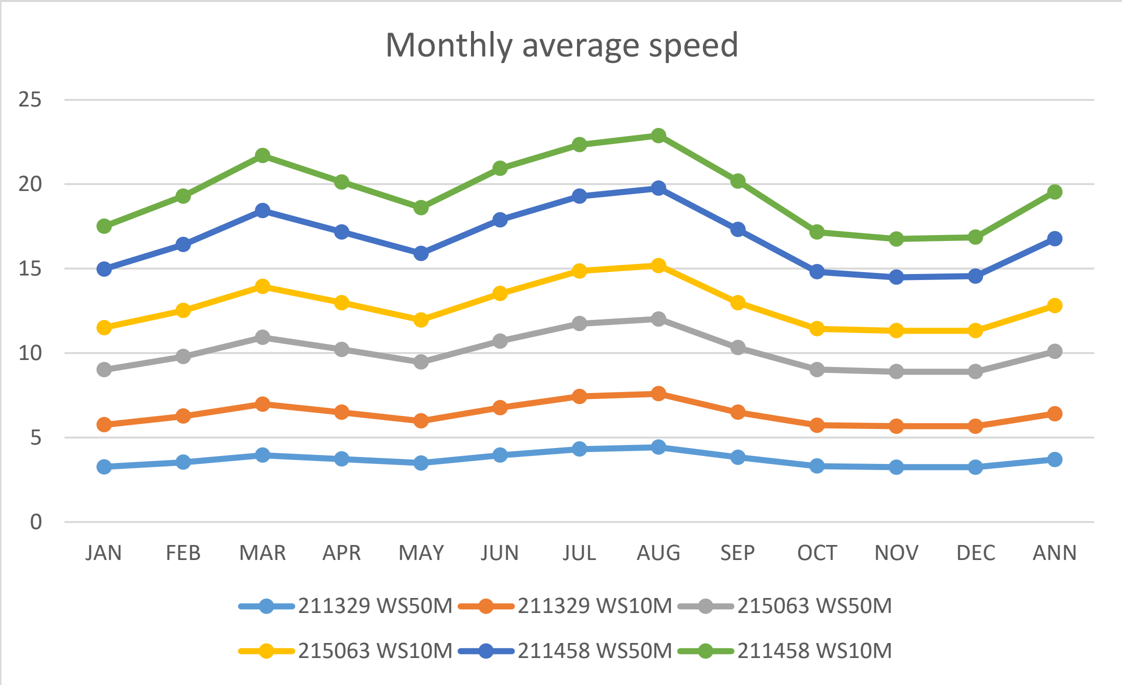

Figure 3.7: Plot of Monthly average wind resource on 3 telecom sites.

3.5 Data Analysis and Materials

The HOMER Pro Software helped in the specification, design and simulation of hybrid system for electricity generation to fully meet and comply with quality, continuity and security of the energy demand. The methodological approach applied was for electrification through a hybrid system combining photovoltaic and wind energy that consisted basically on the following steps:

- Identification, field survey and analysis of energy demand of the Base Transceiver stations in rural telecom selected sites in study;
- Analysis of the temperature, wind speed and solar radiation potential on that geographical region of the selected rural telecom BTS using Excel sheets and HOMER Pro software;
- Analysis of the technical, Economical and environmental feasibility of the hybrid system for electrification of selected rural telecom BTS;
- With the aid of computer tools using HOMER Software was farther proceeded with simulations, comparative analysis of different

configurations of hybrid systems and their costs in power generation to ensure the provision of electricity to the Base Transceiver stations.

- Selection of the best configuration option of hybrid system, that meets quality and lowest cost and electricity demand of selected rural telecom Base Transceiver stations.

3.6 Modeling of Hybrid Energy System Components

Before going to the computer simulation, mathematical modeling of hybrid energy system components is described below. The proposed system contains wind energy sub-system, PV sub-system, diesel generators unit and battery storage sub-system. The theoretical aspects are given below (A, B, C, D, E, and F) and are based on the works of Gupta et al, and Ashok [20].

A. Mathematical Model of Solar Photovoltaic Generator

Using the solar radiation available, the hourly energy output of the PV generator (E_{PVG}) can be calculated according to the following equation [4, 24]:

$$E_{PVG} = G_{(t)} \times A \times P \times \eta_{PVG} \quad \ldots \ldots \ldots \ldots \ldots \ldots \ldots \ldots \ldots \ldots \ldots \ldots \ldots \; (3.1)$$

An assumption was made that the temperature effects (on PV cells) will be ignored.

where G(t) is the hourly irradiance in kWh / m^2

A is the surface area in m^2

P is the PV penetration level factor

η_{PVG} is the efficiency of PV generator

B. Mathematical Model of Wind Energy Generator

Hourly energy generated by wind generator (E_{WEG}) with rated power output (P_{WEG}) is defined by the following expression [4,24, 38]:

$$P_{WEG} = \frac{1}{2}\rho_{Wind} A V^3 C_P(\lambda, \beta) \times \eta_t \times \eta_g \quad \ldots \ldots \ldots \ldots \ldots \ldots \ldots \ldots \ldots \; (3.2)$$

$$E_{WEG}(t) = P_{WEG} \times t \ldots\ldots\ldots\ldots\ldots\ldots\ldots\ldots\ldots\ldots\ldots\ldots (3.3)$$

where ρ_{Wind} is the density of air in 1.22kg/m3

A is the swept area (m2) v is the wind speed (m/s)

C_P is the performance coefficient of the turbine

λ is the tip speed ratio of the rotor blade tip speed to wind speed β is the blade pitch angle (deg) as 0^0

η_t is the wind turbine efficiency

η_g is the generator efficiency

C. Mathematical Model of Diesel Generator

Hourly energy generated by diesel generator (E_{DEG}) with rated power output (P_{DEG}) is defined by the following expression [4]:

$$E_{DEG}(t) = P_{DEG}(t) \times \eta_{DEG} \quad \text{(3.4)}$$

where η_{DEG} is the diesel generator efficiency

For better performance and higher efficiency, the diesel generator will always operate between 80 and 100% of their kW rating.

D. Mathematical Model of Converter

In the proposed scheme, a converter contains both rectifier and inverter. PV, hydro, wind energy generator and battery sub-systems are connected with DC bus while diesel generating unit sub-system is connected with AC bus. The electric loads connected in this scheme are DC loads.

The rectifier is used to transform the surplus AC power from the diesel electric generator to DC power of constant voltage. The diesel electric generator will be powering the load and at the same time charging the battery. The rectifier model is given below:

$$E_{REC-OUT}(t) = E_{REC-IN}(t) \times \eta_{REC} \quad \text{(3.5)}$$

$$E_{REC-IN}(t) = E_{SUR-AC}(t) \quad \text{(3.6)}$$

At any time, t,

$$E_{SUR-AC}(t) = E_{DEG}(t) - E_{Load}(t) \quad \text{(3.7)}$$

Where $E_{REC-OUT}(t)$ is the hourly energy output from rectifier, kWh

$E_{REC-IN}(t)$ is the hourly energy input to rectifier, kWh

η_{REC} is the efficiency of rectifier

$E_{SUR-AC}(t)$ is the amount of surplus energy from AC sources, kWh

E_{DEG} is the hourly energy generated by diesel generator

E. Mathematical Model of Charge Controller

To prevent overcharging of a battery, a charge controller is used to sense when the batteries are fully charged and to stop or reduce the amount of energy flowing from the energy source to the batteries. The model of the charge controller is presented below:

$$E_{CC-out}(t) = E_{CC-IN}(t) \times \eta_{CC} \quad \text{(3.8)}$$

$$E_{CC-IN}(t) = E_{REC-OUT}(t) + E_{SUR-DC} \quad \text{(3.9)}$$

Where $E_{CC-out}(t)$ is the hourly energy output from charge controller, kWh

$E_{CC-IN}(t)$ is the hourly energy input to charge controller, kWh

η_{CC} is the efficiency of charge controller

$E_{REC-OUT}(t)$ is the hourly energy output from rectifier, kWh

E_{SUR-DC} is the amount of surplus energy from DC sources, kWh

F. Mathematical Model of Battery Bank

The battery state of charge (SOC) is the cumulative sum of the daily charge/discharge transfers. The battery serves as an energy source entity when discharging and a load when charging. At any time, t, the state of battery is related to the previous state of charge and to the energy production and consumption situation of the system during the time from t -1 to t.

During the charging process, when the total output of all generators exceeds the load demand, the available battery bank capacity at time, t, can be described by [24, 33]:

$$E_{BAT}(t) = E_{BAT}(t-1) - E_{CC-OUT}(t) \times \eta_{CHG} \quad \text{(3.10)}$$

where $E_{BAT}(t)$ is the energy stored in battery at hour t, kWh

$E_{BAT}(t-1)$ is the energy stored in battery at hour t-1, kWh

η_{CHG} is the battery charging efficiency

On the other hand, when the load demand is greater than the available energy generated, the battery bank is in discharging state. Therefore, the available battery bank capacity at time, t, can be expressed as [24]:

$$E_{BAT}(t) = E_{BAT}(t-1) - E_{Needed}(t) \quad \text{(3.11)}$$

where $E_{Needed}(t)$ is the hourly load demand or energy needed at a particular period of time.

Let d be the ratio of minimum allowable SOC voltage limit to the maximum SOC voltage across the battery terminals when it is fully charged. So, the Depth of Discharge (DOD)

$$DOD = (1 - d) \times 100 \ldots\ldots\ldots\ldots\ldots\ldots\ldots\ldots\ldots\ldots\ldots\ldots\ldots\ldots\ldots \text{(3.12)}$$

DOD is a measure of how much energy has been withdrawn from a storage device, expressed as a percentage of full capacity. The maximum value of SOC is 1, and the minimum SOC is determined by maximum depth of discharge (DOD),

$$SOC_{Min} = 1 - \frac{DOD}{100} \ldots\ldots\ldots\ldots\ldots\ldots\ldots\ldots\ldots\ldots\ldots\ldots\ldots\ldots\ldots\ldots\ldots \text{(3.13)}$$

3.7 Power Generation Model

Total hybrid power generated at any time t, is given by [4, 24]:

$$P(t) = \sum_{WEG=1}^{N_W} P_{WEG} + \sum_{PVG=1}^{N_P} P_{PVG} + \sum_{DEG=1}^{N_D} P_{DEG} \ldots\ldots\ldots \text{(3.14)}$$

Where N_W is the number of wind generators unit

N_P is the number of PV cells unit

N_D is the number of diesel generators unit

This generated power will feed to the loads. The diesel generator has the constraint to always operate between 80 and 100% of their kW rating. When this generated power exceeds the load demand then the surplus of energy will be stored in the battery bank. This energy will be used when deficiency of power occurs in order to meet the load demand. The charged quantity of the battery bank has the constraint $SOC_{MIN} \leq SOC(t) \leq SOC_{MAX}$.

The dump load will draw excess energy produced by the renewable generators or diesel generators but unused when the load does not need all the energy and the battery has reached its maximum capacity and cannot store more energy. The approach involves the minimization of a cost function subject to a set of equality and inequality constraints.

3.8 Economic & Environmental Costs of Energy Systems

This work developed a mathematical model of a system that could deploy the best renewable energy options available at any base station located in any part of a country in the world; where the term Best represents the integral (total sum) of the minimum economic and environmental (health and safety) costs of the considered options. For this purpose, we adopt the Hybrid Optimization Model for Electric Renewable (HOMER Pro).

- **The Annualized Cost of a Component**

The annualized cost of a component includes annualized capital cost, annualized replacement cost, annual O&M cost, emissions cost and annual fuel cost (generator). Operation cost is calculated hourly on daily basis. [24,33]:

- **Annualized Capital Cost**

The annualized capital cost of a system component is equal to the total initial capital cost multiplied by the capital recovery factor. Annualized capital cost is calculated using [24,35]:

$$C_{acap} = C_{cap}.CRF\left(i, R_{proj}\right) \ldots\ldots\ldots\ldots\ldots\ldots\ldots\ldots\ldots\ldots\ldots\ldots \quad (3.15)$$

Where $CRF\left(i, R_{proj}\right)$=capital recovery factor

C_{cap} =initial capital cost of the component

- **Annualized Replacement Cost**

The annualized replacement cost of a system component is the annualized value of all the replacement costs occurring throughout the lifetime of the project, minus the salvage value at the end of the project lifetime [33,35].

Annualized replacement cost is calculated using [33,35]:

$$C_{arep} = C_{rep}.f_{rep}SFF\left(i, R_{comp}\right) - S.SFF\left(i, R_{proj}\right) \ldots\ldots\ldots \quad (3.16)$$

where C_{rep} = replacement cost of the component

SFF ( )= sinking fund factor

i = interest rate

R_{comp}= lifetime of the component

R_{proj} = project lifetime

N = number of years

f_{rep} , a factor arising because the component lifetime can be different from the project lifetime, is given by:

$$f_{rep} = \begin{cases} \frac{CRF\left(i, R_{proj}\right)}{CRF\left(i, R_{proj}\right)}, \ R_{rep} > 0 \\ 0, \ R_{rep} = 0 \end{cases} \ldots\ldots\ldots\ldots\ldots\ldots\ldots\ldots\ldots\ldots\ldots\ldots \quad (3.17)$$

R_{rep} , the replacement cost duration, is given by:

$$R_{rep} = R_{comp}.INT\left(\frac{R_{proj}}{R_{comp}}\right) \ldots\ldots\ldots\ldots\ldots\ldots\ldots\ldots\ldots\ldots\ldots\ldots\ldots \quad (3.18)$$

where INT () is the integer function, returning the integer portion of a real value.

SFF (), the sinking fund factor is a ratio used to calculate the future value of a series of equal annual cash flows, is given by:

$$SFF(i,N) = \frac{i}{(1+i)^N - 1} \text{ ……………………………………………….}(3.19)$$

where N = number of years

The salvaged value of the component at the end of the project lifetime is proportional to its remaining life. Therefore, the salvage value S is given by:

$$S = C_{rep}.\frac{R_{rem}}{R_{comp}} \quad \text{……………………………………………..} (3.20)$$

R_{rem} , the remaining life of the component at the end of the project lifetime is given by:

$$R_{rem} = R_{comp} - (R_{proj} - R_{rep}) \text{ ……………………………….}(3.21)$$

- **Annualized Operating Cost**

The operating cost is the annualized value of all costs and revenues other than initial capital costs and is calculated using: [33,35]:

$$C_{aop} = \sum_{t=1}^{365}\left\{\sum_{t=1}^{24}[C_{oc}(t)]\right\} \text{ ………………………………………...} (3.22)$$

where

$C_{oc}(t)$ is the Cost of operating component

- **Cost of Emissions**

The following equation is used to calculate the cost of emissions [33,35]:

$$C_{emissions} = \frac{C_{CO_2}M_{CO_2} + C_{CO}M_{CO} + C_{UHC}M_{UHC} + C_{PM}M_{PM} + C_{SO_2}M_{SO_2} + C_{NO_X}M_{NO_X}}{1000} \text{ ...} (3.23)$$

where C_{CO_2} = cost for emissions of

C_{CO} = cost for emissions of CO [$/t]

C_{UHC} =cost for emissions of unburned hydrocarbons (UHC) [$/t]

C_{PM}=cost for emissions of particulate matter (PM) [$/t]

C_{SO_2} =cost for emissions of NO [$/t]

C_{NO_X} =cost for emissions of

M_{CO_2}=annual emissions of CO [kg/yr]

M_{CO}= annual emissions of CO[kg/yr]

M_{UHC} =annual emissions of unburned hydrocarbons (UHC) [kg/yr] M PM M_{PM}=annual emissions of particulate matter (PM) [kg/yr]

M_{SO_2} =annual emissions of SO2 [kg/yr] NO [kg/yr]

M_{NO_X} =annual emissions of $NO_X[\frac{kg}{yr}]$

Total cost of a component = Economic cost + Environmental cost

where Economic cost = Capital cost + Replacement cost + Operation & Maintenance cost + Fuel cost (Generator)

Environmental cost = Emissions cost

Annualized cost of a component is calculated using [33,35]:

$$C_{ann} = C_{acap} + C_{arep} + C_{aop} + C_{emission} \ldots\ldots\ldots\ldots\ldots\ldots\ldots\ldots \quad (3.24)$$

Annualized total cost of a component is calculated using [33,35]:

$$C_{ann,tot,c} = \sum_{C=1}^{N_C}\left(C_{acap,c} + C_{arep,c} + C_{aop,c} + C_{emissions}\right) \ldots (3.25)$$

where $C_{acap,c}$= Annualized capital cost of a component

$C_{arep,c}$ = Annualized replacement cost of a component

$C_{aop,c}$= Annualized operating cost of a component

From equation (3.26), the Economic and Environmental cost model through Annualized Total Cost of different Configurations of Power System were derived as follows:

Economic and Environmental cost model of running Diesel Generator only is calculated using:

$$C_{ann,tot,g} = \sum_{g=1}^{N_g}\left(C_{acap,g} + C_{arep,g} + C_{aop,g} + C_{emissions} + C_{af,g}\right) \ldots\ldots\ldots\ldots\ldots\ldots\ldots\ldots \quad (3.26)$$

where $C_{acap,g}$= Annualized Capital Cost of Diesel Generator

$C_{arep,g}$= Annualized Replacement Cost of Diesel Generator

$C_{aop,g}$= Annualized Operating Cost of Diesel Generator

$C_{af,g}$= Annualized Fuel Cost for Diesel Generator

Economic and Environmental cost model of running Wind Power only is calculated as:

$$C_{ann,tot,w} = \sum_{W=1}^{N_w}\left(C_{acap,w} + C_{arep,w} + C_{aop,w} + C_{emissions}\right) \ldots\ldots\ldots\ldots\ldots\ldots\ldots\ldots \quad (3.27)$$

where $C_{acap,w}$= Annualized Capital Cost of Wind Power

$C_{arep,w}$= Annualized Replacement Cost of Wind Power

$C_{aop,g}$= Annualized Operating Cost of Wind power

Economic and Environmental cost model of running Solar Power only is calculated as:

$$C_{ann,tot,s} = \sum_{s=1}^{N_s}\left(C_{acap,s} + C_{arep,s} + C_{aop,s} + C_{emissions}\right) \text{....(3.28)}$$

where $C_{acap,s}$= Annualized Capital Cost of Solar Power

$C_{arep,s}$= Annualized Replacement Cost of Solar Power

$C_{aop,s}$ = Annualized Operating Cost of Solar Power

Economic and Environmental cost model of running Batteries is calculated as:

$$C_{ann,tot,b} = \sum_{b=1}^{N_b}\left(C_{acap,b} + C_{arep,b} + C_{aop,b} + C_{emissions}\right) \dots\dots\dots\dots\dots\dots\dots\dots\dots\dots\dots\dots\dots\dots\dots\dots\dots\dots\dots\dots\dots\dots \text{...(3.29)}$$

where $C_{acap,b}$= Annualized Capital Cost of Batteries Power

$C_{arep,b}$= Annualized Replacement Cost of Batteries Power

$C_{aop,b}$= Annualized Operating Cost of Batteries Power

Economic cost model of Converter is calculated as:

$$C_{ann,tot,c} = \sum_{c=1}^{N_c}\left(C_{acap,c} + C_{arep,c} + C_{aop,c}\right) \dots\dots\dots\dots\dots\dots\dots \text{(3.30)}$$

Where $C_{acap,c}$ = Annualized Capital Cost of Converter Power

$C_{arep,c}$= Annualized Replacement Cost of Converter Power

$C_{aop,c}$ = Annualized Operating Cost of Converter Power

Hybridizing the renewable energy generators (PV and Wind) with existing energy (Diesel) results in seven (7) different topologies as:

Economic and Environmental cost model of running Solar only + Diesel Generator + Batteries + Converter is calculated as:

$$C_{ann,tot,s+g+b+c} = \sum_{s=1}^{N_s}(C_{acap,s} + C_{arep,s} + C_{aop,s} + C_{emissions}) + \sum_{g=1}^{N_g}(C_{acap,g} + C_{arep,g} + C_{aop,g} + C_{emissions} + C_{af,g}) + \sum_{b=1}^{N_b}(C_{acap,c} + C_{arep,c} + C_{aop,c}) + \sum_{c=1}^{N_c}(C_{acap,c} + C_{arep,c} + C_{aop,c}) \dots\dots\dots\dots\dots (3.31)$$

Economic and Environmental cost model of running Wind only + Diesel Generator + Batteries + Converter is calculated as:

$$C_{ann,tot,w+g+b+c} = \sum_{w=1}^{N_w}(C_{acap,w} + C_{arep,w} + C_{aop,w} + C_{emissions}) + \sum_{g=1}^{N_g}(C_{acap,g} + C_{arep,g} + C_{aop,g} + C_{emissions} + C_{af,g}) + \sum_{b=1}^{N_b}(C_{acap,c} + C_{arep,c} + C_{aop,c}) + \sum_{c=1}^{N_c}(C_{acap,c} + C_{arep,c} + C_{aop,c}) \dots\dots\dots\dots.. (3.32)$$

Economic and Environmental cost model of running Hybrid (Wind & Solar) + Diesel Generator + Batteries + Converter is calculated as:

$$C_{ann,tot,w+s+g+b+c} = \sum_{w=1}^{N_w}(C_{acap,w} + C_{arep,w} + C_{aop,w} + C_{emissions}) + \sum_{s=1}^{N_s}(C_{acap,s} + C_{arep,s} + C_{aop,s} + C_{emissions}) + \sum_{g=1}^{N_g}(C_{acap,g} + C_{arep,g} + C_{aop,g} + C_{emissions} + C_{af,g}) + \sum_{b=1}^{N_b}(C_{acap,c} + C_{arep,c} + C_{aop,c}) + \sum_{c=1}^{N_c}(C_{acap,c} + C_{arep,c} + C_{aop,c}) \ldots\ldots\ldots\ldots\ldots (3.33)$$

3.9 The Energy Optimization Model

The process of optimization had been of concern for man for many ages [18]. Previously there were no defined and scientific rules for optimum conditions. But with the passage of time and advancement in science and technology, everything was considered to be based on certain reasons or logics. Mathematical calculations involving process of optimization have become more famous in recent years. True meaning of optimization is to find the best answer for a particular problem. For example, problems dealing with the cost will require the best cost to be as less as possible. On the other hand, problems dealing with profit will see the maximum value as the best answer. So 'Optimum' is the word which is used to demonstrate the meaning of best, and the process of finding the best solution to a particular problem is known as the process of optimization [4]. To solve an optimization problem, we require an optimization algorithm. An optimization algorithm is the algorithm which is used to define an optimized solution for a particular function. Thus, for the stand-alone PV/Wind-Diesel hybrid system with constraints under study, we have the following optimization algorithm.

Minimize

$$Cost = \sum_i C_{PV_i} N_{PV_i} + \sum_j C_{W_j} N_{W_j} + \sum_l C_{DG_l} N_{DG_l} + \sum_m C_{B_m} N_{B_m} + \sum_n C_{C_n} N_{C_n} \ldots\ldots\ldots\ldots (3.34)$$

Subject to the constraints

$$\text{Load} \leq \sum_i C_{PV_i} N_{PV_i} + \sum_j C_{W_j} N_{W_j} + \sum_l C_{DG_l} N_{DG_l} \ldots\ldots\ldots\ldots.... (3.35)$$

$$\text{Maximum Power Wattage} \leq P_{C_n} N_{C_n} \ldots\ldots\ldots\ldots\ldots\ldots...\ldots\ldots..(3.36)$$

$$SOC_{min} \leq SOC(t) \leq SOC_{max} \ldots\ldots\ldots\ldots\ldots\ldots\ldots..\ldots\ldots\ldots (3.37)$$

where C_{PV_i} = Cost of a photovoltaic module

C_{W_j} = Cost of wind turbine

C_{DG_l} = Cost of a diesel generator

C_{B_m} = Cost of a battery

C_{C_n} = Cost of a converter

N_{PV_i} = Number of photovoltaic modules

N_{W_j} = Number of wind turbines

N_{DG_l} = Number of diesel generators

N_{B_m} = Number of battery bank to be use.

N_{C_n} = Number of converters

E_{Si} = kWh generated by photovoltaic module i

E_{Wj} = kWh generated by wind turbine j

E_{DGl} = kWh generated by a diesel generator l

P_{Cn} = Maximum output power of converter n

SOC_{min} = State of battery charge at minimum

SOC_{max} = State of battery charge at maxim

In the optimization procedure, the sizes of system components are decision variables, and their costs and the pollutant emissions are the objective function.

- **Objective Function**

The objective functions to be minimized are the total costs (N) and the pollutant emissions (kg of CO_2).

- **Costs**

The costs objective function is the Total Net Present Cost of the system (NPC), which includes the cost of the initial investment plus the discounted present values of all future costs throughout the total life of the installation. The life of the system is usually considered to be the life of the PV panels - which are the elements that have a longer lifespan. In the following paragraph, the costs taken into account are indicated.

- Cost for purchasing the PV panels, the wind turbine, the batteries, the inverter, the charge regulator, and the Diesel generator.
- Costs of maintenance of the components.
- Costs of replacing the components throughout the life of the system.
- Costs of operation and maintenance of components throughout the life of the system.
- Cost of the fuel consumed throughout the life of the system.

A more detailed description of its calculation can be found in [13, 14, 7,19].

- **Pollutant Emissions**

In order to measure the pollutant emissions, the weight of CO_2, in kg, is considered; it represents the largest percentage of all emissions when Fuel is burnt [1], and it is the main cause of the greenhouse effect. It is considered that the total amount of kg of CO_2 produced by the hybrid system throughout one year is the correct measure of the pollutant emissions and, therefore, it can be used as the objective to be minimized. The developed algorithm has as input data the number of kg of CO_2 produced per liter of fuel consumed by the Diesel generator. This value depends on the characteristics of the Diesel generator and of the characteristics of the fuel, and it usually falls in the 2.4-2.8 kg/L range [1].

Energy Optimization in base stations is being carried out globally by industrial giants such as Ericsson, Chevron and Energy Cybernetics [8] etc. It involves the use of alternatives such as bio fuel, solar energy and wind. In this thesis, the parameters useful for making the decision on the type of energy solution suitable for a site and its location are grouped into the following:

- Total Cost of Energy Generation and;
- Total Environmental impact of each energy solution

These two summarize all the factors we proposed for evaluating the suitability of energy solution for any BTS and location. The model is produced here in the figure (3.7) below.

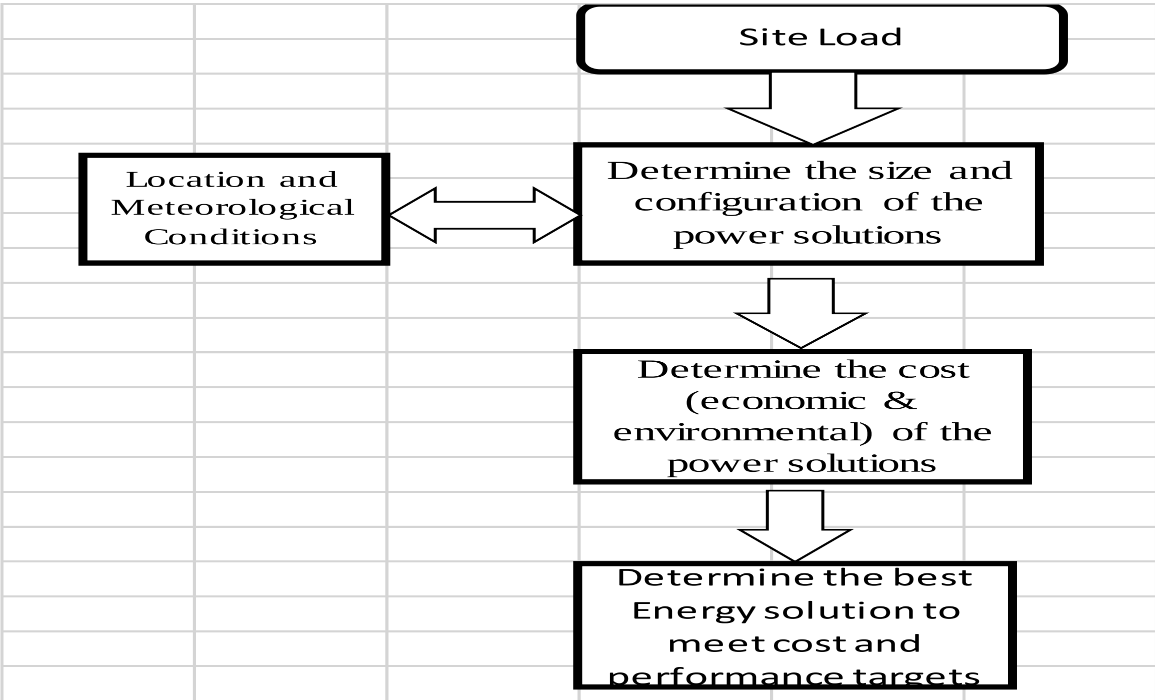

Figure 3.8: Model for choosing Power Solution for a BTS Site [20]

The total net present cost (NPC) of a system is the present value of all the costs that it incurs over its lifetime minus the present value of all the revenue that it earns over its lifetime. Revenues include salvage value and grid sales revenue. The Net Present Cost (NPC) for each component is derived using [23]:

$$CC_{NPC} = \frac{C_{ann,tot}}{CRF(i,R_{proj}} \ldots\ldots\ldots\ldots\ldots\ldots\ldots\ldots\ldots\ldots\ldots\ldots\ldots\ldots\ldots\ldots\ldots\ldots(3.38)$$

The capital recovery factor (CRF) is [23]:

$$CRF = \frac{i.(1+i)^N}{(1+i)^N-1} \ldots\ldots\ldots\ldots\ldots\ldots\ldots\ldots\ldots\ldots\ldots\ldots\ldots\ldots\ldots\ldots\ldots\ldots\ldots\ldots\ldots\ldots\ldots\ldots(3.39)$$

The economic optimization identifies the most financially attractive solution for ten scenarios - various combinations of Diesel Generator, wind, and solar power. The work uses HOMER Pro but this study has tried to go beyond by including a detailed load analysis and suggesting ways of analyzing the results. Data for the six optimized scenarios are reported and graphed to present the viability and financial impact of each scenario.

CHAPTER FOUR
HYBRID SYSTEM ANALYSIS

4.1 Hybrid power system analysis

A hybrid power system is one in which the electrical load is served by two or more power sources. Because renewable energy sources, such as Solar and Wind, are inherently intermittent, frequently they are combined with dispatch able power sources such as utility grid and diesel generators, to ensure the continuous supply of power. Energy storage is often included in hybrid systems that can deliver a certain amount of energy on power demand until its stored energy is exhausted (i.e. Provide a constant flow of uninterrupted power), but it must be recharged at that point. Other advantages of the hybrid system are the stability and immobility of the system and a lower maintenance requirement, thus reducing downtime during repairs or everyday maintenance. In addition to this, as well as being indigenous and free, renewable energy resources also contribute to the reduction of emissions and pollution [27].

4.2 Basic Components of the Hybrid System

The basic components of the hybrid system are the wind plant and the PV system. Others are additional/auxiliary components which help in the full time functioning of the hybrid system. The principle of operation of the basic components has been covered before. The power conditioners are set of power electronics converters which enable to handle the variability of wind and solar resources. They are composed of DC/DC, AC/DC, DC/AC converters. When there is an excess of energy (from the wind and PV), it is directed to the battery through the converter and DC center. In addition, frequency and voltage regulation, control circuitry are to be included in the operation and control center. Similarly, the DC output of the PV panel is connected to the system via the DC center. The DC center is integrated with the system through DC/AC and AC/DC converters. As well as, it is connected to PV and battery components.

4.3 Load Estimation

The term load refers to a demand for electric or thermal energy, if any. Three types of loads can be modeled using HOMER Pro: primary load which is electric demand (9.4kw) that must be served according to a particular schedule, deferrable load which is electric demand that can be served at certain period of time, the exact timing is not important and thermal load which is a demand for heat.

4.4 Load profile of the base station

This study is relied on actual load data and actual meteorological data it could be help in real design analysis for implementation of hybrid renewable energy system for the area in question. The load profile can be examined. The facilities at the BTS site are radio equipment, power conversion equipment, antenna equipment, transmission equipment, and auxiliary equipment. These facilities are all ON for 24hrs (12:00am – 11:00pm) per day except the auxiliary equipment (aviation light) that comes ON only for 13hrs (06:00pm – 7:00am) per day. The power consumptions are assumed to be identical for every day of the year. The daily energy consumption is 111.5kWh/day. The daily average load variation for the base station equipment is shown in table 4.1.

Table 4-1: Maximum Load input for base station

Hour	**Assumed max. load input profile(kw)**
00:00-10:00	4.5
10:00-13:00	5.2
13:00-15:00	4.5
15:00-17:00	5.2
17:00-00:00	4.5
24hour	Total =111kwh/day

Figure 4.1: Homer Pro Output Average Daily load profile of the sites

4.5 Renewable Energy Resources Assessment

The term resource applies to anything coming from outside the system that is used by the system to generate electric power. That includes the four renewable resources (solar, wind) as well as any fuel used by the components of the system. Renewable resources depend extremely on location. The solar resource depends strongly on latitude and climate, the wind resource for large-scale atmospheric circulation patterns and geographic influences. Moreover, at any one location a renewable resource may exhibit strong seasonal and hour-to-hour variability.

The nature of the available renewable resources affects the behavior and economics of renewable power systems, since the resource determines the quantity and the timing of renewable power production. The careful modeling of the renewable resources is therefore an essential element of system modeling. In this section how to model the renewable resources used in this thesis is described.

A.Solar energy resource

To model a system containing a PV array, the solar resource data for the location of interest has been provided. Solar resource data indicate the amount of global solar radiation (beam radiation coming directly from the sun, plus diffuse radiation coming from all parts of the sky) that strikes the Earth's surface in a typical year. The data can be in one of three forms: hourly average global solar radiation on the horizontal surface (kWh/m^2), monthly average global solar radiation on the horizontal surface (kWh/m^2/day), or monthly average clearness index. The clearness index is the ratio of the solar radiation striking earth's surface to the solar radiation striking the top of the atmosphere. A number between zero and one, the clearness index is a measure of the clearness of the atmosphere.

The average solar irradiation is in kWh/m²/day from NASA surface meteorology and solar energy database. Clearness index and the average daily radiation for 22 years are shown in tables 3.9 & 3.10 while summarized by HOMER Pro in figure 4.2 as the monthly solar radiation variation of the sites where the average solar radiation found to be 5.89kwh/m^2/day. The lowest solar radiation profile is indicated in the months of June, July, August, and October Whereas, December, January and February are the sunniest months.

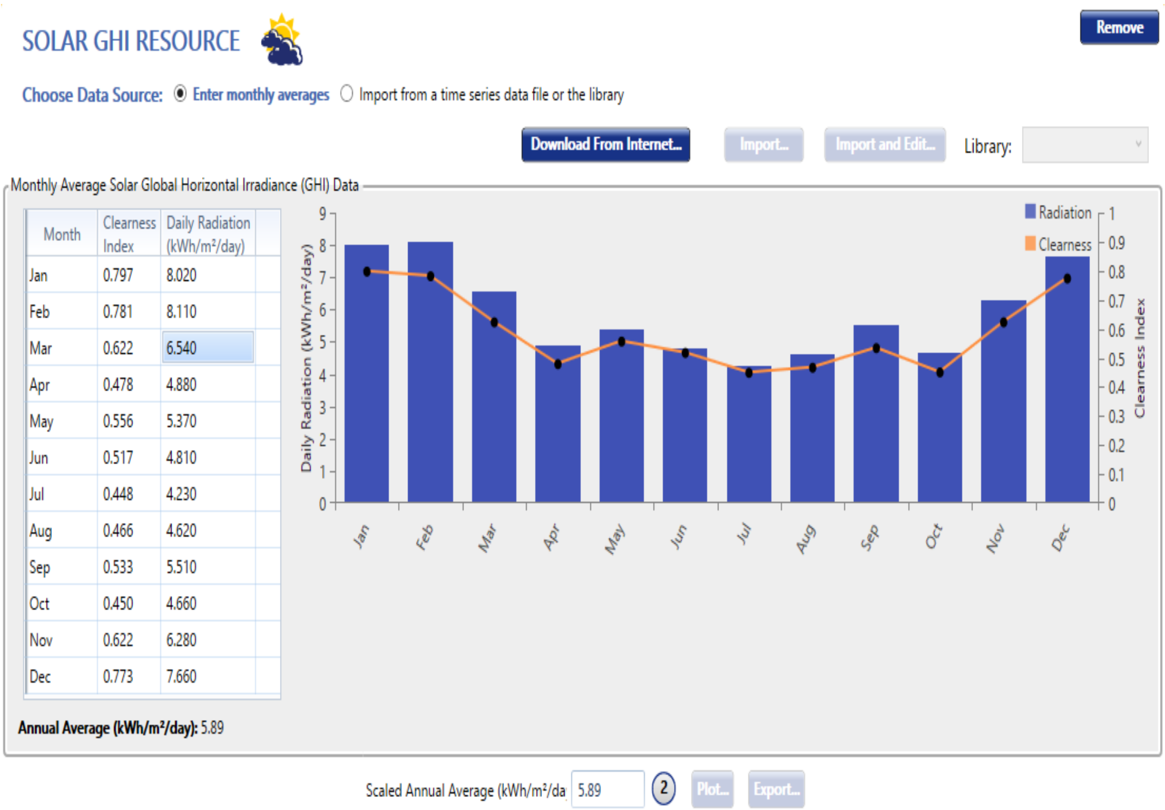

Figure 4.2: HOMER Pro output graphic for Average solar profile for selected locations.

B. Wind energy resource

To model a system comprising one or more wind turbines, the wind resource data indicating the wind speeds the turbines would experience in a typical year has been provided. The user can provide measured hourly wind speed data if available. Otherwise, HOMER Pro. can generate synthetic hourly data from 12 monthly average wind speeds and four additional statistical Parameters: The Weibull shape factor, the autocorrelation factor, the diurnal pattern strength, and the hour of peak wind speed. The Weibull shape factor is a measure of the distribution of wind speeds over the year. The autocorrelation factor is a measure of how strongly the wind speed in one hour tends to depend on the wind speed in the preceding hour [22]. For complex topography the autocorrelation factor is (0.70 - 0.80) while for a uniform topography the range is higher, (0.90 - 0.97). A typical range for the autocorrelation factor is 0.8 – 0.95 [22]. An average value of 0.85 is used here because the selected area is of averagely uniform topography. The diurnal pattern strength is a measure of how strongly the wind speed tends to depend on the time of day [22].

Typical values for diurnal pattern strength range from 0 to 0.4. A value of 0.25 has been selected for calculations. The hour of peak wind speed is the hour of the day that tends, on average, to be the windiest throughout the year. The typical range for the time of peak wind speed is 14:00-16:00[22].

This data can be extrapolated to the designated wind turbine height of 50 m. Monthly average wind speed data for 22 years are shown in tables 4.2,4.3 & 4.4 while summarized by HOMER Pro in figure 4.4 the monthly wind speed variation of the site at 50 m heights where the average wind speed found to be 5.52 m/s. The lowest wind speed profile is indicated in the months of October, November, December and April Whereas, June, July, August and September are the windiest months.

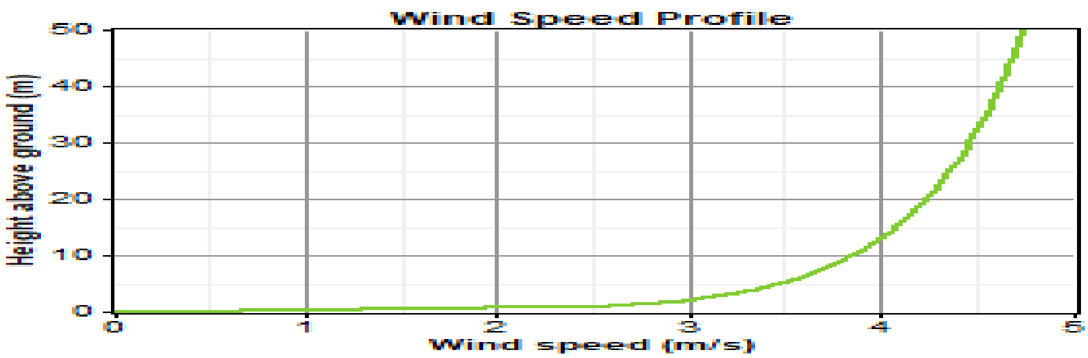

Figure 4.3: Height and wind speed relation

As wind turbine height increase length from ground the wind speed also increase and hence, power production also rises.

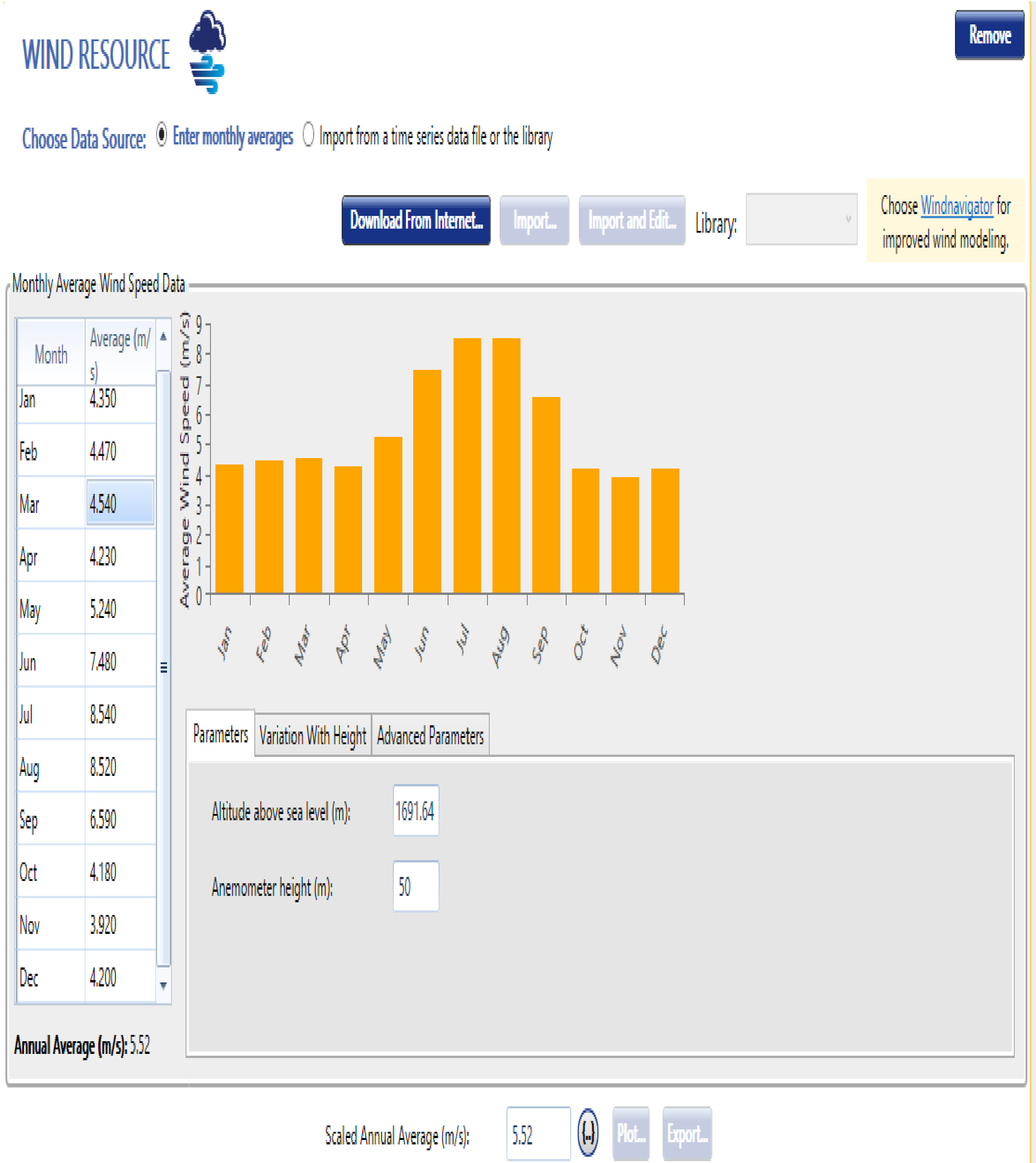

Figure 4.4: HOMER output graphic for wind resource profile for selected locations

Table 4-2: Monthly average wind speed(m/s) for four study sites at 50m height

LAT	LON	Parameter	JAN	FEB	MAR	APR	MAY	JUN	JUL	AUG	SEP	OCT	NOV	DEC	ANN
7.13841	40.71111	WS50M	3.74	4.02	4.43	4.22	4.36	5.66	6.38	6.48	5.37	3.75	3.53	3.62	4.63
7.19931	40.58231	WS50M	3.74	4.02	4.43	4.22	4.36	5.66	6.38	6.48	5.37	3.75	3.53	3.62	4.63
7.24411	40.74021	WS50M	3.74	4.02	4.43	4.22	4.36	5.66	6.38	6.48	5.37	3.75	3.53	3.62	4.63
7.25831	40.83461	WS50M	3.74	4.02	4.43	4.22	4.36	5.66	6.38	6.48	5.37	3.75	3.53	4.13	4.63

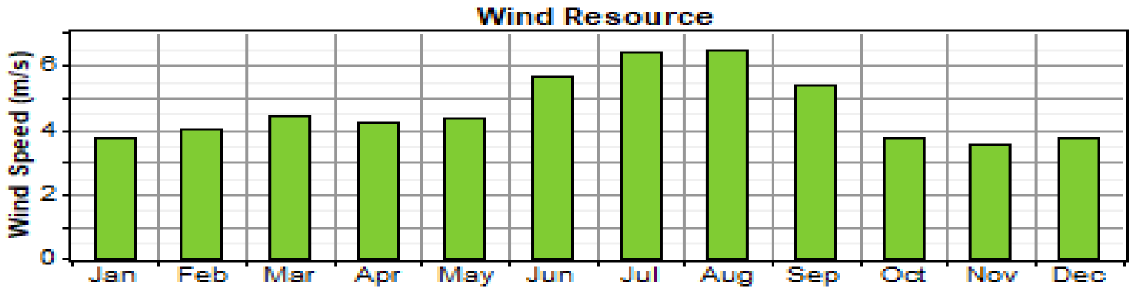

Figure 4.5: HOMER output graphic for wind resource profile for four study sites

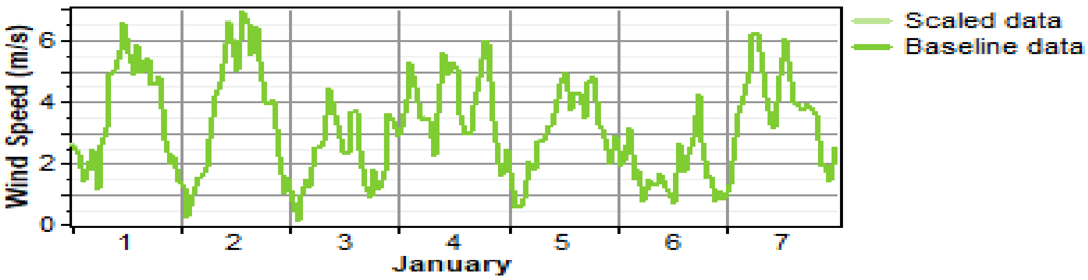

Figure 4.6 Average Hourly wind speed for a year

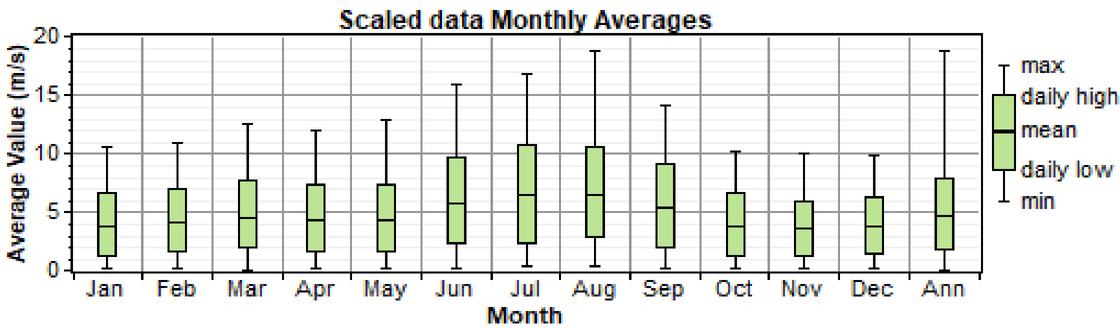

Figure 4.7: Average monthly wind speed for a year 2020

Table 4-3: Monthly average wind speed(m/s) for three study sites at 50m height

LAT	LON	Parameter	JAN	FEB	MAR	APR	MAY	JUN	JUL	AUG	SEP	OCT	NOV	DEC	ANN
7.281	40.31	WS50M	3.26	3.53	3.95	3.72	3.48	3.95	4.31	4.42	3.83	3.3	3.24	3.24	3.69
7.24	40.37	WS50M	3.26	3.53	3.95	3.72	3.48	3.95	4.31	4.42	3.83	3.3	3.24	3.24	3.69
6.88	40.98	WS50M	3.47	3.9	4.49	4.19	3.94	4.37	4.42	4.58	4.33	3.37	3.17	3.23	3.96

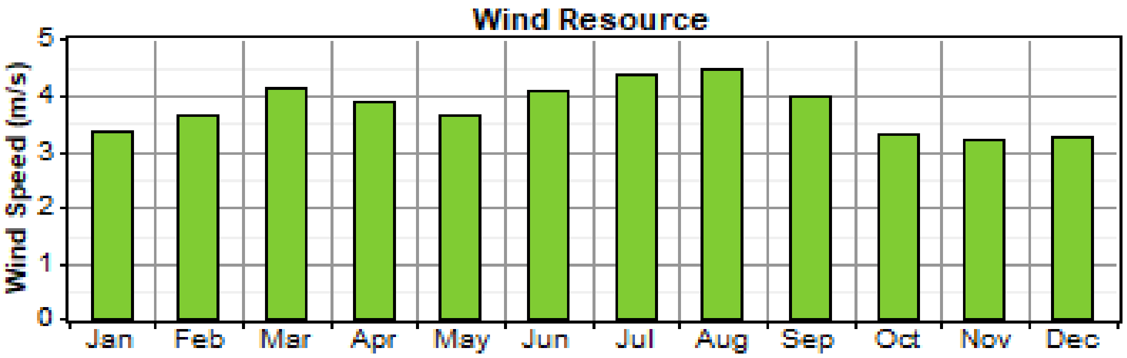

Figure 4.8: HOMER output graphic for wind resource profile for study locations

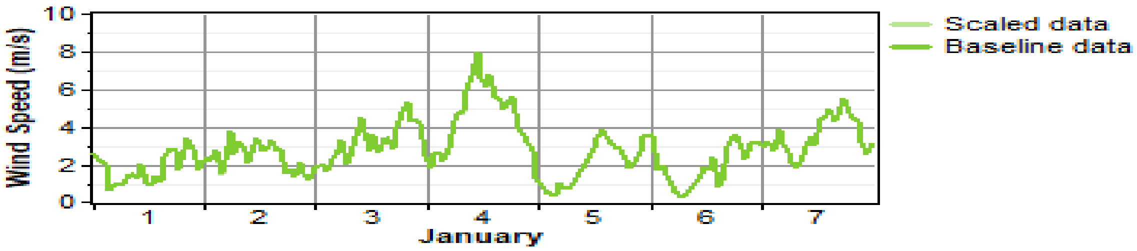

Figure 4.9: Average hourly wind speed for a year 2020.

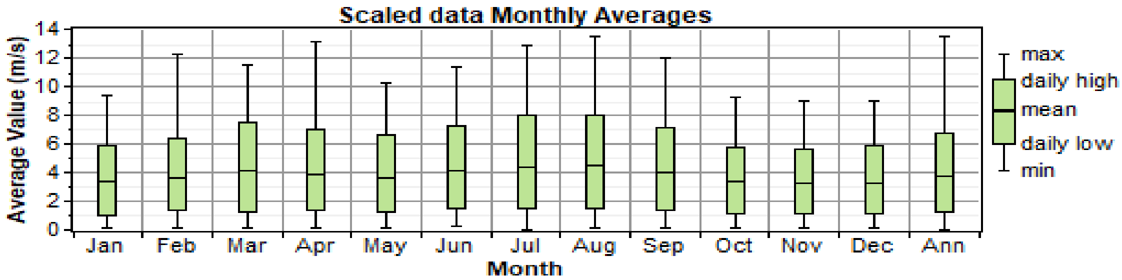

Figure 4.10: Average monthly wind speed for a year

Table 4-4: Monthly average wind resource for nine study sites at 50m height

LAT	LON	Parameter	JAN	FEB	MAR	APR	MAY	JUN	JUL	AUG	SEP	OCT	NOV	DEC	ANN
6.991	40.85	WS50M	4.38	4.54	4.5	4.04	5.26	7.68	8.76	8.74	6.98	4.07	3.81	4.15	5.58
6.549	41.78	WS50M	4.38	4.54	4.5	4.04	5.26	7.68	8.76	8.74	6.98	4.07	3.81	4.15	5.58
6.567	41.61	WS50M	4.38	4.54	4.5	4.04	5.26	7.68	8.76	8.74	6.98	4.07	3.81	4.15	5.58
6.651	41.44	WS50M	4.46	4.52	4.55	4.26	5.27	7.54	8.63	8.57	6.18	4.27	4.03	4.35	5.55
6.721	41.36	WS50M	4.46	4.52	4.55	4.26	5.27	7.54	8.63	8.57	6.81	4.27	4.03	4.35	5.61
6.817	41.26	WS50M	4.46	4.52	4.55	4.26	5.27	7.54	8.63	8.57	6.18	4.27	4.03	4.35	5.55
6.896	41.13	WS50M	4.46	4.52	4.55	4.26	5.27	7.54	8.63	8.57	6.18	4.27	4.03	4.35	5.55
7.235	41.08	WS50M	4.09	4.3	4.61	4.47	5.16	7.06	806	8.1	6.54	4.16	3.87	4	5.38
7.326	41.18	WS50M	4.09	4.3	4.61	4.47	5.16	7.06	806	8.1	6.54	4.16	3.87	4	5.38

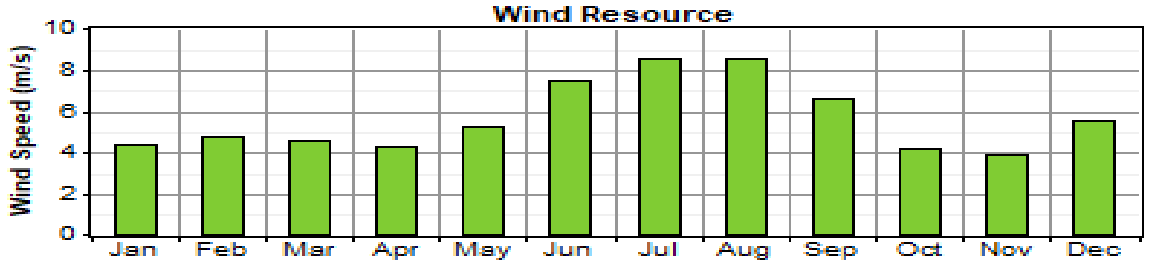

Figure 4.11: HOMER output graphic for wind speed(m/s) profile for nine study sites

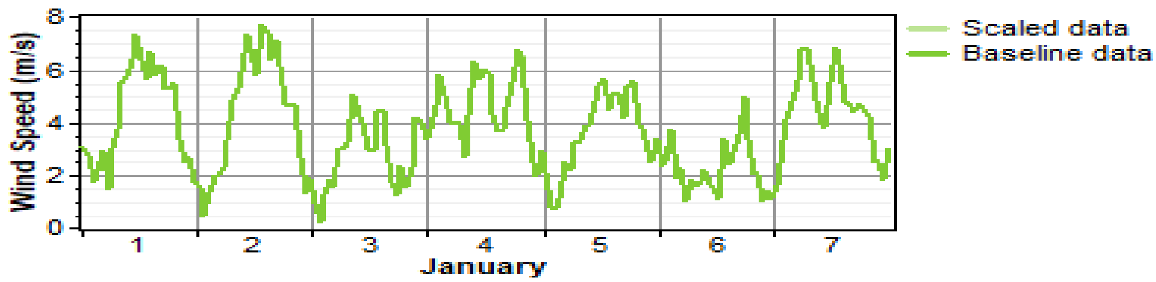

Figure 4.12: Average hourly wind speed for a year

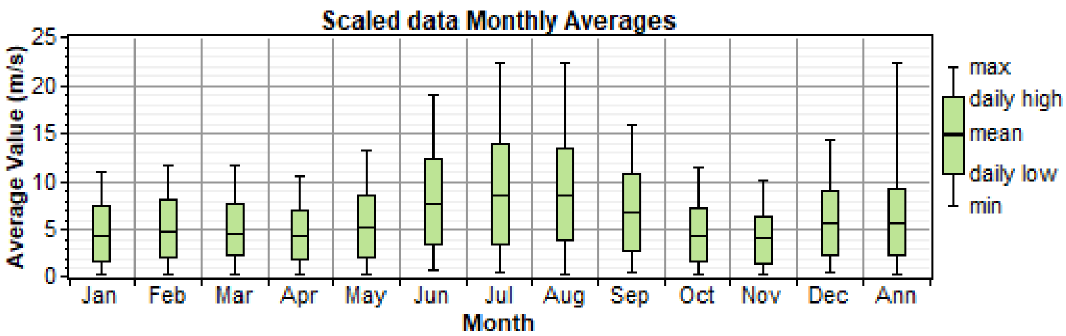

Figure 4.13: Average monthly wind speed for a year 2020

4.6 Components Cost Data and Size Specifications

The HOMER Pro software is used to determine the best optimal sizing and feasibility study of the system. The initial choice of the components size is based on the site load profile. Some of the input values into the software are expressed in size and in quantity. Wind turbines, batteries are the power system components which vary in quantity, and solar PV, diesel generator and converter are other components that vary in size. The main purpose of the work is searching the optimum power system configuration that would meet the load demand with minimum NPC and COE.

Initial capital cost of components: It is the total installed cost deployed to purchase and install the component at the commencement of the project.

O&M cost: It is the cost accounted for maintenance and operation of the system. The entire schema components considered in this study have different operation and maintenance costs. Miscellaneous O&M costs considered by HOMER are like emission penalties, capacity shortage penalty and fixed operation and maintenance costs.

Replacement cost: This is the cost required to replace worn out components at the end of its life cycle. This cost is different from the initial cost of the component, due to the following reasons. At the end of its lifecycle not all of the spheres of the component need to replace, Costs from donors may eliminate or can reduce initial costs, however replacement cost may not account travel costs but initial costs do.

4.6.1 Solar PV Size and Cost

In this project the solar panel considered was a 1 kW, capital cost and replacement cost for 1 kW of PV array are taken as $2500 and $2000, respectively. As the installation cost is taken as 60% of the PV price and the operation and maintenance cost would be 1.7% per year [40]. In this case, four different types of PV arrays are considered to get the optimal size (0,16,24,32,40kW). The lifetime of PV arrays was taken as 25 years and no tracking system was considered. The following default parameters were considered for modeling of the power system like; the de-rating factor was taken as 80%, ground reflectance was also considered as 20%, slope and azimuth taken from the system. The PV de-rating factor is a scaling factor that HOMER applies to the PV array power output to account for reduced output in real-world operating conditions for such factors as ambient temperature, soiling of the panels, wiring losses, shading, snow cover, aging, and so on.

Table 4-5: PV module specifications

Description	Specification
PV module material	Poly/multi-crystalline silicon
Peak power(Pmax)	250wp
Voltage at peak power(Vm)	29.95v
Current at peak power(Im)	8.35A
Open ciecuit voltage(Voc)	37.25v
Short circuit current(Isc)	8.70A
Module efficincy	14%
capital cost/kw	$2500.00
life time	25 year

4.6.2 Wind Turbine Size and Cost

Depending on the wind speed sources the turbine has to generate large amounts of energy to contribute significant renewable fraction and this can be performed using single large wind turbine or a number of smaller turbines. Quantities of turbines, service time, hub height, cost of the component, type of electricity generated, cut-in wind speed is the restrictive values to select wind turbine.

The wind turbine used in this project is Power having the model Generic with a rated capacity of 10 kW in combination of rectifier system to provides DC power. The initial cost of one unit in the current market price is considered as $18000.00. Replacement and annual operational maintenance costs were assumed as $12,509.00 and $200/year, respectively. O&M cost of wind turbine was proposed about 2% of its initial capital cost as given in [40]. Replacement cost of the wind turbine considered in this case is about 69.5% of capital cost after 15year service life. In order to find an optimal size, three different wind turbine options were analyzed: 0, 1, 2, &3 turbines. The operational lifetime of a turbine is considered as 15 years and Hub height is 50m. Wind turbines should be easy to install particularly in remote telecom sites on the tower height.

Table 4-6: Wind Turbine specifications

Description	Specification
Rated out put power	Generic 10kw
Rotor diameter	6m
Cut-in wind speed	2.5m/s
Working wind speed	3-35m/s
Survival wind speed	50m/s
Blade material	Carbon reinforced fiber glass
capital cost	$18,000.00
life time	15 year

4.6.3 Battery Size and Cost

The vented lead acid, tubular-plate, deep cycle battery of Hoppecke 24 Opzs 3000 model battery with one cell, 2 V, 3000 Ah, and 6 kWh is selected in the proposed system, since this the type of battery used in the selected Ethio-telecom BTS site with 24 batteries in one string of 48V. The initial cost of one unit is considered as $2240.00, Replacement and operational maintenance costs were assumed as $1809.00 and $24/year, respectively. In order to find an optimal configuration, the battery bank was assumed to consist of any number of battery string (0, 1,2, &3). Each battery string contains twenty four batteries and the lifetime throughput of each battery is estimated to be 15year.

Benefits

1.Long life design for cyclic or oat application

2.Excellent charge acceptability and deep cycling performance

3.Excellent over discharge recovery capability

4.Superior charging & discharging ability in low current

5. Extend service life under high temperature

Table 4-7: Battery specifications

Description	Specification
Battery Model	Hoppecke 24 Opzs 3000
Battery capacity	3000Ah @ 10hr to 1.80V @ 25˚C(77˚F)
Nominal Voltage	2V
Efficiency	80%
min.state of charge	40%
capital cost	$2,240.00
life time	15 year(10365kwh)

4.6.4 Diesel Generator Size and Cost

The cost of diesel generators available in the market varies, but the DG used in the particular Ethio-telecom BTS site is Deutz air cooled DG with rated output power of 16 kW and 20 kVA with the initial capital cost of $1025.00/kw and the fuel consumption at full load is less than 4 litters. Replacement and operational costs were assumed $820/kW and $0.80/h, respectively. The operating lifetime was also considered 20 year. currently, per liter price of diesel in Ethiopia is around $0.8.

In this study sizes of existing sites DGs were 16kw, I considered Auto size Genset for the simulation. The minimum load ratio was set at 30%.

Table 4-8: Diesel Generator specifications

Deisel Generator Model	Deutz
Rated power	16kw/20kvA(Auto size Genset)
Rated voltage	380 or 220
Rated current	38A
Speed	1500rpm
Frequency	50Hz
Cooling system	Air cooled
Capital cost	$1025.00/kw
life time	20year

4.6.5 Power Converter Size and Cost

A converter needs to maintain the flow of energy between AC and DC power system components. The rated power of the inverter should be equal to or larger than the peak load. The initial installation cost, the replacement cost, and the annual O&M cost per 3 kW are considered $656, $556, and $16, respectively. The lifetime and efficiency of the inverter and Rectifier are set at 15 years and 95%,85% respectively. The sizes of the simulation-values of the applied Converter are 3 to 30 kW.

Table 4-9: MPPT controller specifications

Description	Specification
Converter model	Emerson S48-3000e
Max.out put power	3000w
Regulation method	MPPT
Input voltage	58 to 150VDC
Max.Short circuit current	100A DC
Nominal voltage	48vDC(adj.range:-48 to 58VDC)
Efficiency	≤ 95 %
capital cost	$656
life time	15 year

The PV array, wind turbine, diesel generator, Inverter and battery maintenance costs are estimates based on approximate time required and estimated wages for this sort of work in a remote area of Ethiopia. All initial costs including installation and commissioning, replacement costs and operating & Maintenance costs at sites are summarized in Table 4.10. All costs presented are in USD ($).

Table 4-10: Hybrid Components size & cost Summery

Components	Size	Capital cost	Replacement cost	O&M cost/year	Consider size	lifetime
PV Module	1kw	$2,500.00	$2,000.00	$25/y	10 to 40kw	25years
Generic Wind Turbine	10kw	$18000.00	$12509.00	200/y	0,1,2,3pcs	15years
Hoppecke 24 Opzs 3000Battery	2v,3000 AH, 6kw	$2240.00	$1809.00	$24/y	1,2,3,4 string	15years
Power Converter	1kw	$656	$556	$16/y	3 to 30kw	15years
Diesel generator	1kw	$1025.00/kw	$820.00 /kw	2.8/h	10 to 30kw	20year

Inputs to the HOMER software in simulation have been described (the technical and economic data of all the components of the hybrid system).

The input parameters and system constraints, as described above, were used to simulate hybrid systems and perform optimization analysis. HOMER determines the optimal system by choosing suitable system components (system configuration) depending on parameters like solar radiation, wind speed, diesel price and maximum annual capacity shortage. The feasibility of a configuration is based on the NPC and hourly performance. The results are presented in graphical and tabular forms in chapter five.

4.7 System Architecture and Sizing

This system takes a 9.4kW energy demand for each GSM/UMTS type telecommunications base station which is selected from East Bale, Ethiopia. The system architecture adopted is DC coupled. As shown in the figure 4.14 below, in the hybrid energy system, the primary renewable sources are placed in parallel with a standby secondary non-renewable resource (in this case the diesel generator). The HOMER Pro software is used for this optimization study. As shown in the system architecture, the renewable sources (wind and PV systems) feed into the DC side of the network; the converter converts the DC output of the renewable sources to AC and back, for battery storage, as the case may be. The load is connected to the DC bus side of the network. The diesel generator shown feeds directly into the AC bus of the network.

The renewable sources (solar panels & Wind) and the batteries will share a common set of power conversion equipment. So DC coupling will help to improve the overall energy output of solar-storage hybrid system while optimizing cost and increasing the overall system reliability and flexibility.

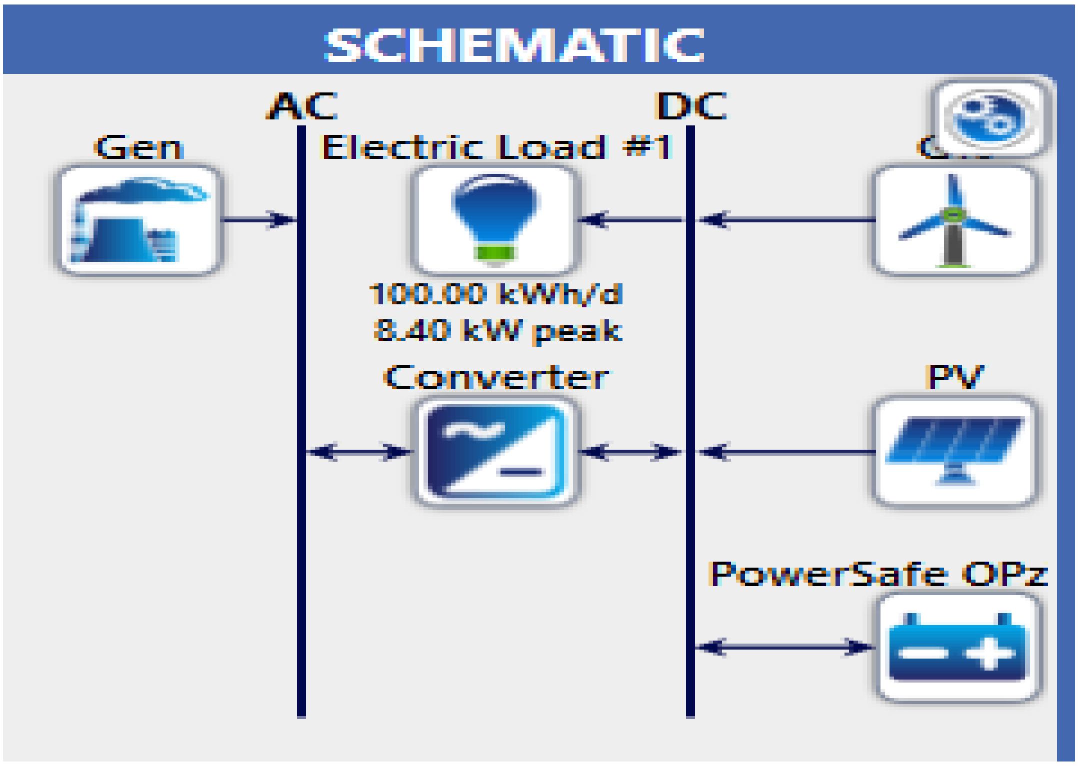

Figure 4.14: System architecture for Optimization study in HOMER Pro

CHAPTER FIVE

RESULTS AND DISCUSSION

5.1 Optimization Results

After introducing all of the input variables, the HOMER Pro software is running repeatedly to get the feasible system configuration; component sizes that meet the load requirement and the input constraints at the lowest NPC and then presents the results of the simulation in terms of optimal systems and sensitivity analysis. The Optimization result displays ten different configurations according to the lowest NPC for further analysis and to increase the chance of finding most optimized system. A hybrid system with less NPC, less COE, higher renewable fraction, less capacity shortage, and minimum fuel consumption would be suggested as optimum system. HOMER simulates every system in all set of component combination (search space) and ranks all the feasible systems according to increasing net present cost. In the case of this study, the software performing 45360 simulations iteration.


Export... Export All...

Sensitivity Cases

Left Click on a sensitivity case to see its Optimization Results.

Compare Economics Column Choi

Sensitivity	Architecture							Cost				System	
G10 Hub Height (m)	PV (kW)	PV-MPPT (kW)	G10	Gen (kW)	PowerSafe OPzV 3000	Converter (kW)	Dispatch	NPC ($)	COE ($)	Operating cost ($/yr)	Initial capital ($)	Ren Frac (%)	Total Fuel (L/yr)
10.0	33.4	27.0			24		CC	$190,340	$0.374	$3,314	$143,170	100	0
50.0	33.4	27.0			24		CC	$190,340	$0.374	$3,314	$143,170	100	0

Optimization Results

Left Double Click on a particular system to see its detailed Simulation Results.

Categorized

Architecture							Cost				System		Ge	
PV (kW)	PV-MPPT (kW)	G10	Gen (kW)	PowerSafe OPzV 3000	Converter (kW)	Dispatch	NPC ($)	COE ($)	Operating cost ($/yr)	Initial capital ($)	Ren Frac (%)	Total Fuel (L/yr)	Hours	Production (kWh)
33.4	27.0			24		CC	$190,340	$0.374	$3,314	$143,170	100	0		
27.0	27.0	1		24		CC	$218,369	$0.427	$4,019	$161,164	100	0		
39.4	27.0	1	20.0	24	1.00	CC	$305,188	$0.588	$6,452	$213,350	96.6	574	250	1,250
33.7	27.0		20.0	48	1.00	CC	$315,812	$0.610	$6,807	$218,931	96.6	574	250	1,250

Figure 5.1: Sensitivity & Optimization results of the system

In the optimization process, the decision variables are sizes of the components; the objective functions are minimizing components cost and pollutant emissions.

5.2 Simulation Results

The detailed result analyses obtained at the end of the simulations are described below:

Table 5-1: Homer economic cost simulation results on existing dual diesel generator sites

Component	Capital ($)	Replacement ($)	O&M ($)	Fuel ($)	Salvage ($)	Total ($)
Generator 1	262,400	219916	1,089,581	70987	-37,711	1,506,435.5
Generator 2	262,400	219916	1,089,581	70987	-30,265	1,506,435.5
Hoppecke 24 OPzS 3000	36,960	13,442	6,712	0	-44	57,070
Converter	19,680	6,046	5,594	0	-1,024	30,295
Other	22,000	0	95,559	0	0	117,559
System	603,440	459,319	2,287,029	141,974	-69,044	3,422,719

Generator 1 & generator 2 are the dual diesel generator used for power generation. One string Hoppecke Opzs 3000AH back up battery, and converter(rectifier) used to convert AC to Dc. Salvage is the remaining value in a component of the power system at the end of the project lifetime

A negative return on investment means the investment properties are actually losing money.in this case the cause of negative return on investment is spending too much on operation and maintenance.

Simulation Results

System Architecture: EnerSys PowerSafe OPzV 3000 (1.00 strings)
Generic flat plate PV (27.0 kW/27.0 kW) HOMER Cycle Charging
Generic 10 kW (1.00)

Hub Height (10.00 m)

Total NPC:	$218,369.20
Levelized COE:	$0.4266
Operating Cost:	$4,019.06

Cost Summary | Cash Flow | Compare Economics | Electrical | Renewable Penetration | EnerSys PowerSafe OPzV 3000 | Generic flat plate PV | Generic 10 kW | Emissions

Cost Type
- Net Present
- Annualized

Categorize
- By Component
- By Cost Type

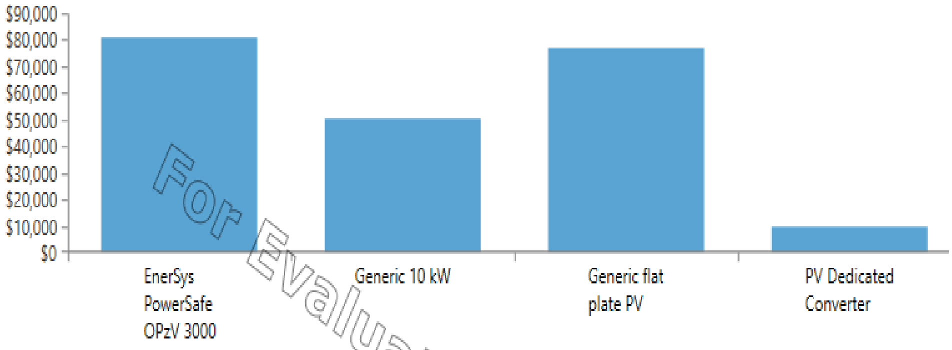

Component	Capital ($)	Replacement ($)	O&M ($)	Fuel ($)	Salvage ($)	Total ($)
EnerSys PowerSafe OPzV 3000	$53,760.00	$22,012.68	$8,198.49	$0.00	($3,130.55)	$80,840.61
Generic 10 kW	$34,000.00	$13,658.53	$5,693.39	$0.00	($2,821.28)	$50,530.64
Generic flat plate PV	$67,500.00	$0.00	$9,607.60	$0.00	$0.00	$77,107.60
PV Dedicated Converter	$5,904.00	$2,440.97	$2,049.62	$0.00	($504.20)	$9,890.39
System	$161,164.00	$38,112.18	$25,549.10	$0.00	($6,456.04)	$218,369.24

Figure 5.2: Simulation result for economic analysis cash flow summary of wind-solar configuration

Simulation Results

System Architecture: HOMER Cycle Charging
Generic flat plate PV (33.4 kW/27.0 kW)
EnerSys PowerSafe OPzV 3000 (1.00 strings)

Hub Height (10.00 m)

Total NPC:	$190,340.20
Levelized COE:	$0.3744
Operating Cost:	$3,314.07

Cost Summary | Cash Flow | Compare Economics | Electrical | Renewable Penetration | EnerSys PowerSafe OPzV 3000 | Generic flat plate PV | Emissions

Cost Type
- Net Present
- Annualized

Categorize
- By Component
- By Cost Type

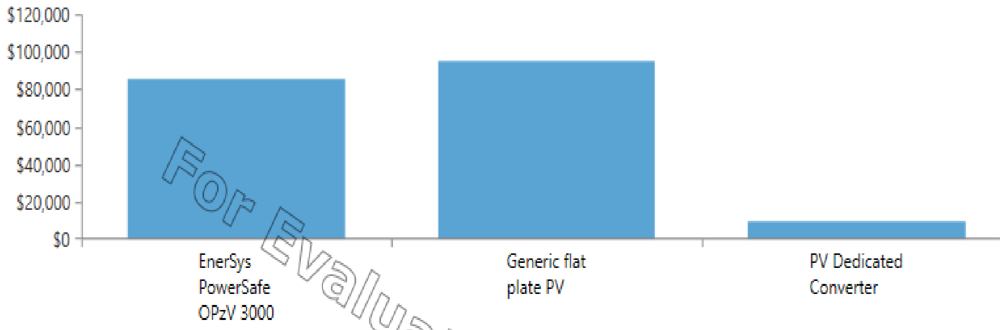

Component	Capital ($)	Replacement ($)	O&M ($)	Fuel ($)	Salvage ($)	Total ($)
EnerSys PowerSafe OPzV 3000	$53,760.00	$23,596.46	$8,198.49	$0.00	($496.39)	$85,058.55
Generic flat plate PV	$83,505.51	$0.00	$11,885.74	$0.00	$0.00	$95,391.25
PV Dedicated Converter	$5,904.00	$2,440.97	$2,049.62	$0.00	($504.20)	$9,890.39
System	$143,169.51	$26,037.43	$22,133.85	$0.00	($1,000.60)	$190,340.19

Figure 5.3: Simulation result for economic analysis cash flow summary of PV configuration

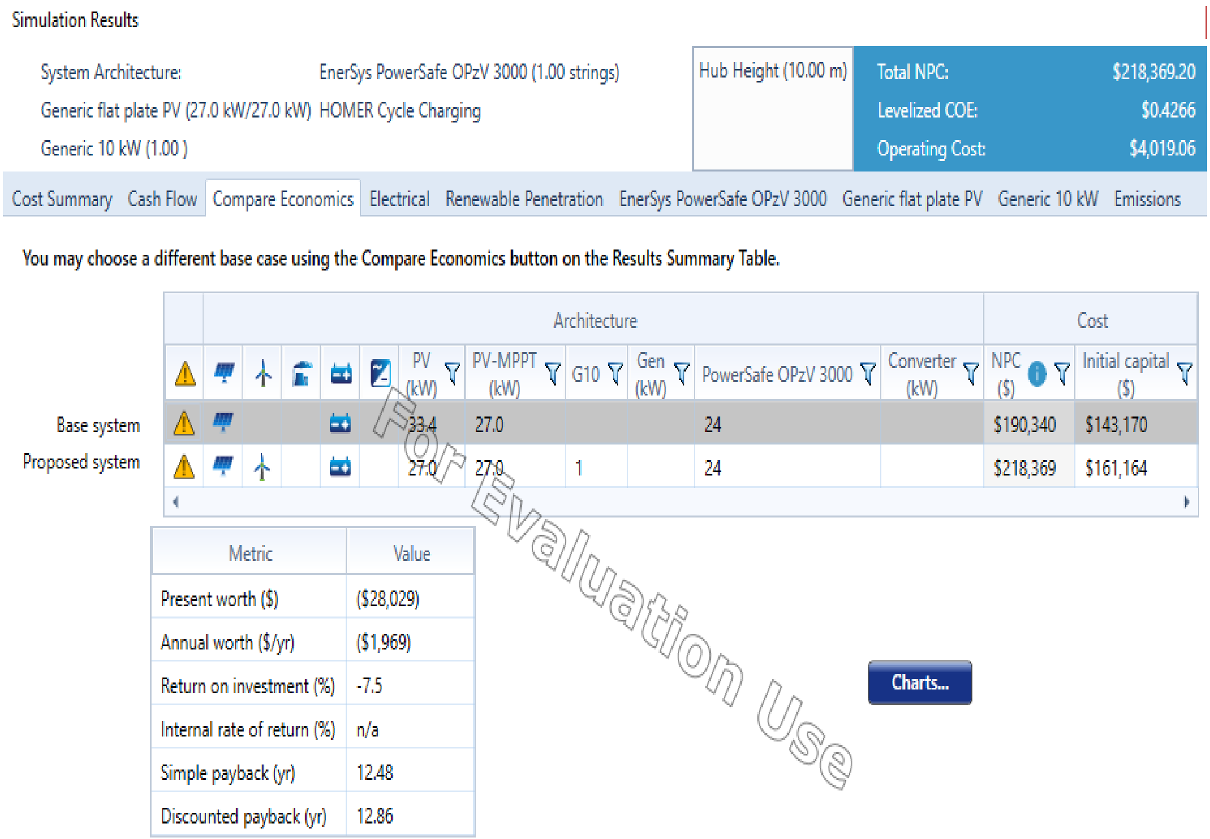

Figure 5.4: Economic comparison of two renewable hybrid system

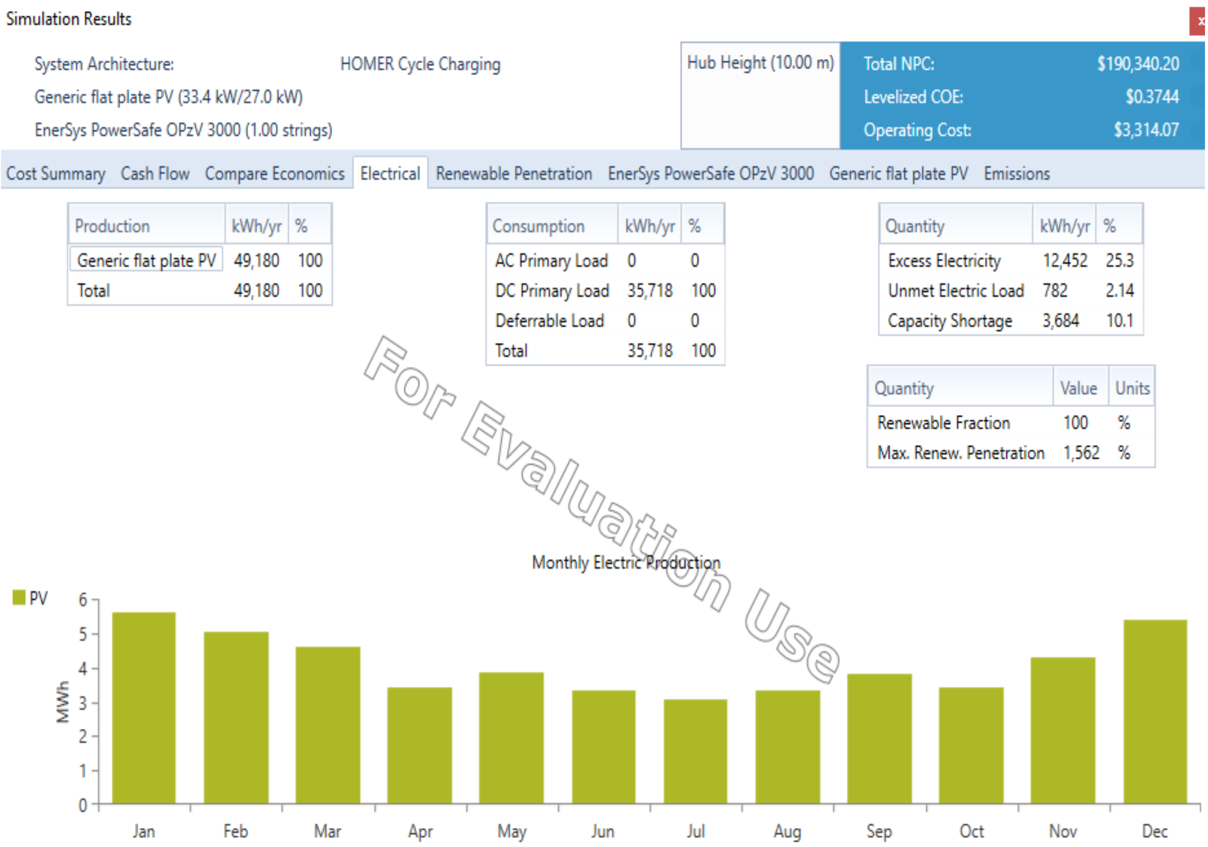

Figure 5.5: Percentage electricity production of components solar hybrid

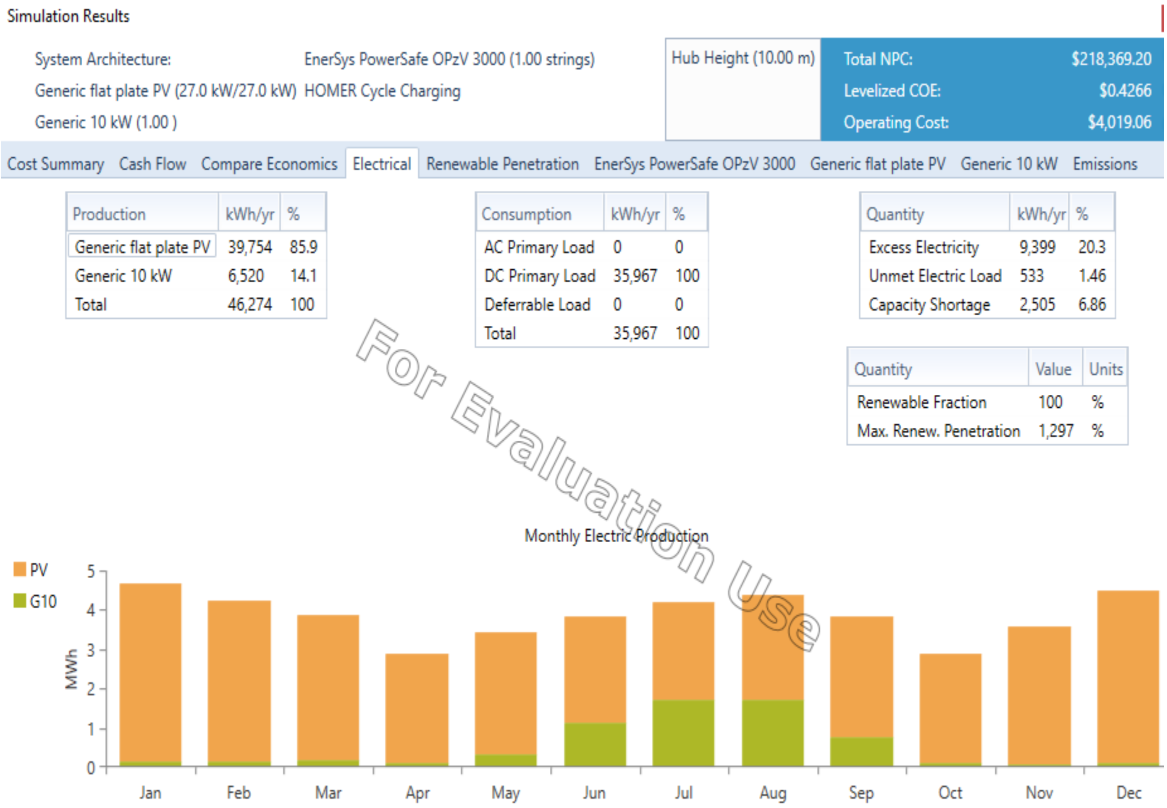

Figure 5.6: Percentage electricity production of components in wind-solar hybrid

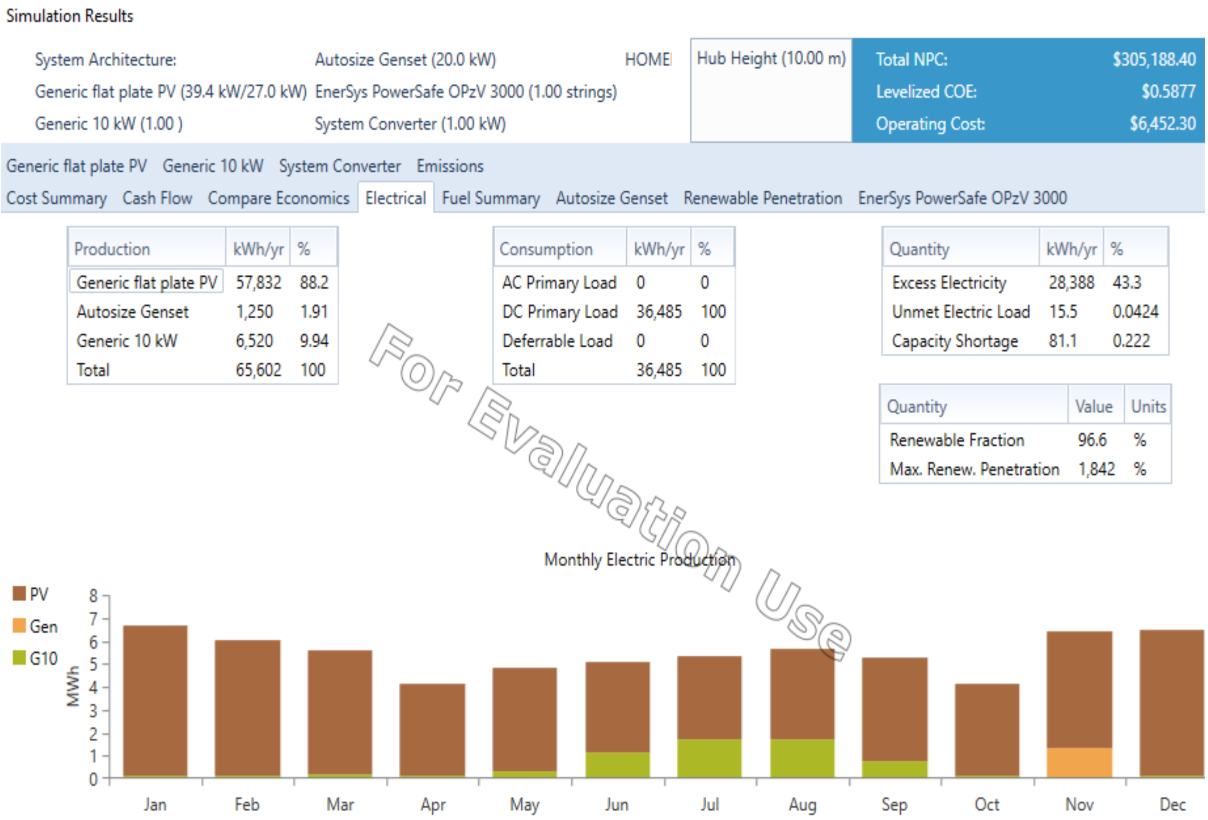

Figure 5.7: Percentage electricity production of components in PV/Wind/DG hybrid

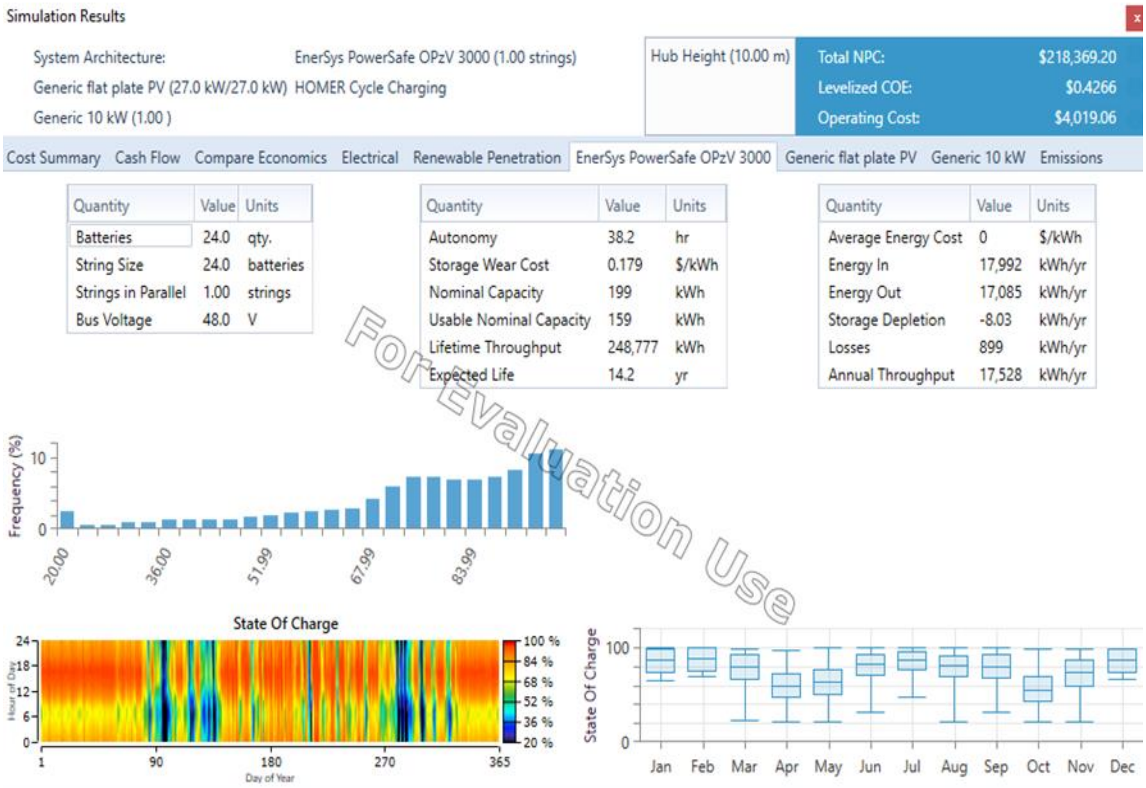

Figure 5.8: Systems Battery state of charge for the renewable system

Life cycle is the number of cycles that a battery can carry out before its capacity reaches 80% of nominal capacity and it is basically determined by battery type and DoD. The higher the DoD, the shorter the life span for all types of batteries. It is advised that even deep cycle batteries should not be regularly discharged below 60% of DoD (40% state of charge). Moreover, all types of batteries perform better at low currents rather than at high ones, both for charge and discharge. Slow charge/discharge procedures prolong the life span of any battery and allow for a sustained high capacity level throughout the life cycle. Fast charging as well as fast discharge drawing high currents can easily lead to worse performance and shorter lifetime for any electrochemical battery type. frequency regulation graph shows sizing methods for renewable integration, peak and load leveling.

Figure 5.8 above shows an overview of the battery performance and state of charge during one year for each scenario. It can be observed that the batteries remain most of the working period charged at the recommended levels (above 40% state of charge or 60% DoD.

5.3 Result Discussions

The popularity of both the individual renewable energy systems and their hybrid configurations stems from many inherent natural features and technological developments. These include:

➢ The renewables:

i)Inexhaustible and readily available natural resources, predominantly present in most parts of Africa;

ii) Relatively environmentally friendly;

iii) Very scalable, from micro- to mega- hydro/wind turbines, and from single-panel to multiple-panel PV (solar) systems; and

iv)They have long lifetime (20-50 years) and very low maintenance cost;

➢ The hybrid systems:

i) Provide more reliable and higher quality energy at lower economic and environmental costs; and

ii) Are more environmentally friendly than any of the conventional energy generators.

Unfortunately, despite these attractions and the abundance of these renewable energy resources, neither the individual renewables nor their hybrid configuration has found considerable applications in Ethiopia. The telecommunications sector of the economy is a case in point. This study has demonstrated that the telecommunications industry is one of the areas where renewable energy systems could be deployed to maximum national economic and environmental benefits, as obtains in many developed and developing countries.

From the simulations result above we compare the four configuration using three major comparison parameters:

A) Economic Cost

The economic cost comparison considers the following major parameters initial capital cost(ICC), operating cost, COE and total NPC as shown in the below Table 5.2 and also figure 5.2,5.3,5.4.

Table 5-2: HOMER Pro economic cost Comparison of six major configurations

Parameter size/cost	**PV/Battery**	**PV/WT/ Battery**	**PV/WT/DG /Battery**	**PV/DG/ Battery**	**WT/DG/ Battery**	**Dual DG/ Battery**
PV size(kw)	33.4	27	39.4	33.7	0	0
Wind Turbine(kw)	0	10	10	0	20	0
Generator(kw)	0	0	20	20	40	40
Battery(quantity)	24	24	24	48	24	24
Converter(kw)	27	27	27	27	39	39
Dispatch strategy	load Following	load Following	load Following	load Following	load Following	load Following
capital cost	143,170	161,164	213,350	218,931	657,050	603,440
Replacement cost	19,245.42	38,112.18	38,119.55	45,069.24	80,241.00	459,319
Fuel cost($)	0	0	459.2	459.2	44,932	141,974
operating cost($)/yr	3,314	4,019	6,452.3	6,807	76,649	241,924
Levelized COE($)/kwh	0.374	0.4266	0.588	0.610	3.829	8.454
Total NPC($)	190,340	218,369	305,188.4	315,812	1,550,283	3,422,719

NPC is the present value of all the costs of installing and operating the system over the project lifetime, minus the present value of all the revenues that it earns over the project lifetime. LCOE is the average cost per kWh of useful electrical energy produced by the system if it should be paying back for itself in reasonable economy terms. OPE is the annualized value of all costs and revenues other than initial capital costs.

i) Wind/PV/Battery System Vs Dual Generator/Battery System

In initial capital cost, the wind/PV/battery hybrid system has $161,164.00, while the dual diesel system has $603,440.00; In comparison, the wind/PV/battery hybrid system saves $442,276.00 to the network operator.

In the operating cost, the wind/PV/battery hybrid system has $4,019/year, while the dual diesel system has $241,924/year; In comparison, the wind/PV/battery hybrid system saves $237,905/year to the network operator.

In the COE, the wind/PV/battery hybrid system has $0.427/kWh, while the dual diesel system has $ 8.454/kWh; In comparison, the wind/PV/battery hybrid system saves $8.027/kWh to the network operator.

In the total NPC, the wind/PV/battery hybrid system has $218,369.00, while the Dual diesel system has $3,422,719; In comparison, the wind/PV hybrid system saves $3,204,350 to the network operator. Finally, based on the comparison parameters, i.e. ICC, operating cost, COE and total NPC of power generation for the BTS site, the hybrid renewable power system is the best in the perspective of economic analysis.

ii) PV/Battery system vs Dual Generator/Battery system

In initial capital cost, the PV/battery hybrid system has $143,170.00, while the Dual diesel system has $603,440.00; In comparison, the PV/battery hybrid system saves $460,270.00 to the network operator.

In the operating cost, the PV/battery hybrid system has $3,314/year, while the dual diesel system has $241,924/year; In comparison, the PV/battery hybrid system saves $238,610/year to the network operator.

In the COE, the PV/battery hybrid system has $0.374/kWh, while the dual diesel system has $ 8.454/kWh; In comparison, the PV/battery hybrid system saves $8.08/kWh to the network operator.

In the total NPC, the PV/battery hybrid system has $190,340 while the Dual diesel system has $3,422,719; In comparison, the PV/Battery hybrid system saves $3,232,379.00 to the network operator. Finally, based on the comparison parameters, i.e. ICC, operating cost, COE and total NPC of power generation for the BTS site, the hybrid renewable power system is the enhanced in the perspective of economic analysis.

iii) Wind/PV/Battery System Vs PV/Battery system

In initial capital cost, the wind/PV/battery hybrid system has $161,164.00 while the PV/Battery system has $143,170; In comparison, the PV/battery hybrid system saves $17,994 to the network operator.

In the operating cost the wind/PV/battery hybrid system has $4019.00 while the PV/Battery system has $3,314.00; In comparison, the PV/battery hybrid system saves $705.00 to the network operator

In the COE, the wind/PV/battery hybrid system has $.427/kwh while the PV/Battery system has $.374/kwh; In comparison, the PV/battery hybrid system saves $0.053/kwh to the network operator.

In the total NPC, the wind/PV/battery hybrid system has $218,369.20 while the PV/Battery system has $190,340.00; In comparison, the PV/battery hybrid system saves $28,029.20 to the network operator. Finally, based on the comparison parameters, i.e. ICC, operating cost, COE and total NPC of power generation for the BTS site, the hybrid renewable power system is the best in the perspective of economic analysis.

B) Electricity Production

Electric production comparison considers the bellow major points as shown on the table 5.3 and on the figure 5.5,5.6,5.7.

Table 5-3: HOMER Pro electricity production Comparison of six major configurations

Production	PV/Battery		PV/WT/ Battery		PV/WT/DG/ Battery		PV/DG/ Battery		WT/DG/ Battery		2DG/ Battery	
	kwh/yr	%	kwh/yr	%	kwh/yr	%	kwh/yr	%	kwh/yr	%	kwh/yr	%
PV array	49,180	100	39,754	86	57832	88	49678	98	0	0	0	0
Wind Turbine	0	0	6,520	14	6520	9.9	0	0	36254	74	0	0
DG	0	0	0	0	1250	1.9	1250	2,45	12515	26	39544	100
Total	49,180	100	46274	100	65,602	100	50,928	100	48,769	100	39544	100
Excess electricity	12452	25	9399	20	28388	43	13416	26	56.1	0.1	0.0001	0
Unmet electric load	782	2.1	533	1.5	15.5	0	107	0.3	0	0	0	0
capacity shortage	3684	10	2505	6.9	81.1	0.2	531	1.5	0	0	0	0
Renewable fraction		100		100		97		97		74	0	0

The unmet load is the proportion of the total load that went unserved because of insufficient generation. The capacity shortage is a shortfall that occurs between the required operating capacity and the actual amount of operating capacity the system can provide. Excess electricity is surplus electrical energy that must be dumped because it cannot be used to serve a load or charge the batteries.

i) Wind/PV/Battery System Vs Dual Generator/Battery System

In the Wind/PV hybrid system, the PV array generates 397,541kwh/year means supplies 85.9% of the annual electricity production, and the wind system contributes 6,520kwh/year (14.1%) of the total electricity with 46,274kwh/year production capacity; while the diesel-only system generates 39,544kwh/year of the total electricity. Since the hybrid system have 6,730kwh/year production benefit.

ii) PV /Battery system Vs Dual Generator/Battery System

In the PV/Battery hybrid system, the PV array generates 49,180kwh/year means supplies 100% of the annual electricity production; while the diesel-only system generates 39,544kwh/year of the total electricity. PV hybrid system have 9636kwh/year production benefit.

iii) Wind/PV/Battery System Vs PV/Battery system

In the PV/Battery hybrid system, the PV array generates 49,180kwh/year means supplies 100% of the annual electricity production; while the Wind/PV/Battery System generates 46,274kwh/year of the total electricity or 100% capacity. PV hybrid system have 2,906kwh/year production benefit.

C) Environmental Impact

Table 5 4: Comparison of simulation results of emissions for three configurations

Pollutant	Emissions (kg/year)			
	PV/WT/ Battery	PV/ Battery	WT/DG/ Battery	Dual DG/Battery
Carbon dioxide(kg/yr)	0	0	12,692	40,102
Carbon monoxide(kg/yr)	0	0	31.3	99
Unburned hydrocarbons(kg/yr)	0	0	3.47	11
Particulate matter(kg/yr)	0	0	2.36	7.46
Sulfur dioxide(kg/yr)	0	0	25.5	80.5
Nitrogen oxides(kg/yr)	0	0	280	883

i) Generator/Battery Vs Wind/PV/ Battery system

The generator in the Generator/Battery system operates for 7,300hr/year, has a fuel consumption of 29,200L/year. It generates 40,102kg/year of carbon dioxide (CO_2), 99 kg/year of carbon monoxide(CO), 11kg/year of unburned hydrocarbons(UHC), 7.46kg/year of particulate matter(PM), 80.5kg/year of sulfur dioxide(SO_2), and 883kg/year of nitrogen oxide(NO) as shown in table 5.4; but in the Wind/PV/Battery hybrid system, no diesel generator in the system so it has a fuel consumption of 0L/year. This system emits 0 kg/year of CO_2, 0 kg/year of CO, 0 kg/year of UHC, 0 kg/year of PM, 0kg/year of SO_2, and 0 kg/year of NO annually into the atmosphere of the location of the BTS station site as shown in table5.4. A 100% decrease was noticed in each pollutant. This was due to the 100% renewable penetration into the existing power (Diesel only) system.

ii) Generator/Battery Vs PV/Battery system

The generator in the Generator/Battery system operates for 7,300hr/year, has a fuel consumption of 29200L/year. It generates 40,102kg/year of carbon dioxide (CO_2), 99 kg/year of carbon monoxide(CO), 11kg/year of unburned hydrocarbons(UHC), 7.46kg/year of particulate matter(PM), 80.5kg/year of sulfur dioxide(SO_2), and 883kg/year of nitrogen oxide(NO) as shown in table 5.4; but in the PV/Battery hybrid system, no diesel generator in the system so it has a fuel consumption of 0L/year. This system emits 0 kg/year of CO_2, 0 kg/year of CO, 0 kg/year of UHC, 0 kg/year of PM, 0kg/year of SO_2, and 0 kg/year of NO annually into the atmosphere of the location of the BTS station site as shown in table5.4. A 100% decrease was noticed in each pollutant. This was due to the 100% renewable penetration into the existing power (Diesel only) system.

iii) Generator/Battery Vs Wind/Generator/Battery system

The generator in the Generator/Battery system operates for 7,300hr/year, has a fuel consumption of 29,200L/year. It generates 40,102kg/year of carbon dioxide (CO_2), 99 kg/year of carbon monoxide(CO), 11kg/year of unburned hydrocarbons(UHC), 7.46kg/year of particulate matter(PM), 80.5kg/year of sulfur dioxide(SO_2), and 883kg/year of nitrogen oxide(NO) as shown in table 5.4; but in the Wind/DG/Battery hybrid system The generator operates for 2,277.6hr/year, has a fuel consumption of 9,110.4L/year. It generates 12,692kg/year of carbon dioxide (CO_2), 31.3 kg/year of carbon monoxide(CO), 3.47kg/year of unburned hydrocarbons(UHC), 2.36kg/year of particulate matter(PM), 25.5kg/year of sulfur dioxide(SO_2), and 280kg/year of nitrogen oxide(NO) as shown in table 5.4. A 74%

decrease was noticed in each pollutant. This was due to the 74% renewable penetration into the existing power system.

Table 5-5: Comparison of simulation of Diesel-only System and Diesel in Hybrid System

Quantity (unit)	**PV/WT/DG/Battery**	**WT/DG/Battery**	**Dual DG/Battery**
Hours of operation(hr/yr)	1	3,268	4,174
Operational life(yr)	20,000	6.12	4.79
Capacity factor(%)	0.00342	22.1	28.2
Fuel consumption(L/yr)	2.48	11,923	15,229
Specific fuel consumption(L/kwh)	0.517	0.385	0.385
Fuel energy input(kwh/yr)	24	117,323	149,849
Mean electrical efficiency(%)	19.7	26.4	26.4

Diesel only system is the energy source is dual diesel generator for twenty-four hours per day, but diesel in hybrid system single backup generator used when the renewable resource (solar & wind) intermittent.

5.4 Sensitivity Analysis & Result

As it is seen from all sensitivity cases considered above in this study, it is clear that the renewable hybrid system is best of all other hybrid systems for all sensitivity cases considered. As a result, it can be concluded that it is best to power the BTS site in the study area through a renewable based hybrid system, i.e. first PV/Battery system, second Wind/PV/Battery system than the dual diesel generator alone configuration.

Table 5-6: Optimal Ranking of the Hybrid System Types [as Generated by HOMER Pro]

Ranking	Homer Pro Optimization Result
1	PV/Battery hybrid power system
2	PV/Wind/Battery hybrid power system
3	PV/Wind/DG/Battery hybrid power system
4	PV/DG/Battery hybrid power system
5	PV/Wind/2DG/Battery hybrid power system
6	PV/2DG/Battery hybrid power system
7	Wind/DG/Battery hybrid power system
8	Wind/2DG/Battery hybrid power system
9	DG/Battery hybrid power system
10	2DG/Battery hybrid power system

The above major scenarios resulted from the simulations are described in details below: The result is based upon the system with 111kWh/day telecom load at 5.89kWh/m2/day of solar radiation, 5.52m/s of wind speed and $0.8/L diesel price.

Table 5-7: HOMER Pro Design, Analysis Model summery

Project in put	**Analysis**	**Result**
▪ Load profile ▪ Economic cost ▪ Site specific metrological data (solar radiation, wind speed, temperature). ▪ System component specification	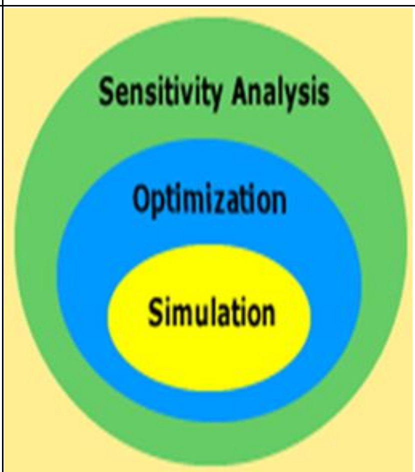	▪ Economic & Engineering ▪ System sizing ▪ Performance detail ▪ Financial report ▪ Print out report

6. CONCLUSION AND RECOMMENDATION

6.1 Conclusion

Providing a reliable, secure power and energy system is one of the main issues in cellular networks. Accordingly, this study examined supplying the needed energy for a GSM/UMTS type base station located at East Bale, Ethiopia by renewable hybrid system with Big storage battery so as to provide feasibility and reliable electric power. The optimum criteria, including economic and technical feasibility parameters, were analyzed using the HOMER Pro software package developed by the U.S. National Renewable Energy Laboratory (NREL).

Moreover, the best optimal hybrid system configurations PV/Battery system after considering Economical comparison the net present cost (NPC) with the Levelized cost of energy (LCOE)), electric production comparison and (i) OPEX savings and (ii) GHG emissions with the conventional DG/Battery/Converter system. Findings indicated that PV/Battery hybrid system is the most economically viable option with a total cost of $190,340.00 for the whole system project life time, i.e. 25 years and for the diesel generator system the total cost is $3,422,719 for 20 years' life time. And the levelized cost of energy (COE) for PV/Battery systems is $.374 and Dual Diesel generator system is $8.454/kWh. This implies the hybrid system saves $3,232,379 in terms of Net Present cost and $8.08/kWh in terms of Levelized cost of energy and have 9,636kwh/year electric production benefit to the network operator.

Also, simulation results show that the renewable energy source (RES) based hybrid energy system can decrease amount of air pollutants as compared to the conventional diesel generator only and so a reduction of 40,102kg/year of CO_2, 99 kg/year of CO, 11 kg/year of UHC, 7.46 kg/year of PM, 80.5 kg/year of SO_2, and 883 kg/year of NO_x is observed and saves about 177,467 liters of fuel per annum to the network operator. A sensitivity analysis is also done to analyze the effects of probable variation in solar radiation, wind speed, diesel price and average annual energy usage of the system load in the optimal system configurations and the simulation results show that the proposed system is effective to supply the site at all conditions.

In summary, this paper has verified the predictions that the proposed hybrid system is superior to the rest systems which have diesel system for power generation at the BTS site from the perspective of both economic, electric production and environmental analyses.

- Best renewable hybrid system is PV/Battery system composed of PV=33.4kw, MPPT=27kw, one string 3000AH/2v Battery (Zero fuel consumption).
- Second enhanced renewable hybrid system is PV/Wind/Battery system composed of PV=27kw, Wind turbine =10kw, MPPT=27kw, and one string 3000AH/2v Battery (Zero fuel consumption).
- Third good renewable hybrid system is PV/Wind/DG/Battery system composed of PV=39.4kw, Wind turbine =10kw, MPPT=27kw, DG=20kw and one string 3000AH/2v Battery (minimized fuel consumption).

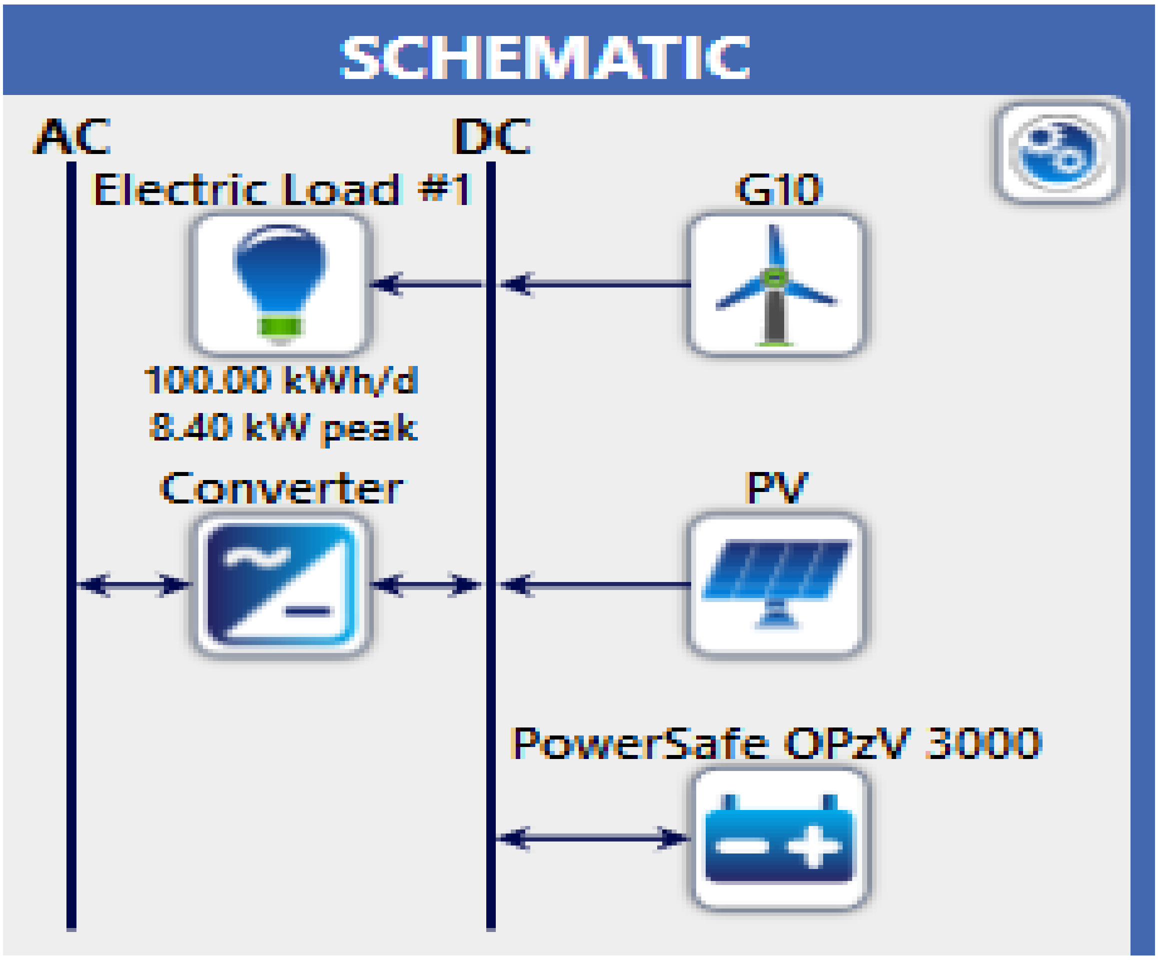

Figure 5.9: Recommended Hybrid system from Homer result

6.2 Recommendation

The researcher has recommended that to implement a renewable-energy based hybrid system for ensuring reliability and cleanly powering of the site since utilizing renewable-energy based hybrid system for powering BTS sites will decrease the operating cost of the telecom company which has direct impact on the low-income rural telecom subscriber, also reduce the diesel fuel usage, thereby bring low greenhouse gas emission to the environment and also the study energy resource map for nearby community. Finally, the information gained from the entire thesis can be applied in the design, execution, or development of HRES for any mobile tower applications in other locations in the country.

6.3 Future work

Further follow up studies are required to be carried for the design and development of reliable hybrid systems of the BTSs considering shelter and indoor type BTS load consumptions including fuel and controlling system for enhancing the reliability of a hybrid system for remote and inaccessible locations.

REFERENCES

[1]. Emmanuel D.Rogdakis, Irene P.koronaki,(2018), “Renewable Energy Engineering: Solar, Wind, Biomass, Hydrogen and Geothermal Energy System. Bentham” ,1–400P.

[2]. Ersan Kabalci,(2020),”Hybrid Renewable Energy systems and micro grids” ,:1-526p.

[3]. Patel, M.R., (2006) Wind and Solar Power Systems: Design, Analysis, and Operation. 2nd Ed. Boca Raton: Taylor & Francis Group,3-358pp.

[4]. HOMER® Pro Version 3.7 User Manual, (2016), HOMER® Energy 1790 30th St Suite 100 Boulder CO 80301 USA

[5]. Mehrpooya, M.; Mohammadi, M.; Ahmadi, E.(2018), “Techno-economic-environmental study of hybrid power supply system: A case study in Iran. Sustain”. Energy Technol. Assess, 25, 1–10pp.

[6]. Owusu, P.A.; Asumadu-Sarkodie, S.(2016),“A review of renewable energy sources, sustainability issues and climate change mitigation” Cogent.Eng. ,3p.

[7]. Misrak Girma, (2016)"Viability of Solar/Wind and Hybrid Water Pumping System for Off-Grid Rural Areas in Ethiopia." Addis Ababa University Docterial Thesis.1-260pp.

[8]. Olatomiwa L,Mekhilef S,Huda ASN,et al.(2015)”Techno-economic-analysis of hybrid PV diesel-battery and PV-Wind-Diesel-battery power system for mobile BTS: the way forward for rural development ”Energ Sci Eng., 1–285pp.

[9]. Shahzad, M.K.; Zahid, A.; Rashid, T.U.; Rehan, M.A.; Ali, M.; Ahmad,(2017)” Techno-economic feasibility analysis of a solar-biomass off grid system for the electrification of remote rural areas in Pakistan using HOMER software”. Renew. Energy, 106, 264–273p.

[10]. Vincent Anayochukwu Ani,(2015) "Energy optimization at GSM base station sites allocated in rural areas” Nigaria,1-210p.

[11]. Strnad, I.; Prenc, R.,(2017) “Optimal sizing of renewable sources and energy storage in low-carbon micro grid nodes”. Electr. Eng., 100, 1661–1674pp.

[12]. Arul, P.; Ramach and aramurthy, V.K.; Rajkumar, R.,(2015)” Control strategies for a hybrid renewable energy system: A review. Renew. Sustain”. Energy. Rev., 42, 597–608pp.

[13]. Dlatomiwa, L.; Mekhilef, S.; Ismail, M.; Moghavvemi, M.,(2016) “Energy management strategies in hybrid renewable energy systems: A review. Renew. Sustain”. Energy. Rev., 62, 821–835pp.

[14]. Vivas, F.; Heras, A.D.L.; Segura, F.; Andújar, J., (2018)“A review of energy management strategies for renewable hybrid energy systems with hydrogen backup. Renew. Sustain”. Energy. Rev., 82, 126–155.

[15]. Jung, T.; Kim, D.; Moon, J.; Lim, S.,(2018) “A scenario analysis of solar photovoltaic grid parity in the Maldives: The case of Malahini resort”. Sustainability, 10,4045.

[16]. Sigarchian, S.G.; Paleta, R.; Malmquist, A.; Pina, A.(2015) “Feasibility study of using a biogas engine as backup in a decentralized hybrid (PV/wind/battery) power generation system—Case study Kenya”. Energy, 90, 1830–1841pp.

[17]. Rezzouk, H.; Mellit, A.(2015) “Feasibility study and sensitivity analysis of a stand-alone photovoltaic–diesel–battery hybrid energy system in the north of Algeria. Renew. Sustain”. Energy. Rev., 43, 1134–1150pp.

[18]. Madziga, M.; Rahil, A.; Mansoor, R.,(2018) “Comparison between three off-grid hybrid systems (solar photovoltaic, diesel generator and battery storage system) for electrification for Gwakwani village, South Africa”. Environments , 5, 57.

[19]. Sisay Fitwi and Dr.Getachew B., (2015), “Feasibility Study of Standalone PV/Wind/Biogas Hybrid System for Rural Electrification: (A Case Study of Midrwa community in Adigrat District)”. Addis Ababa University,1-92p.

[20]. Onwumere , Michael (2017).”An Economic analysis on the viability of harnessing wind energy of power generation in Kaduna state, Nigeria.5.124pp.

[21]. Lemlem M ,(2016) "Optimum Design and Analysis of Solar PV/Diesel Hybrid Power Generation System for Cheri Alga Irrigation Site and Electrification of the Nearby Community at Kosha Kebele, Jimma” Master Thesis,9,1-96.

[22]. Natei Ermias, Ashenafi Abebe, (2017)"Evaluations of Wind Speed Distribution and Wind Power Potential over Ethiopia.", http://scienceq.org/Journals/JPCS. php.

[23]. Cheng, L.;Wang,W.;Wei, S.; Lin, H.; Jia, Z.(2018) “An improved energy management strategy for hybrid energy storage system in light rail vehicles”. Energies, 11, 423p.

[24]. Li, H.; Eseye, A.T.; Zhang, J.; Zheng, D. (2017)”Optimal energy management for industrial micro grids with high-penetration renewables”. Prot. Control Mod. Power Syst., 2.

[25]. Acharya D,(2013) “Solar and Wind Hybrid Power for an Extremely Remote Mobile Base Station”. Guelph Eng J 1-10. ISSN: 1916-1107pp.

[26]. Brenna, M.; Foiadelli, F.; Longo, M.; Abegaz, T.(2016) "Integration and optimization of renewables and storages for rural electrification". Sustainability, 8, 982pp.
[27]. Halabi, L.M.; Mekhilef, S.; Olatomiwa, L.; Hazelton, J.(2017) "Performance analysis of hybrid PV/diesel/battery system using HOMER: A case study Sabah, Malaysia". Energy Convers. Manag., 144, 322–339pp.
[28]. Ambekar P, Sengar KP (2015) "Cost Analysis of a hybrid system by using An Optimalzation Technique". Int. J Adv. Technol. Eng. Res (IJATER) 5: 2250-3536pp.
[29]. Nag, A.K.; Sarkar, S. (2018) "Modeling of hybrid energy system for futuristic energy demand of an Indian rural area and their optimal and sensitivity analysis". Renew. Energy, 118, 477–488.
[30]. Singh, A.; Baredar, P.; Gupta, B.(2017) "Techno-economic feasibility analysis of hydrogen fuel cell and solar photovoltaic hybrid renewable energy system for academic research building". Energy Convers. Manag., 145, 398–414pp.
[31]. Dereje Derebew (2015)"Ethiopia's Renewable Energy Power Potential and Development Opportunities" Ministry of Water and Energy.1-40p
[32]. Berino Francisco Silinto & Nelso Alberto Bila ,(2015), "Feasibility Study of Solar-Wind Hybrid Power System for Rural Electrification at the Estatuene Locality in Mozambique",KTH Indu.Eng.&Mang,1-224p
[33]. Subodh paudel, (2015)," Optimization of Hybrid PV/Wind Power System for Remote Telecom Station" Junior Researcher, IEEN,Nepal,8,1-212p
[34]. Rehman, S, El-Amin, I (2015) Study of a solar pv/wind/diesel hybrid power system for a remotely located population near Arar, Saudi Arabia. Energy Exploration & Exploitation 33(4): 591–620.
[35]. Rehman, S, Sahin, AZ (2015) Performance comparison of diesel and solar photovoltaic power systems for water pumping in Saudi Arabia. International Journal of Green Energy 12: 702–713.
[35]. Mohamad Shahrizal Mohd Noor1,a, Zuraimy Adzis1,b, Yanuar Z. Arief1,c *, Nor Asiah Muhamad ,(2016),"Feasibility Analysis of Stand-Alone Renewable Energy Supply for Telecommunication Tower Using Homer" Applied Mechanics and Materials Vol. 818 ,pp 223-227.
[37]. Areef Kassam., (2021),"HOMER Software Training Guide for Renewable Energy Base Station Design", GSM Association, Available in http://www.homerenergy.com

[38]. Solar and Wind energy (2021) available in
https://energypedia.info/wiki/Ethiopia_Energy_Situation
[39]. NASA/SSE. Surface meteorology and energy (2013) Available at
http://eosweb.larc.nasa.gov/sse.
[40]. Electrical Equipment product suppliers and current price (2021) Available in
http://www.alibaba.com